

*IN VITRO RESPIRATORY SYNCYTIAL VIRUS INFECTION
IN GUINEA PIG ALVEOLAR MACROPHAGES*

by

PHILOMENA MIEWCHING KAAN

B. Sc., Simon Fraser University, 1985
M. Sc., University of British Columbia, 1995

A THESIS SUBMITTED IN PARTIAL FULFILMENT OF
THE REQUIREMENTS FOR THE DEGREE OF

DOCTOR OF PHILOSOPHY

In

THE FACULTY OF GRADUATE STUDIES

(Department of Experimental Medicine)

Experimental Medicine Program

We accept this thesis as conforming to the required standard

THE UNIVERSITY OF BRITISH COLUMBIA

February 2002

© Philomena Miewching Kaan, 2002

In presenting this thesis in partial fulfilment of the requirements for an advanced degree at the University of British Columbia, I agree that the Library shall make it freely available for reference and study. I further agree that permission for extensive copying of this thesis for scholarly purposes may be granted by the head of my department or by his or her representatives. It is understood that copying or publication of this thesis for financial gain shall not be allowed without my written permission.

Department of Experimental Medicine

The University of British Columbia
Vancouver, Canada

Date February 25, 2002

ABSTRACT

Respiratory syncytial virus (RSV) is the most common cause of acute bronchiolitis in infants. Alveolar macrophages (AM), cells which play major roles in lung defense mechanisms, are major targets for RSV infection *in vivo* and *in vitro*. This thesis examines the effects of cell maturation, age and sex of the host, and interaction of environmental particulates (PM10) on *in vitro* RSV infection of guinea pig AM. In addition, the expression of protein kinase in RSV-infected AM was studied. Electron microscopy localized immunogold labeled RSV antigens in the lysosomes of mature AM that restrict RSV replication while gold particles were observed in the cytoplasm of immature AM that support viral replication. Using RSV Yield as a measure of virus progeny per RSV immunopositive AM, immature AM from young animals showed a significantly higher RSV Yield compared to the same AM subpopulation from adult animals. The data concerning animal gender showed that the distribution of AM subpopulation from both sexes is similar but the RSV Yield of mature AM was greater from male than female guinea pigs. The introduction of PM10 during RSV infection of AM resulted in suppression of RSV Yield and RSV-induced cytokine production. The study of protein kinase expression identified Rsk, PKB and p70 S6K as potential candidates and MAPK and PKB as major pathways involved in RSV-mediated signal transduction in AM. In conclusion, the response of guinea pig AM to *in vitro* RSV infection is associated with expression of candidate protein kinases and is influenced by cell maturation, age and sex of the host animal, and interaction with extrinsic factors such as air pollution.

TABLE OF CONTENTS

| | |
|--|-----|
| Abstract | ii |
| Table of Contents | iii |
| List of Tables | ix |
| List of Figures | x |
| List of Abbreviations | xii |
| Acknowledgements | xv |
| Dedication | xvi |
| CHAPTER 1 Overview | |
| General Introduction | 1 |
| Organization of Thesis | 2 |
| CHAPTER 2 Respiratory Syncytial Virus | |
| History and Classification | 3 |
| Characteristics | 4 |
| RSV infections in Humans | 5 |
| Epidemiology | 6 |
| Pathology | 6 |
| Pathogenesis | 7 |
| Important Issues | 10 |
| Animal models of RSV Infection | 11 |
| RSV <i>in vitro</i> infection | 12 |
| Epithelial Cells | 12 |
| Alveolar Macrophages | 14 |
| Summary | 15 |

CHAPTER 3 Alveolar Macrophages

| | |
|------------------------------------|----|
| Introduction | 17 |
| Origin of Macrophages | 17 |
| Heterogeneity of Macrophages | 18 |
| Morphology of Alveolar Macrophages | 20 |
| Light Microscopy | 20 |
| Electron Microscopy | 20 |
| Functions of Alveolar Macrophages | 20 |
| Phagocytosis | 21 |
| Inflammatory Activity | 25 |
| Regulation of Lung Homeostasis | 27 |
| Summary | 28 |

CHAPTER 4 General Materials & Methods

| | |
|--------------------------------|----|
| Cell Culture | 29 |
| HEp-2 Cells | 29 |
| L929 Fibroblasts | 30 |
| Virus Culture | 30 |
| RSV Propagation | 30 |
| Harvest & Concentration of RSV | 31 |
| RSV Titer Determination | 31 |
| Animals | 32 |
| Alveolar Macrophage Harvest | 32 |
| Bronchoalveolar Lavage | 32 |
| Cell Processing | 33 |

| | |
|---|----|
| Isolation of Macrophage Subpopulations | 33 |
| <i>In vitro</i> RSV Exposure | 34 |
| CHAPTER 5 Effect of Cell maturation– an EM study | |
| Introduction | 35 |
| Hypothesis & Specific Aims | 36 |
| Experimental Protocols | 37 |
| Study Design | 37 |
| Immunogold Labeling & Transmission Electron Microscopy | 39 |
| Results | 41 |
| Isolation of AM Subpopulations | 41 |
| Localization of RSV Particles | 41 |
| Discussion | 45 |
| CHAPTER 6 Effect of Age of host animal | |
| Introduction | 47 |
| Hypothesis & Specific Aims | 49 |
| Experimental Protocols | 49 |
| Study Design | 49 |
| Cytospin Preparation | 51 |
| Immunocytochemistry | 51 |
| Viral Plaque Assay | 52 |
| Results | 54 |
| Distribution of AM Subpopulations | 54 |
| Effect of Age on RSV Immunopositivity | 55 |
| Effect of Age on RSV Replication | 57 |

| | |
|---|----|
| | vi |
| Effect of Age on RSV Yield | 59 |
| Summary of Results | 60 |
| Discussion | 60 |
| CHAPTER 7 Effect of Sex of host animal | |
| Introduction | 63 |
| Hypothesis & Specific Aims | 64 |
| Experimental Protocols | 65 |
| Study Design | 65 |
| Detection of IL-6 & IL-8 by ELISA | 67 |
| Detection of TNF α by Bioassay | 69 |
| Results | 72 |
| Distribution of AM Subpopulations between the Sexes | 72 |
| Effect of Sex on RSV Immunopositivity | 73 |
| Effect of Sex on RSV Replication | 73 |
| Effect of Sex on RSV Yield | 75 |
| Effect of Sex on Cytokine Production | 75 |
| Summary of Results | 76 |
| Discussion | 77 |
| CHAPTER 8 RSV Interaction with PM10 | |
| Introduction | 80 |
| Hypothesis & Specific Aims | 83 |
| Experimental Protocols | 84 |
| Study Design | 84 |
| PM10 Exposure | 88 |

| | |
|---|-----|
| | vii |
| Flow Cytometry | 89 |
| Immunofluorescent Staining of RSV Antigens | 90 |
| Results | 91 |
| Effect of PM10-RSV Interaction on the Phagocytic Ability of AM | 91 |
| Effect of PM10-RSV Interaction on RSV Immunopositivity | 93 |
| Effect of PM10-RSV Interaction on RSV Replication | 95 |
| Effect of PM10-RSV Interaction on RSV Yield | 96 |
| Effect of PM10-RSV Interaction on IL-6 Production | 97 |
| Effect of PM10-RSV Interaction on IL-8 Production | 98 |
| Effect of PM10-RSV Interaction on TNF α Production | 99 |
| Summary of Results | 100 |
| Discussion | 100 |
| CHAPTER 9 Expression of Protein Kinases in RSV infection | |
| Introduction | 106 |
| Hypothesis & Specific Aims | 111 |
| Experimental Protocols | 112 |
| Study Design | 112 |
| Cell Lysate Preparation | 114 |
| Protein Assay | 114 |
| Western Blot | 115 |
| Results | 116 |
| Discussion | 119 |

| | |
|--------------------------------------|------|
| | viii |
| CHAPTER 10 Concluding Remarks | 125 |
| BIBLIOGRAPHY | 127 |
| APPENDIX | 154 |

LIST OF TABLES

| | | |
|-----------|--|-----|
| Table 3.1 | Ligands recognized by AM via receptors. | 22 |
| Table 3.2 | Major products released by AM. | 24 |
| Table 6.1 | Distribution of AM subpopulations in adult and juvenile guinea pigs. | 54 |
| Table 6.2 | RSV Yield in AM subpopulations from adult and juvenile guinea pigs. | 59 |
| Table 7.1 | Distribution of AM subpopulations in juvenile male and female guinea pigs. | 72 |
| Table 7.2 | RSV Yield in AM from male and female guinea pigs. | 75 |
| Table 7.3 | Cytokine profile of guinea pig AM following RSV exposure. | 76 |
| Table 8.1 | Chemical components of EHC-93. | 88 |
| Table 8.2 | Effect of PM10-RSV interaction on RSV Yield. | 96 |
| Table 9.1 | Summary of data from KPKS-1.0 | 117 |
| Table 9.2 | Protein kinases detected in guinea pig AM following RSV infection. | 118 |

LIST OF FIGURES

| | | |
|------------|--|----|
| Figure 5.1 | Experimental design of EM study. | 38 |
| Figure 5.2 | Isolation of AM subpopulations by density gradient centrifugation. | 42 |
| Figure 5.3 | Electron micrograph of immunogold-RSV particles in AM. | 43 |
| Figure 5.4 | Electron micrograph of RSV-infected HEp-2 cell. | 44 |
| Figure 6.1 | Experimental design for effect of age of host animal on RSV infection. | 50 |
| Figure 6.2 | Immunostaining of guinea pig AM subpopulations with anti-RSV antibody | 56 |
| Figure 6.3 | Effect of age of host animal on RSV immunopositivity | 56 |
| Figure 6.4 | Formation of a syncytium on HEp-2 monolayer. | 58 |
| Figure 6.5 | Effect of age of host animal on RSV replication | 58 |
| Figure 7.1 | Experimental design for effect of sex of host animal on RSV infection. | 66 |
| Figure 7.2 | Effect of sex of host animal on RSV immunopositivity | 74 |
| Figure 7.3 | Effect of sex of host animal on RSV replication | 74 |
| Figure 8.1 | Experimental design for study of PM10-RSV interactions in AM. | 84 |
| Figure 8.2 | PM10-exposed AM. | 86 |
| Figure 8.3 | Electron micrograph of AM containing PM10. | 86 |
| Figure 8.4 | Effect of PM10-RSV interactions on AM granularity. | 92 |
| Figure 8.5 | Representative histograms of HEp-2 cells and guinea pig AM with and without RSV infection. | 94 |
| Figure 8.6 | Effect of PM10-RSV interactions on RSV immunopositivity. | 94 |
| Figure 8.7 | Effect of PM10-RSV interactions on RSV replication. | 95 |
| Figure 8.8 | Effect of PM10-RSV interactions on IL-6 production by AM. | 97 |
| Figure 8.9 | Effect of PM10-RSV interactions on IL-8 production by AM. | 98 |

| | | |
|-------------|--|-----|
| Figure 8.10 | Effect of PM10-RSV interactions on TNF α production by AM. | 99 |
| Figure 9.1 | Experimental design for detection of protein kinases in RSV-infected AM. | 113 |
| Figure 9.2 | Representative autoradiogram of the KPKS-1.0. | 117 |

LIST OF ABBREVIATIONS

| | |
|-------------------------------|--|
| ABC-AP | avidin-biotin complex-alkaline phosphatase |
| AM | alveolar macrophage(s) |
| BSA | bovine serum albumin |
| C/EBP | CCAAT-enhancer binding proteins |
| CFU-GM | colony forming unit – granulocyte, monocyte |
| CTL | cytotoxic T lymphocytes |
| dH ₂ O | distilled water |
| EBV | Epstein-Barr virus |
| ECP | eosinophil cationic protein |
| EIA | immunoabsorbent assay |
| ELISA | enzyme-linked immunosorbent assay |
| ERK2 | extracellular signal-regulated kinase |
| EU | endotoxin unit |
| FACS | Fluorescence-Activated Cell Sorter |
| FBS | fetal bovine serum |
| FI-RSV | formalin-inactivated RSV |
| FKHRL 1 | Forkhead transcription factor |
| GM-CSF | granulocyte/monocyte-colony stimulating factor |
| GSK3 | glycogen synthase kinase 3 |
| H ₂ O ₂ | hydrogen peroxide |
| HIV | Human Immunodeficiency Virus |
| HSV | Herpes Simplex Virus |
| ICAM-1 | Intercellular adhesion molecule-1 |
| ICE | IL-1 β converting enzyme |

| | |
|-----------------------------|--|
| IFN $\alpha/\beta/\gamma$ | interferon alpha/beta/gamma |
| Ig | immunoglobulin |
| IgA | immunoglobulin A |
| IgE | immunoglobulin E |
| IgG | immunoglobulin G |
| IL- | interleukin- |
| iNOS | inducible nitric oxide synthase |
| IRF-1 | transcriptional activator interferon regulatory factor |
| JNK | c-jun N-terminal kinases |
| KPKS-1.0 | Kinetworks TM Protein Kinase Screen |
| LTB ₄ | leukotriene B4 |
| LTC4 | leukotriene C4 |
| m.o.i. | multiplicity of infection |
| MAPK | mitogen-activated protein kinase |
| MCP | monocyte chemotactic protein |
| M-CSF | monocyte colony stimulating factor |
| MEM | minimum essential medium |
| MFI | mean fluorescence intensity |
| MIP | macrophage inflammatory protein |
| NEG | negative control |
| NF κ B | nuclear factor – kappa B |
| NO | nitric oxide |
| O ₂ ⁻ | superoxide anion |
| OH ⁻ | hydroxyl radical |
| PBS | phosphate buffered saline |

| | |
|-------------------------|--|
| PDK-1 | phosphoinositide-dependent kinase |
| PFK-2 | 6-phosphofructo 2-kinase |
| PGE2 | prostaglandin E2 |
| PH | pleckstrin homology |
| PI-3,4,5-P ₃ | phosphatidyl inositides-3,4,5-triphosphate |
| PI-3,4-P ₂ | phosphatidyl inositides-3,4-diphosphate |
| PI3K | phosphatidyl 3-OH kinase |
| PKB | protein kinase B |
| PM10 | particulate matter, aerodynamic diameter <10 microns |
| PMN | polymorphonuclear leukocytes |
| PP2A | protein phosphatase 2A |
| RANTES | Regulated upon activation, normal T cells expressed and secreted |
| RSV | respiratory syncytial virus |
| RSVRE | RSV response element |
| SD | standard deviation |
| SEM | standard error of mean |
| TNF α | tumor necrosis factor alpha |
| TRAF | TNF-receptor associated factors |

ACKNOWLEDGEMENTS

I wish to thank Dr. R.G. Hegele for his guidance and support even when my ideas were seemingly wild and bizarre. Thank you for being a great teacher in experimentation, critical thinking and writing skills so pertinent in a scientific career. Special thanks go to members of my advisory committee, Dr. J.C. Hogg, Dr. E. Thomas and Dr. D.C Walker for their constructive criticisms. To various past and present members of the McDonald Research Laboratories (MRL), I wish to express my gratitude for your willingness to share with me your technical expertise: Dr. A. Dakhama, my predecessor, who taught me virology techniques; Ms. J. Hards and Dr. M. Elliott for discussion and advice concerning immunocytochemistry; Ms. D. Zhou and Ms. F. Chu, my good friends, who are experts in ELISA and EM techniques; Mr. S. Tsang for advice and assistance in TNF bioassay; Mr. G. Osborne of the UBC Flow Cytometry Facility for consultation on flow cytometry; Dr. K. Ashfaq for assistance in preparation of cell lysates; Ms. D. Minshall and Ms. L. Carter of the MRL Animal Care Facility; Mr. S. Greene and Mr. D. English for photographic expertise; Ms. Y. D'Yachova for statistical consultations. I am also indebted to Dr. R.R. Schellenberg (MRL) for the gift of L929 cells, Dr. C. Sherlock and members of the UBC Virology Laboratory for supply of HEp-2 cells and Dr. S.F. van Eeden (MRL) and Dr. R. Vincent of Health Canada for the gift of PM10 particles. Special thanks also go to Dr. S. L. Pelech and members of Kinexus Bioinformatics Corporation for advice and discussion on protein kinases and performing the protein kinase screen. I would also like to acknowledge the following people for their critical review and comments on selected chapters in this thesis: Dr. A. Sandford (Chapter 7), Dr. S.F. van Eeden (Chapter 8), Dr. H. Luo (Chapter 9) and Dr. V. Duronio of Jack Bell Research Laboratory (Chapter 9). I am also grateful to the British Columbia Lung Association for the financial support during my PhD program. Last but not least, I would not have made it this far without the love and support of my husband, Oon-Sim, and my son, Iain, who puts everything into perspective.

DEDICATION

This thesis is dedicated to

THE CREATOR

Of

All Creatures Great and Small

CHAPTER 1

OVERVIEW

GENERAL INTRODUCTION

Acute bronchiolitis is a lung infection in which inflammation is primarily localized to the non-cartilaginous airways. The majority of hospitalized cases of acute bronchiolitis are the result of infection by respiratory syncytial virus (RSV) (1). RSV-bronchiolitis is a serious condition among infants (1) as well as immunocompromised adults and the elderly (2). For infants, acute bronchiolitis is the most common single cause of hospital admission throughout the developed world (3). In the United States, RSV-bronchiolitis hospitalization rates among children less than 1 year of age were 31.2 per 1000 in 1996 (4) resulting in an annual estimated rate of 91,000 hospital admissions and 4500 deaths (5). In addition, the annual bronchiolitis hospitalization rates have increased more than 2-fold in recent years (4). Based on the numbers reported by Shay *et al.* (4) this translates to an estimated cost of approximately US\$585 million per annum (6). In British Columbia, the reported hospitalization rate for bronchiolitis is similar to that of the US for the same period (7) although no estimated cost has been reported. A significant percentage of previously healthy children have been reported to develop chronic pulmonary function abnormalities after RSV infection (8). There is compelling evidence, both epidemiologic and clinical, that RSV-bronchiolitis in infancy is associated with reactive airway disease that may persist for several years (9). Thus, from the public health as well as economic perspectives, continuing efforts to understand and attenuate the severity of RSV infection among young children is warranted.

ORGANIZATION OF THESIS

The focus of this thesis is a guinea pig model of *in vitro* RSV infection in alveolar macrophages (AM), cells that are believed to harbor the virus for long periods. Chapters 2 and 3 provide background information on RSV and AM which are also focal points of this thesis. The general features of the Materials and Methods are described in Chapter 4. Chapters 5 through 7 describe investigations of the effects of cell maturation, age and sex of the host on *in vitro* RSV infection in guinea pig AM. Chapter 8 examines the interactive effects of RSV infection and air pollution (using PM10) on guinea pig AM functions. As presented in Chapter 9, the last study examines the expression of protein kinases involved in RSV-mediated signal transduction in guinea pig AM. The Concluding Remarks section of this thesis provides a summary of the major findings and some suggestions for future directions.

CHAPTER 2

RESPIRATORY SYNCYTIAL VIRUS

HISTORY & CLASSIFICATION

Respiratory syncytial virus (RSV) was first isolated as an agent responsible for causing colds in chimpanzees by Morris and coworkers in 1956 (10). Subsequently, Chanock *et al.* obtained two isolates (Long strain and Snyder strain) from children with lower respiratory tract infections and these isolates were indistinguishable from the chimpanzee coryza agent. This virus was renamed RSV because of the cell fusion that is characteristic of its cytopathic effect in continuous cultured cell lines (11, 12).

RSV belongs to the *Paramyxoviridae* family that consists of 2 subfamilies, *Paramyxovirinae* and *Pneumovirinae* (13). The subfamily *Paramyxovirinae* is made up of the genus *Paramyxovirus* (e.g., human parainfluenza virus types 1 & 3), *Rubulavirus* (e.g., mumps, human parainfluenza virus types 2 & 4) and *Mobillivirus* (e.g., measles virus). RSV belongs to the fourth genus *Pneumovirus* of the *Pneumovirinae* subfamily. Other members of pneumoviruses include bovine-, ovine- and caprine-RSV and pneumonia virus of mice. Distinctive features of RSV include the number and order of genes and the lack of hemagglutinin and neuraminidase activity (13). There are two major antigenic strains of RSV, subgroup A and B, with subtypes within each group. The most extensive antigenic and nucleotide sequence differences between the two groups are found on the G glycoprotein (14). Both RSV A and RSV B can circulate simultaneously during a seasonal outbreak. Initially it was thought that group A RSV infections may cause more severe disease (15); however, two recent larger studies have failed to show such a difference (16, 17).

CHARACTERISTICS

RSV is an enveloped virus and ranges in diameter from 150 – 300 nm. The viral envelope is a lipid bilayer derived from the plasma membrane of the host cell. Electron microscopy of ultrathin sections of infected tissue reveals RSV as a pleomorphic, round or filamentous particles with spikes of transmembrane surface glycoproteins (F, G, SH) embedded in the envelope (18). Two non-glycosylated matrix proteins (M and M2) line the inside of the viral envelope. The nucleocapsid, which comprises the RNA genome bound continuously to the nucleoprotein (N) with clumps of small phosphoproteins (P) and large nucleoproteins (L), is located within and is protected by the viral envelope.

The RSV genome constitutes a single-stranded RNA molecule of negative polarity and contains 15,222 nucleotides (19). The genome transcribes 10 subgenomic monocistronic mRNAs coding for 8 structural and 2 non-structural proteins. RSV infection is initiated by attachment of the virion to a susceptible cell by the G protein, a surface glycoprotein. The cell receptor for RSV is still not known. Recent studies have led to the speculation that the RSV G protein, whose conserved region has sequence and structural homology to the TNF receptor, may be involved in antiviral and apoptotic effects of TNF (20). Following viral attachment, cellular proteolytic enzymes cleave the F glycoprotein into its subunits (F1 and F2) (13). Recent studies of x-ray crystallography on human RSV F protein revealed hairpin structures thought to be responsible for bringing viral and cellular membranes into close juxtaposition and facilitating membrane fusion and subsequent viral entry (21). These 2 surface glycoproteins, F and G, are the only RSV proteins capable of inducing protective neutralizing antibodies in the host (13). In addition, the F protein promotes viral spread by infecting adjacent uninfected cells resulting in the formation of giant cells or syncytia. RSV replicates solely in the cytoplasm with no requirements for host cell nuclear functions (22). The virion polymerase (P and L) transcribes the negative-strand RNA genome to produce viral proteins. The negative-strand RNA also

serves as a template for synthesis of the positive-strand RNA. The virion complementary RNA is then copied into progeny negative-strand RNA. The virion is assembled with progeny negative-strand RNA and structural proteins and then released by budding from the host cell membrane (13).

RSV INFECTION IN HUMANS

RSV is a major pathogen responsible for severe respiratory tract infections not only in the young but also in the elderly and immunocompromised adults (2). RSV is the only known virus that causes severe disease at a time when specific maternal antibodies are still present in the serum (23). The peak incidence for infants infected with RSV is between 6 weeks and 6 months but particularly those under 3 months of age (24). Nearly all children become infected with RSV by their second year of life but not all of them acquire severe infantile lower respiratory tract disease. As there is no long-term or complete immunity induced by natural infection, RSV reinfections are common throughout life; however subsequent infections are progressively less severe (25). The incubation period with RSV is on average 2 to 8 days, after which RSV replicates in the nasopharyngeal epithelium. In most normal healthy children, RSV infection is contained within the upper respiratory tract resulting in a cold-like clinical symptom. However, in a percentage of these infants, RSV spreads to the lower respiratory tract and these infants may be acutely ill with cyanosis and respiratory distress and eventually develop bronchiolitis and/or pneumonia (26). For unexplained reasons, the risk for hospitalization in infants infected with RSV has risen from 1% in 1988 to 3% in 1999 (4, 27). It is estimated that 50% to 90% of children hospitalized with bronchiolitis and 5% to 40% of children hospitalized with pneumonia are associated with RSV infection (26).

Epidemiology

Distinct seasonal epidemics of RSV infections, as characterized by increase in hospital admissions of pediatric bronchiolitis, have been documented. In temperate countries, the peak period of RSV activity is generally mid winter; in tropical areas, RSV outbreaks are usually during the rainy season (13).

Among the host factors that have been reported to influence RSV infection are genetic predisposition (28, 29), age (see Chapter 6), sex (see Chapter 7) and socioeconomic status (30). Immunocompromised and institutionalized adults, especially the elderly, are at high risk of severe RSV infection (2). In children, male infants are approximately 1.4 to 1.9 times as likely to be hospitalized for RSV-associated bronchiolitis as female infants (31-33). In middle-income populations, approximately 1 in every 1000 patients with RSV required hospitalization; in contrast, this rate is five-fold to ten-fold higher in lower-income populations (34).

Pathology

RSV is a cytopathic virus that infects adjacent cells in the airway epithelium by formation of multinucleated giant cells or syncytia. The pathological observation seen in bronchiolitis is considered to be a consequence of some combination of direct cytopathic effects induced by viral replication and the resulting host inflammatory response, the relative importance of each being unclear (35). The histological picture of bronchiolitis includes necrosis and sloughing of respiratory epithelial cells. The peribronchiolar spaces are infiltrated with inflammatory cells including lymphocytes, plasma cells, granulocytes (neutrophils, eosinophils) and macrophages. The submucosal and adventitial tissues become edematous and result in excessive mucus secretion. These processes cause obstruction of the small bronchioles, with either collapse or emphysema of the distal airways (36).

Pathogenesis

A number of theories, based on immunologic and non-immunologic factors, have been postulated for the pathogenesis of RSV-bronchiolitis (37). The severity of RSV infection in children with high levels of circulating but non-specific antibodies induced by formalin-inactivated RSV (FI-RSV) vaccine has suggested that immunologic mechanisms may contribute to RSV diseases (38). Almost all components of the immune system have been implicated in the pathogenesis of RSV infection (39). Concerning non-immunologic factors, anatomical and functional differences in the lungs of young children (40, 41) as well as the role of pulmonary surfactant (42) have been implicated in the pathogenesis of RSV-bronchiolitis (see section on Non-immunologic Factors).

Humoral Immunity

The role of RSV-specific antibodies in the pathogenesis of RSV-bronchiolitis is controversial. RSV-specific IgE antibodies were detected in secretions of infants with bronchiolitis and are associated with disease severity and subsequent recurrent wheezing (43-45). Welliver *et al.*, who correlated high levels of IgE in bronchiolitic patients with a decrease in circulating CD8+ cells, postulated that the IgE response might initiate a cascade of mediators that induce inflammation in the lungs of RSV-infected infants (46). Subsequently, increased levels of leukotriene C4 (LTC4) and eosinophil cationic protein (ECP), both mediators involved in airway bronchospasm and inflammation, were detected in the lungs of RSV-bronchiolitic children (47, 48). However, since most children produce IgE to RSV early in life, it has been suggested that it is the level of IgE and the duration of response, rather than the production *per se*, that is the important determinant in development of RSV associated lower respiratory tract infection (49).

On the other hand, several studies have also shown the potential benefits and protective effects of RSV-specific antibodies. Although maternal antibody does not provide complete

protection during infancy, several studies have demonstrated that high levels of maternal antibodies (e.g., RSV-specific IgG, IgA and IgM) correlated with lower infection rates and decreased severity in children with RSV-bronchiolitis, suggesting a protective role for these antibodies (30, 34). Studies have indicated that RSV-specific antibodies (IgA in the nasopharynx and serum IgG in the lower respiratory tract) are boosted with each subsequent reinfection (24). Moreover, the lower frequency of RSV-bronchiolitis among children with high titers of RSV-neutralizing antibodies (>1:100) provides further support for a protective role in these antibodies (50). In addition, trials of hyperimmune RSV globulin in high-risk infants have been considered successful in the prevention of RSV-induced lower respiratory tract infections (51, 52).

Cellular Immunity

Due to obvious ethical reasons, there are limited data about the role of cellular immunity in RSV disease in humans. Evidence supporting a role of cell-mediated immunity in the pathogenesis of RSV bronchiolitis emerged from the unfortunate experience of the unsuccessful FI-RSV vaccine, and the study of RSV disease in immunocompromised individuals. Infants given the FI-RSV vaccine were not protected against subsequent natural RSV infection and many of them manifested unusually severe illness with high rates of hospitalization and mortality (53). Follow-up laboratory findings by Chin *et al.* (54) revealed lung infiltrates of neutrophils and eosinophils as well as blood eosinophilia, both of which were not associated with primary RSV infection and suggested an enhanced cell-mediated inflammatory (Th2 type) response (25). This hypothesis was supported by subsequent studies demonstrating a Th2 type response in FI-RSV vaccinated mice and a Th1 type response in mice when challenged with wildtype RSV (55).

However, alternative evidence suggests that cell-mediated immunity may play a central role in the clearance of established RSV infection. For example, cancer or bone marrow transplantation patients undergoing immunosuppressive chemotherapy have more severe RSV

infection and prolonged virus shedding (56-58). In addition, detection of RSV-specific cytotoxic T lymphocytes (CTL) in the peripheral blood of infected adults has been associated with decreased clinical symptoms (59, 60).

Non-immunologic Factors

Besides immunologic mechanisms, the anatomy of the lungs has been considered to play a role in severe RSV infection in infancy. By virtue of the relatively lower maximal expiratory flows at functional residual capacity, infants with smaller and narrower airways may be more prone to develop wheeze at the time of RSV bronchiolitis (40, 61). In addition, evidence from *in vitro* studies indicated that plasma proteins leaking into the airways as a result of inflammatory process may degrade and/or inhibit the function of pulmonary surfactant, which in turn could cause blockage of conducting airways and contribute to increased airway resistance (62, 63). Support for this possibility came from the work by Dargaville *et al.* (42) who demonstrated a deficiency of surfactant protein A with impaired functional activity in lavage fluids of infants with RSV bronchiolitis. Furthermore, administration of exogenous surfactant has been reported to alleviate disease symptoms in animal studies (37, 64) as well as in clinical studies (65, 66).

Important Issues

At this point, I would like to draw attention to some issues in relation to RSV infections in humans. First, as discussed earlier, RSV infection during infancy can induce either a Th1 type or Th2 type immune response depending on host and viral factors (67). However, classifying the immune response of RSV bronchiolitis in humans should be carried out with reservations. One should bear in mind that the dichotomy for activated T cells was originally described in the mouse (68)¹ and the distinction between the 2 subsets of cells is not as definitive in humans.

Secondly, the prevalence of asthma and atopy has been and is still on the increase over the past 3 decades (70, 71). This increase prevalence of respiratory allergies may be due to the interaction of independent factors (e.g., environmental and lifestyle) resulting in altered allergy-related immune responses (71). The Hygiene Hypothesis (72) may be a plausible explanation for the current unfavorable trend in asthma and atopy. The impact of the interaction between RSV and environmental particulates on AM function (see Chapter 8) may provide insights on this issue.

¹ CD4+ T helper lymphocytes (Th0) play a major role in the modulation of immune responses. These Th0 cells differentiate into 2 subclasses: Th1 and Th2. Th1 responses are usually observed in infectious diseases involving intracellular pathogens (e.g., bacteria and viruses) and delayed-typed hypersensitivity while Th2 responses deal with parasitic infections. Th2 responses are also associated with allergy-related diseases such as asthma. These subclasses of cells are distinguished by their different cytokine profiles: Th1 cells produce IL-2 and IFN γ , both of which mediate help for the generation of cytotoxic T cells. Th2 cells secrete IL-4, IL-5, IL-10 and IL-13, cytokines which induce B cells to produce specific immunoglobulins (69).

ANIMAL MODELS OF RSV INFECTION

Although it is not clear that the immune response demonstrated in animals can be directly extrapolated to human infection, animal studies have contributed much to the understanding of immunopathogenic mechanisms in RSV disease. These *in vivo* systems have facilitated the testing of many hypotheses that would have been otherwise deemed unethical or impractical if experiments were attempted in humans. Since the isolation of RSV, numerous animal models of RSV infection have been developed using primates, cotton rats, mice, calves, sheep, guinea pigs, rats, ferrets and hamsters (73-75).

As in humans, the manifestation of RSV disease in different animal models varies with age, genetic makeup and immunologic status (73). In experiments using primates, only the chimpanzee appears to be highly permissive to RSV replication even though other primate species could be infected by intranasal instillation of RSV (13). Among the animal species used as models of lower respiratory tract infection with RSV, one popular animal model is the Balb/c mouse. While RSV infection produces asymptomatic bronchiolitis, this model has been useful in the study of cell-mediated immunity in RSV infections (76). This model system provided the evidence that the cell-mediated enhancement of RSV disease seen in humans was due to an imbalance of Th1 and Th2 lymphocyte response to the FI-RSV vaccine. In the murine model, RSV induces a Th1 type CD4+ response characterized by production of Th1 cytokines (IFN γ , IL-2, IL-12) and cytotoxic T cells (55, 59, 77). In contrast, immunization with inactivated virus or G subunit viral proteins induces a Th2 CD4+ response with the corresponding cytokines (IL-4 and IL-5) and no CTL (55). In addition, studies with mice also indicated that RSV-specific CD8+ lymphocytes can clear virus from persistently infected, immunodeficient mice, but acute pulmonary damage occurs and may be associated with fatality (67, 78). Thus, both CD4+ and CD8+ lymphocytes are involved in both recovery and the pathologic response even though CD4+ cells have been demonstrated to be more antiviral (i.e., 4-fold less in cell number to

decrease lung virus titer and produce similar effects) and more immunopathogenic than CD8+ cells in RSV infected mice (79).

The guinea pig model for RSV infection is the basis of RSV research in our laboratory and in this thesis. Besides the extensive knowledge of airway physiology in this species, Hegele *et al.* (80, 81) were the first to successfully induce acute and persistent RSV infection and demonstrated RSV genome as well as viral antigens in airway epithelial cells and AM from RSV-infected guinea pigs. Riedel and coworkers (82) demonstrated hyperresponsiveness to histamine challenge and viral persistence in RSV-infected guinea pigs even after resolution of virus-induced inflammation in the lung. Moreover, Dakhama *et al.* (83) demonstrated that RSV could infect and replicate in guinea pig AM in cell culture medium.

RSV INFECTION *IN VITRO*

In vitro experiments permit the isolation and manipulation of a microenvironment in a controlled and systematic manner. In most diagnostic virology laboratories, RSV infection is determined by rapid antigen detection test kits (for example, enzyme immunoabsorbent assay (EIA) kits, and immunofluorescent techniques). However, the detection of infectious virus by cell culture remains the gold standard. This technique is used throughout this thesis for detection of replicating RSV as well as quantification of viral titers. RSV-sensitive, transformed human epithelial cells, HEp-2 cells were used for RSV detection because of their characteristic cytopathic effect of syncytia formation as a result of the fusion of cell membranes between infected and uninfected adjacent cells.

Epithelial Cells

Since the airway epithelial cell is the primary target for RSV infection, it is speculated that these cells and the soluble factors (cytokines and mediators) derived from them are

responsible for initiation of airway immune responses and inflammatory processes (84, 85). In epithelial cells, viral replication causes upregulation of multiple cytokines, chemokines and adhesion molecules by triggering intracellular signaling pathways (86-88). *In vitro* infection in epithelial cells with RSV activates transcription factors such as activator protein-1 (AP-1), nuclear factor-kappa B (NF- κ B), NF-IL6 and CCAAT-enhancer binding proteins (c/EBP) (89, 90). A major cytokine induced by RSV infection is interleukin-8 (IL-8) (91, 92). IL-8 is a potent chemotactic agent for neutrophils (93). Clinical studies have demonstrated that lavage fluid from RSV-infected infants contains a predominance of neutrophils (94). Another cytokine that is worthy of mention is interleukin-6 (IL-6). IL-6 is detected in respiratory secretions during RSV infection *in vivo* (95) as well as in RSV infected epithelial cell cultures *in vitro* (95-98). During RSV infection IL-6 may play an immunoregulatory role by promoting humoral and cellular defense mechanisms (99). IL-6 plays a major role involved in isotype switch, differentiation and synthesis of IgA (100). On the other hand, IL-6 may play a proinflammatory role by contributing to the symptoms and signs of acute infections (99). Therefore it appears that RSV may cause inflammation in part through the production of these proinflammatory cytokines from epithelial cells in the lung.

In addition to the accumulation of neutrophils, eosinophils have been demonstrated in the inflammatory infiltrates from autopsied lungs of children infected with RSV (53). Studies by Becker *et al.* (101) demonstrated that RSV infection of human airway epithelial cells caused the production of an important eosinophil chemoattractant, RANTES (Regulated upon activation, normal T cells expressed and presumably secreted). Garofalo *et al.* (47) demonstrated the increased levels of ECP in lavage fluid sampled from RSV-infected infants. Moreover, subsequent studies have indicated that degranulation of the accumulated eosinophils and the release of ECP may be mediated via upregulation of CD18 molecules on the RSV infected epithelial cells (102).

Other cytokines that have been implicated in the promotion of the inflammatory response induced by RSV infection include interferon- β (IFN β), interleukin-1 α (IL-1 α), macrophage inflammatory protein-1 α (MIP-1 α) and monocyte chemotactic protein (MCP) (92, 102, 103). Enhanced expression of IFN β and IL-1 α causes upregulation of the major histocompatible complex (MHC) class I molecules on the surface of the epithelium, which in turn results in activation of CD8+ T cells and increases local inflammation (103, 104). MIP-1 α and MCP are known chemotactic and activator factors for monocytes, basophils and eosinophils. In addition, MIP-1 α has been shown to stimulate the production of IgE and IgG4 by human B cells (105) and to induce degranulation of natural killer cells (106), thereby contributing to the augmentation of local inflammation.

Alveolar Macrophages

Besides epithelial cells, AM (107, 108), eosinophils (109), T cells and neutrophils (110) are also cell targets for RSV infection. AM are the first line of defense against inhaled pathogens (biologic and non-biologic) and are in direct encounter with the virus during RSV infection. In addition, AM are the pivotal cell type that link the external environment to within the lung. For these reasons, AM are very important and are the cell type of focus in this thesis work. Panuska *et al.* examined bronchoalveolar lavage cells from adult transplant patients with RSV infection and found both AM and epithelial cells were infected with RSV *in vivo* (107). Studies investigating susceptibility of blood monocytes, AM and cord blood to RSV infection indicated a role for intrinsic cellular factors in the restriction of viral infection (83, 108). Panuska *et al.* (111) demonstrated that human AM are able to support prolonged RSV replication *in vitro*. Although AM are susceptible to RSV infection, in comparison to epithelial cells, the infection is usually abortive after the initial cycles of viral replication (112, 113). In addition, RSV does not

induce cytopathic effects in AM and only a fraction or subpopulation of AM was susceptible to RSV regardless of the dose of infectious virus used. This observation has also been reported in mice (114), cattle (115) as well as in guinea pig (83).

The effects of *in vitro* RSV infection on AM have been studied (83, 111, 114). Exposure of AM to RSV has been reported to stimulate the immunoregulatory functions and depress the microbicidal activity of these cells (114). With regards to cytokine expression, as demonstrated in epithelial cells, RSV induced upregulation of IL-1 (114), IL-6 (114, 116, 117) and IL-8 (116, 117) in AM. Of particular interest is tumor necrosis factor- α (TNF α), a marker of macrophage activation. TNF α is induced in RSV-infected AM but not expressed in epithelial cells infected by RSV (91, 114, 116, 117). TNF α is synthesized and secreted in large quantities by macrophages in response to various proinflammatory stimuli (e.g., lipopolysaccharide). More importantly, TNF α is mediated by NF- κ B activation and induces macrophage synthesis of several key proinflammatory cytokines (e.g., IL-1, IL-6, GM-CSF), chemokines (e.g., RANTES, IL-8, MCP-1 and MIP-1 α) as well as inflammatory mediators (e.g., leukotrienes, reactive oxygen species). The combined effects of these mediators on cell recruitment and cell activation are likely to play a fundamental role in the pathogenesis of RSV disease. In contrast to epithelial cells, there is limited published literature on how RSV modulates these mediators via intracellular signaling pathways in AM (see Chapter 9).

SUMMARY

This year, 2002, marks the 46th anniversary since the discovery of RSV. While the impact of RSV from public health and economic perspectives is appreciable, there are numerous issues that remain controversial. These include the pathogenic/ protective role of RSV against development of allergies in later life, the role of RSV in reactive airway disease, and whether

RSV infection induces a Th1 or Th2 response in humans. Epidemiological studies suggest that the influence of viral infection on the developing immune system depends on the type of viral infection, the age, sex, and genetic background of the host and environmental factors. The purpose of this thesis is to examine the relationship between RSV infection and anti-viral immune response by evaluating some of these factors in a controlled environment in order to better understand the nature of RSV disease.

CHAPTER 3

ALVEOLAR MACROPHAGES

INTRODUCTION

The alveolar macrophages (AM) play major roles in the lungs defense against bacterial infections (e.g., *Mycobacterium*, *Pseudomonas*), parasitic infections (e.g., *Leishmania*), viral infections (e.g., HIV, RSV), chronic inflammation (e.g. particulates, silicosis, asbestosis) and in response to cigarette smoke and air pollutants (118). As “gatekeepers”, AM are responsible for clearance of microorganisms and small inhaled particulate material in the alveolar space. The aim of this chapter is to provide a basic review of AM biology in general and highlight issues that are relevant to RSV infection in AM.

ORIGIN OF MACROPHAGES

Macrophages originate from a pluripotent stem cell (colony-forming unit granulocyte-macrophage (CFU-GM)) in the bone marrow (119, 120). In response to growth factors, such as interleukin-3 (IL-3), granulocyte-macrophage colony stimulating factor (GM-CSF) and macrophage colony stimulating factor (M-CSF), the pluripotent stem cells from the bone marrow develop into myeloid stem cells that eventually become promonocytes (121, 122). As the promonocytes mature, they leave the bone marrow and enter the blood stream to become blood monocytes. Monocytes circulate in the blood stream for 1 – 2 days and continue to mature within the blood stream. Monocytes are randomly distributed and recruited into different organs, i.e. Kupffer cells in the liver, Langerhan cells in the skin, osteoclast cells in bone, microglial cells in the central nervous system, peritoneal macrophages in the intestine and pulmonary macrophages in the lung. In lung capillaries, blood monocytes traverse the blood vessel wall by a process known as diapedesis and mature into pulmonary macrophages (123). Recruitment

from the bone marrow is the dominant mechanism for renewal of the pulmonary macrophage population. This recruitment process is mediated by monocyte-specific chemoattractants including MIP-1, MIP-2 and monocyte chemoattractant protein-1 (MCP-1) (124, 125). In addition, a very low percentage (0.5%) of AM proliferates locally and contributes to the alveolar pool of cells (126). *In vitro* experiments have demonstrated that human AM are capable of proliferation in response to GM-CSF (127).

HETEROGENEITY OF MACROPHAGES

Macrophages are tissue-specific and in different tissues they are morphologically and functionally distinct depending on the microenvironment in which they mature. However, the basic functions of macrophages remain similar despite their ability to excel in specific functions at various body sites. For example, AM are excellent at phagocytosis and secretion of nitric oxide (NO) but are somewhat deficient at antigen presentation. In contrast, macrophages in the spleen and lymph nodes are excellent at antigen presentation. Macrophage heterogeneity is therefore a reflection of the local microenvironment of the cell and its involvement in various physiological or pathological processes (118).

Pulmonary macrophages are the only macrophages living in an aerobic environment and are categorized into 4 different types based on their localization: intravascular macrophage, dendritic cell, interstitial macrophage and AM (128). Intravascular macrophages are located on the endothelial cells of the pulmonary capillaries (129). These cells are highly phagocytic and are responsible for clearance of pathogens entering the lung via the blood stream (130). Apparently, these cells have been described in humans, pigs, cats, dogs and sheep but not in rodents (131). Dendritic cells, located in the lung interstitial tissue, are poor phagocytes (132, 133). High amounts of Class II antigen expression on the surface of dendritic cells make them suited for antigen presentation and accessory function (128). Interstitial macrophages are located

in the lung connective tissue. Like AM, interstitial macrophages are effective phagocytes, function as antigen presenting cells as well as produce cytokines (e.g., TNF α , IFN α/β) and oxygen radicals (131). Unlike AM, they have an increased ability to replicate and synthesize DNA *in vitro* (134, 135) and are much more effective in stimulating T-cell responses to antigens (136). Morphometric comparisons of AM, interstitial macrophages and blood monocytes indicated that interstitial macrophages represent a transitional stage of maturation between blood monocytes and AM (137). AM are localized on the alveolar epithelial surface within a film of surfactant. As a first line of defense, AM possess high phagocytic and microbicidal potential. In addition, AM are also involved in inflammatory activities and regulation of lung homeostasis (see below) (136). Since AM can be easily obtained by bronchoalveolar lavage (>95% purity), in comparison to other types of pulmonary macrophages, these cells have been most extensively studied (138).

AM that are newly recruited into the alveolar space continue to undergo maturation (136). AM represent a morphologically and functionally heterogeneous population. As AM mature, they increase in size; ranging from 12 μm (generally the newly recruited cells) to 40 μm (the older and sometimes multinucleated AM) in diameter (139). Taking advantage of these size and density differences, several investigators (140-142) have fractionated AM into different subpopulations using density gradient centrifugation and characterized these subpopulations and studied their heterogeneity based on receptor expression, release of mediators such as oxygen radicals and tissue factor, cytotoxicity, migration and pinocytosis (140, 143, 144). Likewise, the methodology of isolating AM into subpopulations has been applied in 3 studies (Chapters 5, 6 and 7) in this thesis work. In addition, Sibille *et al.* (131) have established that the response of each subpopulation of AM to different stimuli (including response to RSV – see Chapters 5 and 6) may be markedly heterogeneous. In humans, the distribution of AM subpopulations is known to vary with different disease states. For example, the predominance of small monocyte-like AM

has been observed in acute inflammation whereas an increase in larger and more mature AM is associated with chronic lung disorders (145).

MORPHOLOGY OF AM

Light Microscopy

AM are large irregular shaped cells with prominent ruffled membranes ranging from 12-40 μm in diameter. The kidney-shaped nucleus, usually eccentrically placed within the cell, contains fine nuclear chromatin with one or two prominent nucleoli. Newly recruited AM have a relatively smaller cytoplasm-to-nucleus ratio while mature AM have a larger ratio due to an abundant cytoplasm with an increased number of cytoplasmic inclusions (146). Besides cytoplasmic vacuoles, fine granules and multiple large azurophilic granules are seen in the cytoplasm (147).

Electron Microscopy

Electron microscopy shows the multi-lobulated nucleus with fine clumps of chromatin. The cytoplasm contains well-developed Golgi complex, numerous vesicles, vacuoles and pinocytic vesicles, large mitochondria and lysosomes. Membrane bound, electron dense vesicles filled with ingested biological or inert particulate material are also visible. The ruffled cell membrane of the AM exhibits irregular microvilli or pseudopods that are involved in amoeboid movement and phagocytosis (147).

FUNCTIONS OF AM

AM perform their function as “gatekeepers” mainly through phagocytosis (when the alveolar space is invaded by inhaled pathogens), recruitment of inflammatory cells (in response to tissue and vascular changes), and regulation of lung homeostasis. These functions are carried

out and assisted by the wide range of surface receptors and large spectrum of secretory products within membrane bound organelles within the AM.

Phagocytosis

As the resident phagocyte of the alveolar space, AM play major role in defending the host against invasion by a wide variety of small particles (0.5 μm to 3.0 μm diameter) that are inhaled into the distal airways (148). These inhaled substances may be of biological (for example, bacteria, viruses, fungi and protozoa) as well as non-biological (for example, asbestos, particulate material) nature (128). Since AM are among the first cells encountering the virus in the event of a RSV infection, these cells play a major role as a first line of defense. However, and more importantly, AM trigger the immune response cascade through activation of granulocytes (see section on Inflammatory Activity). In addition to invading pathogens, AM also play an important part in scavenging apoptotic, senescent and damaged cells. Through phagocytosis and the production of oxygen radicals and proteases, most of the microorganisms and particulates are eliminated by the AM (128).

Phagocytosis is a special form of endocytosis; unlike pinocytosis, a constitutive process that occurs continuously, phagocytosis is a receptor-mediated process that requires the transmission of extracellular signals to the interior of the cell to initiate the response (149). The main features of phagocytosis are attachment, engulfment, phagosome formation and maturation, digestion and membrane retrieval (118). AM move toward inhaled particles guided by a gradient of chemotactic molecules. Particle attachment and engulfment may be facilitated by the presence of specific receptors on the surface of the cell and opsonins that coat the inhaled particles. Several classes of receptors that promote phagocytosis have been characterized (see Table 3.1).

Table 3.1 Ligands recognized by AM via receptors
 (Extracted from Lohman-Matthes ML *et al.* (128), with permission)

| Immunoglobulins | Complement |
|---|--|
| IgG1, IgG2a (murine) | C3b, iC3b, C4b, C3d, C5a |
| IgG2b, IgG3 (murine) | |
| IgG1, IgG3 monomers (human) | Lipoproteins |
| IgG complexes (human) | Low density lipoproteins |
| IgE, IgA (murine and human) | β -very low density lipoproteins |
| Proteins | Lectins with specificity for |
| Fibronectin, fibrin | α -linked galactose residues |
| Lactoferrin, transferrin | N-acetylgalactosamine residues |
| GM-CSF, CSF-1 | N-acetylglucosamine residues |
| Interferon- γ , IL-4, IL-1Ra | α -linked fucose residues |
| IL-2, insulin | Mannose residues |
| | N-acetylneuramine residues |
| Surface markers | |
| Class II molecules, CD11a, CD11b, CD11c, CD14, CD18, CD54 | |
| Molecules recognized by monoclonal antibodies: | |
| 25F9 (mature macrophages), 27E10 (inflammatory macrophages), Ki M2, Ki M8 (mature macrophages), RM31 (inflammatory macrophages), RFD1, RFD7, RFD9 | |

Ig: immunoglobulin; GM-CSF: granulocyte-macrophage colony stimulating factor;
 IL: interleukin

Three major groups of receptors that play important roles in the attachment stage of phagocytosis are: the Fc receptors (which recognize the Fc region of antibodies coating inhaled pathogens), the complement receptors (which recognize the cleaved products of the third component of the complement C3) and lectin-binding receptors (which recognize lectins on microorganisms) (128). However, the specific AM receptor(s) that recognize RSV is yet to be determined, although the toll-like receptors are thought to be involved (150). Opsonization is an essential mechanism that enhances the initial stages of phagocytosis. Opsonins were initially discovered as factors that “butter” the particles to make them “appetizing” to phagocytes (151). Opsonins are soluble components in the alveolar space that facilitate phagocytosis by increasing the recognition and endocytosis of different pathogens by the AM through their binding to a specific receptor on the cell surface (131). Examples of opsonins include surfactant phospholipids, glycoproteins (e.g., fibronectin), proteins (e.g., IgG, IgA) and complement fragments (C3b)

(131). For example, antibodies may coat inhaled pathogens so that the Fc regions are exposed on the exterior. When the Fc portions of antibodies attach to the Fc receptors on the surface of AM, intracellular signals are triggered. These signals initiate the reorganization of cytoskeletal microfilaments at the site of attachment and result in the extension and fusion of the AM pseudopods and consequently engulfment of the inhaled particle (149). A number of hypotheses have been proposed for the mechanisms involved in the engulfment stage of phagocytosis. In Fc- and complement receptor-mediated uptake of inhaled particles, a “zipper” mechanism guided macrophage pseudopods to circumferentially envelop the attached particle (152). The bacterium *Legionella pneumophila* enters the macrophage via an alternative coiling mechanism in which the microbial outer wall components induce the cell membrane to wrap around the organism in myelin-like configurations (153). Alternatively, engulfment could also occur independent of opsonins; for example, certain bacteria possess surface determinants or carbohydrate residues that interact with the mannose-fucose receptor on the surface of the AM (154).

Engulfed particles are contained in large membrane-bound endocytic vesicles called phagosomes within the cytoplasm. The diameters of the phagosomes are determined by the size of the ingested particle and could be as large as the AM itself (149). At this stage, recycling of membrane and receptors takes place via sorting endosomes which are acidic vesicles that dissociate receptors from ligands and are responsible for shuttling of cell membrane and receptors back to the cell surface (155). The phagosomes containing the ingested particles fuse with primary lysosomes and mature into secondary lysosomes or phagolysosomes (156).

The primary lysosomes contain lysosomal enzymes, which comprise more than 40 different acid hydrolases and are optimally active at a pH of about 5, that are involved in the degradation of phagocytosed material (131). In addition, AM possess granules containing oxygen metabolites (such as superoxide anion (O_2^-), hydrogen peroxide (H_2O_2) and hydroxyl radical (OH^-)) and other enzymes that can be released into the phagosomes or the external

environment during phagocytosis to destroy ingested materials (see Table 3.2) (157). AM are equipped with various ways to degrade and eliminate ingested matter. Degradation of ingested matter in the AM depends on the nature of the ingested substance and/or the opsonins that are involved. For example, Fc-mediated phagocytosis results in the release of oxygen radicals and arachidonic acid metabolites (158, 159). In contrast, complement receptor-mediated phagocytosis does not involve oxygen or arachidonic metabolites but induces secretion of IL-1 (160).

Table 3.2 Major products released by AM
(Extracted and modified from Sibille Y *et al.* (131), with permission)

| Proteins | Enzymes |
|--|---|
| Antiproteases (e.g. α 1-proteinase inhibitor) | Lysozyme, β -glucuronidase |
| Other inhibitors (e.g. IL-1 inhibitor) | Acid hydrolase |
| Glycoprotein (e.g. fibronectin) | Angiotensin converting enzyme |
| Complement components (e.g. C2, C4) | Elastase: serine and metalloenzyme |
| Binding protein (e.g. transferrin, ferritin) | Collagenase (fibroblast-like, gelatinase) |
| Free fatty acids | Plasminogen activator |
| Antioxidants (e.g. Glutathione) | Cysteine proteinase (cathepsin L) |
| Coagulation factors (e.g. Factors V, VII) | |
| Cytokines | Biologically active lipids |
| Interleukin-1 α , Interleukin-1 β | Thromboxane A2 |
| Interleukin-6 | Prostaglandins |
| Tumor necrosis factor | 5-hydroxyeicosatetraenoic acid |
| Interferon- α , Interferon- γ | Leukotrienes |
| Colony stimulating growth factors | Platelet activating factor |
| Transformation growth factor- β | |
| Fibroblast growth factor, insulin growth factor-1 | |
| Neutrophil-activating factor | |
| Enzyme-releasing peptide | |
| Neutrophil chemotactic factor | |
| Platelet-derived growth factor | |
| Histamine releasing factor | |

Following degradation of the ingested material, AM are removed from the alveoli by a number of routes. Some AM are transported up the airway by the mucociliary escalator while other AM migrate to the regional lymph nodes via peribronchial lymphatics. In addition, pathogen-containing AM can also be scavenged and phagocytosed by other AM (131).

Although AM are well-equipped with a large spectrum of enzymes with microbicidal activities for destruction of many microorganisms, certain pathogens have evolved anti-immune strategies to counteract macrophage defenses in order to survive, parasitize and replicate within these cells. For example, *Mycobacterium tuberculosis* releases sulpholipids that prevent the fusion of lysosomes and phagosomes thereby avoiding exposure to the lysosomal enzymes (161). The Epstein-Barr virus (EBV) synthesizes a homologue of interleukin-10 (IL-10) so that its anti-inflammatory properties are retained; however the ability to stimulate lymphocytes is lost (162). While it has been postulated that RSV induces IL-10 production in AM to prevent complete anti-viral immunity (163); direct evidence is lacking and further investigations are needed to provide insights on the evasion strategies used by this virus to circumvent macrophage defenses. Regardless of the evasion strategy utilized by RSV, this virus is capable of causing productive infection in isolated human AM (111).

Inflammatory Activity

AM play an important role in the recruitment of additional inflammatory cells during the initial phase of lung inflammatory response when the load of inhaled material is overwhelmed and resident AM are insufficient to mount an adequate response (136). In the lung of the normal individual, AM are a major source of chemotactic factors (131). AM release various chemotactic factors to recruit inflammatory cells such as polymorphonuclear leukocytes (PMN), monocytes and lymphocytes. In the event of a RSV infection, AM play major roles in the activation and recruitment of granulocytes with PMN being the first cells recruited to the site of infection (164).

On interaction with pathogens or other stimuli such as complement, AM become stimulated and release chemotactic factors that attract PMN from the capillary lumen into the alveolar space. There are numerous macrophage-derived chemotactic factors for PMN (131); however, a few that are of particular interest include leukotriene B4 (LTB₄) (165), TNF α (166), interleukin-8 (IL-8) (167, 168), and MIP-1 α (169).

Upon stimulation by IgG or IgE immune complexes, AM release several arachidonic acid metabolites including LTB₄. As one of the earliest factors identified, LTB₄ is considered as the predominant PMN chemotactic factor secreted by human AM (165). LTB₄ is a potent proinflammatory mediator and chemoattractant for PMN as well as eosinophils (170, 171). LTB₄ increases pulmonary vessel permeability by inducing plasma leakage and leukocyte adhesion (172). In addition, LTB₄ in combination with other mediators (e.g., PAF and 5-HETE), mediates enzyme degranulation of PMN (173).

During phagocytosis or stimulation by calcium ionophore (174), LPS and other microbial agents, IL-2, GM-CSF and IL-1 stimulate AM to produce TNF α , a potent chemotactic factor for monocytes and PMN (166). TNF α was initially identified for its ability to induce hemorrhagic necrosis of certain tumors (175). Subsequently, TNF α was shown to have cytotoxic effects *in vitro* against various human tumors. TNF α is involved in the induction of IL-1, GM-CSF, IL-6 and intercellular adhesion molecule-1 (ICAM-1) production (176). In addition, TNF α activates PMN, enhances their phagocytic capabilities, and induces secretion of H₂O₂ (177, 178). Moreover, TNF α is responsible for monocyte differentiation and the subsequent release of IL-1 from these cells (179). IL-1 stimulates the release of granule proteins (lysozyme and lactoferrin) in PMN (178). TNF α induces upregulation of IL-6, which in turn induces the proliferation of immature and mature T cells (180). IL-6 also acts on B-lymphocytes as a differentiation factor and induces immunoglobulin secretion (181, 182).

LPS stimulation of AM causes the release of IL-8 (168), a potent chemoattractant for PMN and T cells (183, 184). In addition to recruitment of PMN to sites of infection, IL-8 also regulates PMN activation. IL-8 increases the microbicidal ability of PMN by enhancing phagocytosis, O_2^- generation and granule release (185). Indeed, production of these proinflammatory cytokines (i.e. TNF α , IL-8 and IL-6) has been enhanced during RSV infection (116).

MIP-1 α is produced by AM as well as PMN and epithelial cells during lung inflammation (186). MIP-1 α has been shown to have chemoattractant activity for T cells, eosinophils and basophils (187). MIP-1 α also plays a role in regulation of hematopoiesis through stimulation of other inflammatory mediators (e.g., TNF α , IL-1, IL-6, histamine). Increased MIP-1 α expression has been observed in animal models of bacterial sepsis, silicosis and oxidant-induced lung injury (188-190). In addition, recent studies have demonstrated high levels of MIP-1 α expression in AM from asthmatic individuals (191, 192). Recent studies have demonstrated that *in vitro* RSV infection of AM stimulated the expression of MIP-1 α (193). Moreover, increased expression of MIP-1 α has recently been associated with severe RSV bronchiolitis in infants (194).

Regulation of lung homeostasis

During inflammation, AM may elaborate many proinflammatory factors in concentrations that result in irreversible injury to the lung. In addition, AM may release cytokines and other factors that affect the function of other cells such as epithelial cells and fibroblasts (136). AM play an important role in the maintenance of lung homeostasis by the secretion of various inhibitory factors against inflammatory cells. For example, AM can inhibit PMN activity through the release of prostaglandin E2 (PGE2). *In vitro* studies have shown that

PGE2 can inhibit PMN and monocyte chemotaxis as well as the release of O₂⁻ anions by PMN (195). Furthermore, recent studies by Thomassen *et al.* (196) have demonstrated that AM may regulate lung homeostasis via the release of NO which downregulate AM production of proinflammatory cytokines TNF α and MIP-1 α .

SUMMARY

AM play a pivotal role in the innate immune response in defending the host against invading pathogens. As a first line of defense, AM limit the spread of infection and stimulate the immune response cascade through activation of granulocytes as well as activation of cytotoxic and helper T cells and the production of specific immunoglobulins. Despite the tightly regulated mechanisms against invaders, the RSV has devised strategies to not only evade subsequent immunosurveillance but also to survive within infected AM with productive replication of virus progeny. The study of RSV infection in different AM subpopulations and the viral impact on cytokine production as well as activation of signaling cascades in these cells will further our understanding of AM functions.

CHAPTER 4

GENERAL MATERIALS & METHODS

CELL CULTURE

All cell culture work was carried out in a Biosafety cabinet (Forma Scientific, Marietta, OH) housed in a Level II containment facility. All solutions and equipment that come into contact with cells were steam sterilized or purchased as “sterile” from the manufacturers. Proper aseptic techniques were practiced and used accordingly.

HEp-2 cells

HEp-2 cells, a transformed human cell line isolated from epidermoid carcinoma of the larynx, were purchased from American Type Culture Collection (ATCC) (Manassas, VA). HEp-2 cells were seeded in T75 flasks (Corning; Corning, NY) containing minimum essential medium (MEM) (Life Technologies, Burlington, ON, Canada) supplemented with 10% heat-inactivated fetal bovine serum (FBS; Life Technologies) and 50 µg/mL gentamycin (Life Technologies) and incubated in an incubator (Fisher Scientific, Nepean, ON) at 37°C in an atmosphere of humidified air and 5% CO₂. The cell line was maintained by sub-culturing the confluent monolayers. When cells were confluent the culture medium was removed and the monolayer was rinsed with sterile phosphate buffered saline (PBS, pH 7.4; Sigma). A 1 mL solution of trypsin (0.25%)-EDTA (0.02%), prewarmed at 37°C, was added to the flask. The flask was rocked gently to ensure even distribution of the trypsin solution and incubated at 37°C for 5 minutes. The cells were detached by slapping the flask in a vertical position. The enzymatic action of trypsin was inhibited by the addition of fresh culture medium containing FBS. The sub-cultivation ratio as recommended by the supplier for HEp-2 cells is between 1:4 and 1:10. Freezer stocks of HEp-2 cells were prepared by the above trypsinization procedure followed by a

5-minute centrifugation in PBS at 1000 $\times g$. The cells were re-suspended in a 3 mL solution of culture medium: DMSO (9:1) and stored as 1 mL aliquots in cryovials. Cells were frozen in a “slow-freeze” procedure by standing on ice for a half-hour, kept in the -20°C freezer for 1 hour, then kept in the -70°C freezer overnight and transferred to liquid nitrogen tanks for long term storage the following day.

L929 Fibroblasts

TNF α -sensitive L929 fibroblasts were a gift from Dr. R.R. Schellenberg, McDonald Research Laboratories, St. Paul’s Hospital, Vancouver, BC. L929 cells were cultured in T75 flasks of RPMI medium (Life Technologies) containing 10% FBS, 10 mM Glutamine, 100 units/mL penicillin, 100 μ g/mL streptomycin and 250 ng/mL amphotericin B. The subcultivation ratio as recommended by the original supplier (ATCC) is 1:6. The procedure to maintain the cell line and to store freezer stocks is as described for HEp-2 cells.

VIRUS CULTURE

RSV Propagation

The Long strain, type A of human RSV was purchased from ATCC. RSV stocks were propagated on monolayers of HEp-2 cells in MEM supplemented with 2% FBS and 50 μ g/mL gentamycin. RSV infection of HEp-2 cells induces the cytopathic effect of multiple cells fusing to form a mega-cell or syncytium. RSV was harvested when syncytial formation peaked in the monolayers of HEp-2 cells. A crude RSV stock was prepared by scraping infected cell monolayers with a sterile cell scraper and the cells and supernatant were transferred to 50 mL tubes for short term storage in the -70°C freezer. This crude preparation of RSV was used for regeneration of viral stocks.

Harvest and Concentration of RSV

Concentrated stocks of RSV were prepared by mechanical disruption of the syncytia-filled monolayers of HEp-2 cells using sterile 3 mm glass beads (Fisher Scientific) over a vortex for 30 seconds. The cell suspension was transferred to 50 mL tubes and underwent centrifugation at $1500 \times g$, 4°C for 15 minutes to sediment the cellular debris. The clear supernatant (containing free virus and soluble macromolecules such as inflammatory mediators) was applied on to Centriplus™ concentrators (Amicon, Beverly, MA) with molecular cut-off at 100,000 Daltons to concentrate the virus as well as to remove soluble macromolecules synthesized during viral infection of HEp-2 cells. The clear supernatant was spun in the concentrator unit at $3000 \times g$, 25°C for 75 minutes and the virus-enriched retentate was stored in 1 mL aliquots in the -70°C freezer.

RSV titer determination

HEp-2 cells were seeded in 6-well plates (Corning; Corning, NY) at a density of 5×10^5 cells/well. Overnight culture at this density usually results in cells reaching approximately 80–90% confluence. Ten-fold serial dilutions (10^{-1} to 10^{-7}) of RSV stocks were prepared using MEM. HEp-2 cells were exposed to 1 mL of the serially diluted RSV and viral adsorption was allowed to take place over 90 minutes at 37°C in a 5% CO₂ incubator (Fisher Scientific). The plates were gently agitated intermittently at 15-minute intervals to ensure even distribution of virus over the cells. The wells were washed in PBS and 1 mL of medium-agarose mixture (1:1, 2X MEM with 2% FBS:1% agarose) was applied. The agarose mixture was allowed to solidify at room temperature before returning to the CO₂ incubator. The cells were cultured until syncytia were visible (7 – 10 days) and were fixed in 4% paraformaldehyde (Ted Pella Inc, Redding, CA) at room temperature for 30 minutes. The agarose layers were removed and the wells rinsed with dH₂O. The adherent monolayer was fixed in methanol (BDH Chemicals,

Toronto, ON, Canada) and air-dried. To enhance visualization of the syncytia formation, the cells were stained with 0.1% neutral red (Life Technologies) for 1 minute and then washed with running tap water. The syncytia were counted under an inverted light microscope. The number of plaque forming units per milliliter (pfu/mL) (i.e., the amount of replicating virus per milliliter of stock) was determined by the number of syncytia counted divided by the corresponding dilution factor.

ANIMALS

Juvenile Cam Hartley guinea pigs of both sexes, 22 to 29 days old (250 g to 300 g body weight) and female retired breeders (>1000 g) were purchased from Charles River Laboratories (Montreal, QC, Canada). The animals were housed in metal cages with corncob bedding and access to guinea pig chow (Purina, Ralston Purina Company, St. Louis, MO), alfalfa cubes and water. The animals were allowed to acclimatize for at least 5 days before being used for experiments. The guinea pigs were maintained in accordance with standards of the Canadian Council on Animal Care (197).

ALVEOLAR MACROPHAGE HARVEST

Bronchoalveolar Lavage

The guinea pigs were killed by intraperitoneal administration of pentobarbital (Euthanyl; MTC Pharmaceuticals; Cambridge, ON, Canada) at a dose of 40mg/kg body mass. When the animal was fully euthanized (no response to forceps pinch test or spontaneous respiration), bronchoalveolar lavage was performed *in situ*. The animal was positioned ventral side up and a longitudinal cut was made through the skin from below the jaw line to the bottom of the sternum. The trachea was exposed and a small horizontal cut was made between two cartilage rings. A 21-gauge cannula was inserted approximately 1 cm into the trachea and secured with a piece of

suture thread. The lungs were lavaged by intratracheal instillation of 5 mL aliquots of sterile non-pyrogenic normal saline solution (Baxter, Toronto, ON, Canada), pre-warmed at 37°C, totaling 100 mL. The instilled fractions were gently aspirated and pooled together in 2 x 50 mL centrifuge tubes and kept on ice until processed. This procedure of bronchoalveolar lavage performed on guinea pigs results in a typical yield of 10-15 million AM per animal.

Cell Processing

The BAL fluids were centrifuged at 500 $\times g$ for 10 minutes at 4°C. The resultant cell pellets from the same animal were pooled together and re-suspended in 5 mL Hank's balanced salt solution (HBSS, Life Technologies) and counted in a hematocytometer.

Isolation of Macrophage Subpopulations

Columns of discontinuous gradients were prepared fresh in 15 mL transparent polypropylene centrifugation tubes (Corning) immediately before use. This method was adapted from Dakhama *et al.* (83) using 3 concentrations of metrizamide (Nycomed Pharma AS; Oslo, Norway), 18%, 20% and 22% prepared in H-saline². Cell pellets from the same animal were pooled together and counted; the cell suspensions were spun down again at 500 $\times g$ for 10 minutes at 4°C and the pellet re-suspended in 3 mL of 18% metrizamide solution. This cell preparation was gently overlaid a 15-mL polypropylene centrifugation tube containing 3 mL of 20% metrizamide overlaid to another 3 mL of 22% metrizamide solution. A 4 mL overlay of H-saline was applied over the cell suspension to prevent dehydration during centrifugation. After centrifugation at 1,200 $\times g$ for 45 minutes at 18°C, the cells were collected from each interface and washed in 5 mL HBSS.

² H-saline is a HEPES-buffered saline solution containing 10mM HEPES (pH 7.4, Sigma-Aldrich, Toronto, ON, Canada), 150mM NaCl, 0.1% glucose and 0.1% gelatin.

In vitro RSV exposure

After washing, viability of the AM was determined by trypan blue dye exclusion test and the cell concentration was adjusted to 1×10^6 /mL. The AM were seeded in 6-well plates at a density of 2×10^6 cells/well and allowed to adhere for 30-60 minutes. For an infection with a multiplicity of infection (m.o.i.) of 3, the viral stock concentration was adjusted to 6×10^6 pfu/mL of which 1 mL was applied to each well. Viral adsorption with intermittent agitation of 6-well plates was carried out over 90 minutes. The wells were washed with PBS and fresh MEM containing 5% FBS were added (2 mL/well) followed by overnight incubation at 37°C in a 5% CO₂ incubator.

CHAPTER 5

EFFECT OF CELL MATURATION- AN EM STUDY

INTRODUCTION

AM exist as an heterogeneous population in the lung *in vivo* (143). Using density gradient centrifugation, subpopulations of AM can be separated based on the inverse relationship of cellular maturation and buoyant density (141, 143). By examining subpopulations of AM based on their stage of maturation, our laboratory (83) has demonstrated that cell maturation may be an important factor in the susceptibility of these cells to acute RSV infection *in vitro*. Using immunocytochemistry and viral plaque assay, to determine the proportion of RSV-positive cells and the amount of intracellular replicating virus respectively, Dakhama *et al.* (83) showed that immature AM were significantly more susceptible to RSV infection and supported RSV replication more efficiently compared to their matured cellular counterparts. While it is known that AM of different maturation stages are morphologically and functionally different (141, 143), it is not understood if the different subpopulations respond differently to RSV infection. Dakhama *et al.* (83) have shown that immunostaining of RSV antigens manifest a distinct granular pattern in the cytoplasm of mature AM while a less granular and more diffuse cytoplasmic staining is found in intermediate and immature AM. These observations suggest that mature AM may be structurally better equipped to deal with RSV infection when compared to the relatively immature AM. Ultrastructural studies of RSV infection in HEp-2 cells (18, 22) and eosinophils (109) have been documented; however, prior to the publication of this work (83), there have been no ultrastructural studies of RSV in AM. Arslanagic *et al.* (18) showed two mechanisms by which RSV mature in HEp-2 cells. Maturation of RSV particles occurred on the internal vesicle membrane within the cytoplasm before being delivered to the plasma membrane by transport vesicle and were subsequently released into the extracellular space by exocytosis.

The other pathway for RSV maturation, a widely accepted maturation process for most paramyxoviruses, newly synthesized viral proteins are assembled and packaged on the plasma membrane of infected cells and mature by budding through the plasma membrane (13). In the work by Garcia *et al.* (22), RSV antigens, as recognized by RSV-specific antibodies conjugated to colloidal gold particles, were detected in electron-dense inclusion bodies found in the cytoplasm in close proximity to cell nuclei of RSV-infected HEp-2 cells. Kimpfen *et al.* (109) demonstrated that RSV particles could be taken up by phagocytic vacuoles in eosinophils within 2 hours following exposure of the cells to virus.

HYPOTHESIS AND SPECIFIC AIMS

On the basis of the above observations, we speculate that the maturation stage of AM may be a determining factor in the outcome of RSV infection and the **Working Hypothesis** is:

Differences in RSV replicative outcome in subpopulations of guinea pig AM may be due to differences in the intracellular compartmentalization of RSV during its life cycle in these cell subpopulations.

The **Specific Aims** of this study are:

1. To isolate heterogeneous guinea pig AM into 3 subpopulations by density gradient centrifugation.
2. To determine intracellular localization of RSV antigens in these AM subpopulations following *in vitro* infection using immunogold labeling and transmission electron microscopy.

EXPERIMENTAL PROTOCOLS

Study Design

The design of this study is shown in Figure 5.1. Briefly, juvenile female guinea pigs ($n=3$) were killed and heterogeneous AM were obtained by *in situ* bronchoalveolar lavage. The AM were isolated into three subpopulations, "immature", "intermediate" and "mature", by density gradient centrifugation. The cells were transferred to 6-well plates (2×10^6 cells per well) after washing in cold RPMI medium and left in the incubator (37°C , 5% CO_2) for 30 minutes to allow viable AM to adhere to the plates. Non-adherent cells were washed off and the 3 subpopulations of AM were exposed to RSV at an m.o.i. of 3. At 24 hours post-infection, the cells were collected into pellets and processed by standard EM procedures before being embedded and cured in plastic blocks. Ultra-thin sections of cells were prepared and immunogold labeling was performed. Examination of these cells was carried out by transmission electron microscopy. Positive control HEp-2 cells were used in parallel with the guinea pig AM through the experimental procedures.

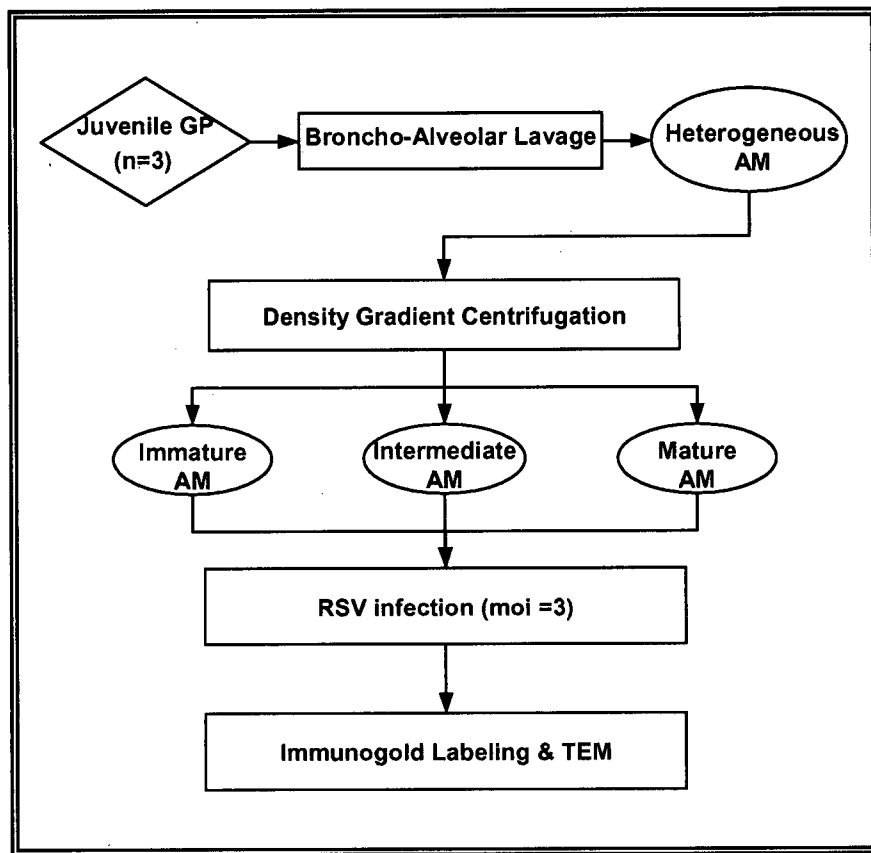


Figure 5.1 Experimental design of EM study – a cell maturation effect on *in vitro* RSV infection in guinea pig AM.

Immunogold Labeling & Transmission electron microscopy

Cell Processing and Fixation

At 24 hours post-infection, RSV-exposed AM were scraped off 6-well plates with a sterile cell scraper and washed in PBS. The AM were collected into a pellet by centrifugation at 4°C, 400 $\times g$ for 10 minutes. After aspirating off the PBS, the cell pellets were gently dislodged and fixed in 0.1M sodium cacodylate buffer (pH7.4, Marivac Ltd., Halifax, NS, Canada) containing 2.5% glutaraldehyde (BDH Chemicals) for 1 hour at 4°C. The cells were spun down and resuspended in a minimum amount of cacodylate buffer. This cell suspension was transferred to rubber mould. An equal volume of tepid 2% (w/v) low-melting point agarose (Sigma) was added to the cell suspension, mixed thoroughly and allowed to set in the refrigerator. The agar block was cut into 2 mm³ cubes, transferred to glass vials, washed thrice in cacodylate buffer and then fixed in 1% osmium tetroxide for 1 hour in the dark. The cubes were washed in 3 changes of dH₂O followed by an hour fixation in saturated uranyl acetate. Excess uranyl acetate was washed off in 3 changes of dH₂O. Unless otherwise mentioned, all electron microscopy products/reagents were purchased from Electron Microscopy Services, Fort Washington, PA.

Infiltration and Embedding

Prior to infiltration, the cubes containing AM were passed through a series of increasing concentrations of alcohol, (30%, 50%, 70%, 90% and 3X100%) at 10-minute intervals. The cubes were washed thrice in 100% propylene oxide for 10 minutes each. Immediately before use, equal volumes of Epon Mixture I³ was mixed with propylene oxide and used as infiltration fluid. After aspirating off the propylene, the freshly prepared infiltrating fluid was added to the cubes. The vials of cell cubes were left to infiltrate overnight on a rotator with their lids off. The

³ Recipe for Epon Mixture I:

Prepare Stock using 62 mL of Epon 812, 81 mL of Araldite 502 and 5 mL of DBP (Dibutyl Phthalate). Mix 1 part Stock to 1 part DDSA (Dodecetyl Succinic Anhydride) and 1.5% (v/v) DMP30 (2,4,6-Tri (dimethylaminomethyl) phenol).

cubes were then transferred the following day to rubber moulds, embedded in fresh 100% Epon Mixture I and left to cure overnight in a 60°C oven in a fume hood.

Grid Preparation and Cutting

Specimen grids made of nickel with a diameter of 3.05 mm and standard hexagonal mesh were used for supporting ultra-thin sections of cells. The grids were coated with 0.5% formvar in ethylene dichloride. Semi-thin sections (0.5 µm thickness) were cut using a glass knife fitted with a trough of dH₂O. These sections were stained with Toluidine Blue O and examined under light microscope to locate areas of interest. Ultra-thin sections, between 60 nm (gray color) and 90 nm (silver color) in thickness, were sectioned using a fresh glass knife. The sections floating in the trough of dH₂O were transferred onto the dull side of formvar-coated grids with the aid of a wire loop.

Immunogold Labeling and Visualization

Ultra-thin sections of specimens that were mounted on nickel grids were pretreated with 2% sodium metaperiodate to unmask antigenic sites (198). The sections were first incubated with 5% normal goat serum to minimize background staining and then incubated with NCL-RSV2 (Novocastra Laboratories; Newcastle-Upon-Tyne, UK), a pool of monoclonal antibodies with specificities for RSV fusion protein (F), phosphoprotein (P) and the 22K membrane-associated protein (M2). The feasibility of the antibodies directed against the P and M2 proteins have been demonstrated by Garcia *et al.* (22) for intracellular localization. The primary antibody was used at a empirically determined working dilution of 1:50 in PBS for 1 hour at 37°C. Consecutive sections incubated with non-immune mouse IgG₁ served as controls for immunostaining. Excess primary antibodies were washed off using PBS. Specific antibody-antigen reaction sites were labeled by incubation of goat anti-mouse immunoglobulins conjugated to 10 nm diameter gold particles (1:50 dilution, Dakopatts) for 30 minutes at 25°C. Three changes of PBS plus a final wash in dH₂O was performed. The sections were

counterstained with uranyl acetate and lead citrate prior to viewing under a Philips 400 electron microscope (Philips 400; N.V. Philips' Gloeilampen-fabrieken; Eindhoven, The Netherlands).

RESULTS

Isolation of AM subpopulations

Figure 5.2 shows heterogeneous AM harvested by bronchoalveolar lavage isolated into 3 distinct fractions on a metrizamide gradient following density gradient centrifugation. The subpopulation of AM recovered at the 20-22% metrizamide interface was designated as "immature", those recovered at the 18-20% metrizamide interface were designated as "intermediate", and those residing in the 18% metrizamide-H-saline interface were "mature" AM (83).

Localization of RSV particles

All three subpopulations of AM were exposed to RSV (m.o.i.=3) and immunolabeled with a pool of anti-RSV monoclonal antibodies. Examination by transmission electron microscopy revealed aggregates of colloidal gold particles in the lysosomal compartment of mature AM (Figure 5.3A). In contrast, clusters of gold particles were seen in perinuclear distribution in the cytoplasm of intermediate AM (Figure 5.3B) and in immature AM (Figure 5.3C), the gold particles associated with electron-dense material, that had the ultrastructural appearance of free RSV nucleocapsid. Positive control RSV-infected HEp-2 cells (Figure 5.4), which showed gold particles within cytoplasmic regions and budding of virus progeny around the cell membrane, confirmed the specificity of immunogold labeling by our TEM technique.

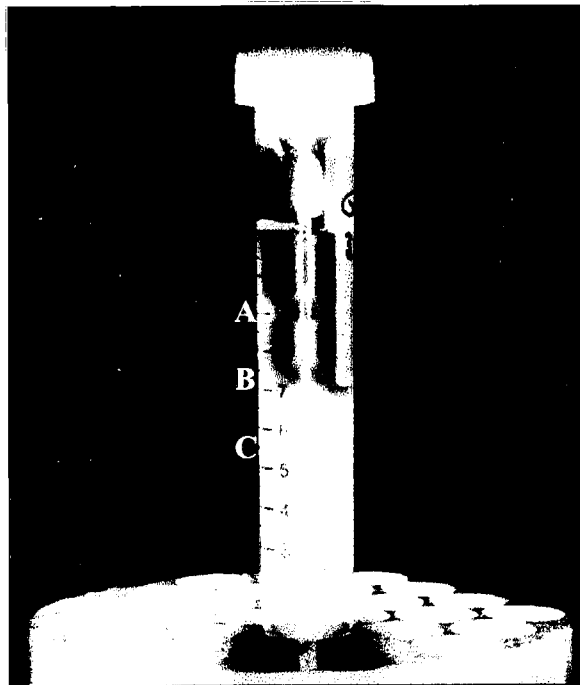


Figure 5.2 Isolation of AM subpopulations by density gradient centrifugation. Heterogeneous AM obtained from bronchoalveolar lavage were separated into hypodense mature (A), intermediate (B) and high density immature (C) subpopulations on a discontinuous metrizamide gradient.

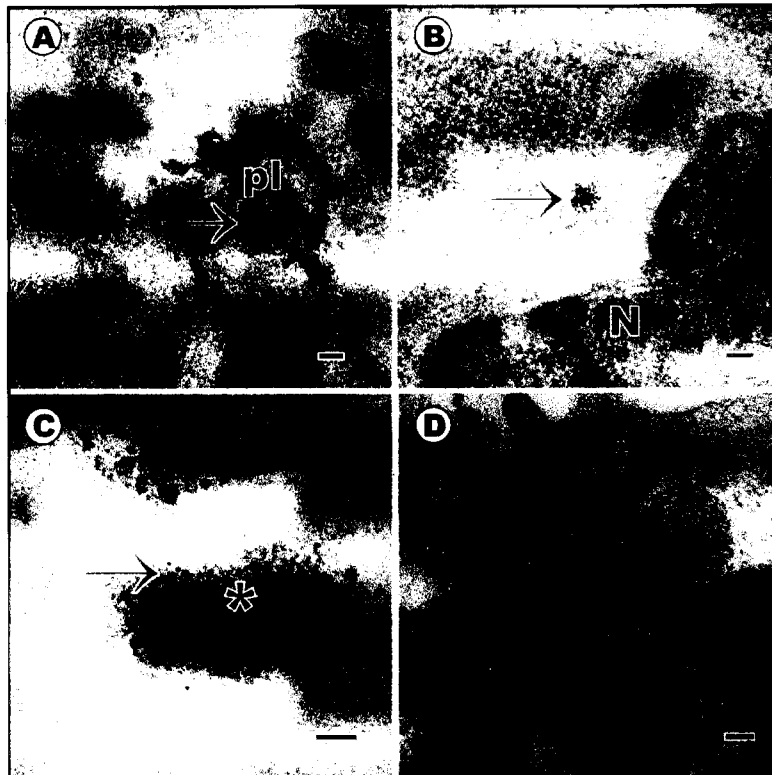


Figure 5.3 Electron micrograph of immunogold labeling of RSV particles using anti-RSV antibodies in AM subpopulations. Scale bar represents 50 nm.

- (A) Mature AM: colloidal gold labeled RSV particles (arrow) were observed in phagolysosome (pl).
- (B) Intermediate AM: colloidal gold particles (arrow) found in cytoplasm near the nucleus (N).
- (C) Immature AM: colloidal gold particles localized to viral nucleocapsid (asterisk) in cytoplasm.
- (D) Immature AM: negative control.



Figure 5.4 Electron micrograph of RSV-infected HEp-2 cell. Arrow indicates colloidal gold localized to RSV progeny budding from cell membrane. Scale bar represents 100 nm.

DISCUSSION

The objectives of this study were to localize RSV proteins within infected AM by electron microscopy and compare intracellular compartmentalization of RSV in the three subpopulations of guinea pig AM. The results showed that immunogold labeled-RSV particles were found in different intracellular compartments of AM according to their degree of maturation. More specifically, colloidal gold particles were observed in the lysosomal compartment of mature AM, whereas gold particles were found in the cytoplasm of intermediate and immature AM. These observations are consistent with and extend the light microscopic observations made by Dakhama *et al.* (83) in that RSV infection of mature AM yielded a granular staining pattern (which we interpreted as corresponding to lysosomes) while that of intermediate and immature AM produced a diffuse cytoplasmic staining pattern (which we interpreted as corresponding to free cytosolic virus).

Ultrastructural studies on functional studies of subpopulations of human AM have been described (199). Transmission electron microscopic analysis by Nakstad *et al.* (199) revealed mostly primary lysosomes and very few secondary lysosomes in high density immature AM in contrast to large mature AM with numerous secondary lysosomes. Primary lysosomes are membrane-bound organelles which contain lytic enzymes for intracellular digestion but have not yet become engaged in enzymatic digestive activities. When a phagosome (with its phagocytosed material) fuses with a primary lysosome, the resulting merged organelle is referred to as a secondary lysosome or phagolysosome (156). Thus localization of colloidal gold particles in the phagolysosomes of mature AM, in contrast to the free cytoplasmic colloidal gold particles found in intermediate and immature AM, suggests that mature AM were more able to contain the viral particles within the lysosomal compartment than less mature AM subpopulations. Since virus-associated colloidal gold particles were found in the phagolysosomes of mature AM, this localization may be pertinent to the mechanisms by which

mature AM inactivate RSV and restrict viral replication. On the other hand, the observation of virus-associated colloidal gold particles free in the cytoplasm of intermediate and immature AM is similar to observations made in RSV-infected epithelial cells (22). Furthermore, in immature AM, the colloidal gold particles were associated with electron dense material that showed morphologic features typical of paramyxovirus nucleocapsids (22, 200). The observations made in intermediate and immature AM suggest that these cells were less able to inactivate RSV and thereby have a tendency to support viral replication.

Qualitative observations, such as those described here, represent a limitation of the current study but are nonetheless valuable because the differences in RSV-AM interactions show distinct patterns of ultrastructural localization that extend light microscopic observations. Although the proportions of AM subpopulations in children have not been determined (due to practical and ethical reasons), most of the AM in the lungs of normal adults are of the mature subpopulation which are relatively more capable of conferring protection (201); this may be an explanation for immunocompetent adults to rarely develop serious RSV-bronchiolitis. Investigations to examine the relative proportions of AM subpopulations between the ages in animal studies (see Chapter 6 – Effect of age of host animal) would provide new information to improve our understanding of the interactions between RSV and AM.

In summary, the ultrastructural observations of immunogold labeled-RSV particles in different intracellular compartments of AM according to their degree of maturation supports the hypothesis that differences in RSV outcome in subpopulations of AM may be due to differences in intracellular compartmentalization of RSV, with the mature subpopulation of AM containing viral antigens within phagolysosomes.

CHAPTER 6

EFFECT OF AGE OF HOST ANIMAL ON RSV INFECTION

INTRODUCTION

The age of the host animal is a major determinant in the ability of the cell to contain viral infections. Increased resistance to disease in the course of growth, development and maturation of the host appears to be a general characteristic in humans and other species. Age-dependent resistance of macrophages to viral infections has been demonstrated in animal models. Some examples, included but not limited to, are herpes simplex virus (HSV) (202, 203) and rabies virus (204). Several theories to explain the age-related resistance against viral infections have been postulated; included are maturation of immunological reactivity, augmented IFN production and reduction in number of cell surface viral receptors (205).

As mentioned in the overview, the age of the host is one of the determinants affecting RSV infection. In children, the severity of primary pulmonary disease due to RSV infection is inversely proportional to age (1). The nature of the maturation process that renders in most adults the ability to confine RSV infection in the upper respiratory tract is still not well understood. Although numerous animal models of RSV infection have been developed, only a limited number of these models have included the age dependency phenomenon (73). Using the ferret model, Prince and Porter (206) showed that RSV could replicate in the lungs of infant but not adult animals. Similarly, data from our laboratory has demonstrated that juvenile guinea pigs are more susceptible to acute bronchiolitis than adult guinea pigs when inoculated with human RSV (207).

While the effect of age on *in vitro* RSV infection in subpopulations of AM has not been examined, it has been studied in different virus-host systems. Hirsch *et al.* (202) showed that HSV-infected macrophages from suckling mice released more progeny virus than adult mouse

macrophages. *In vitro* studies by Morgensen (203) showed that HSV-2 infection of peritoneal macrophages from 3-week old and 8-week old mice correlated age-related resistance with an increased restriction of viral replication, as determined by plaque assay.

Recent studies of *in vitro* RSV infection in AM have demonstrated that viral infection is restricted to a subset or subpopulation of cells (83, 108, 113). Midulla *et al.* (108) studied the "permissiveness" of various cell types to RSV infection by examining the proportion of RSV-positive cells following *in vitro* exposure to RSV. Cirino *et al.* (113) showed that only approximately one-third of AM exposed to RSV were capable of replicating RSV and restriction of viral replication may be related to cellular differentiation. Dakhama *et al.* (83) extended this observation: in addition to examining the proportion of RSV-positive cells following *in vitro* RSV infection, they included in their investigation the amounts of replicating virus in RSV-exposed AM. However, none of these studies examined the effect of age of the host animal on RSV infection in conjunction with subpopulations of AM. Various investigators (83, 108, 113) have used the term "permissiveness" in their reports in a rather vague manner and without precise definition. To avoid confusion, this term will not be used in this thesis. A more complete understanding of the interaction between RSV and AM could be achieved by considering the ability of RSV to enter cells as well as the ability of cells to support viral replication as one entity. Therefore, in this thesis, a new term, **RSV Yield**, will be used. The RSV Yield of a cell is defined as the amount of viral replication (as determined by plaque assay) per RSV-immunopositive cell (as determined by RSV immunostaining). Mathematically,

$$\text{RSV Yield} = (\text{pfu per million AM}) \div (\% \text{ RSV-immunopositive AM})$$

The investigations in this study examined the effect of age of guinea pigs on *in vitro* RSV infection by analyzing the distribution of the AM subpopulations and the RSV Yield of AM subpopulations between juvenile and adult animals.

HYPOTHESIS AND SPECIFIC AIMS

The Working Hypothesis of this study is:

The susceptibility of guinea pig AM to *in vitro* RSV infection is dependent on the age of the host animal and the state of cell maturation.

The Specific Aims of this study are:

1. To examine the distribution of AM subpopulations between juvenile and adult guinea pigs.
2. To determine and compare the uptake of RSV in AM subpopulations isolated from juvenile and adult guinea pigs.
3. To determine and compare RSV replication of RSV in AM subpopulations isolated from juvenile and adult guinea pigs.
4. To determine and compare the RSV Yield in AM subpopulations isolated from juvenile and adult guinea pigs.

EXPERIMENTAL PROTOCOLS

Study Design

The design of this study is shown in Figure 6.1. Six adult female guinea pigs (retired breeders, >1000 g) and five one month-old, juvenile female guinea pigs (250 – 300 g) were used in this study. Since puberty in the female guinea pigs occur around 10 weeks of age, young sows at one month of age are considered to be sexually immature (208). Heterogeneous AM were obtained by bronchoalveolar lavage immediately following killing. The cells were isolated into 3 subpopulations (immature, intermediate and mature) by means of density gradient centrifugation. These cells were exposed to RSV at a m.o.i.=3 for 90 minutes with intermittent agitation, and harvested at 24 hours post-exposure. The susceptibility of AM subpopulations to

RSV infection and replication were determined by a combination of immunostaining of cytopsin preparations and viral plaque assays, and RSV Yield was calculated.

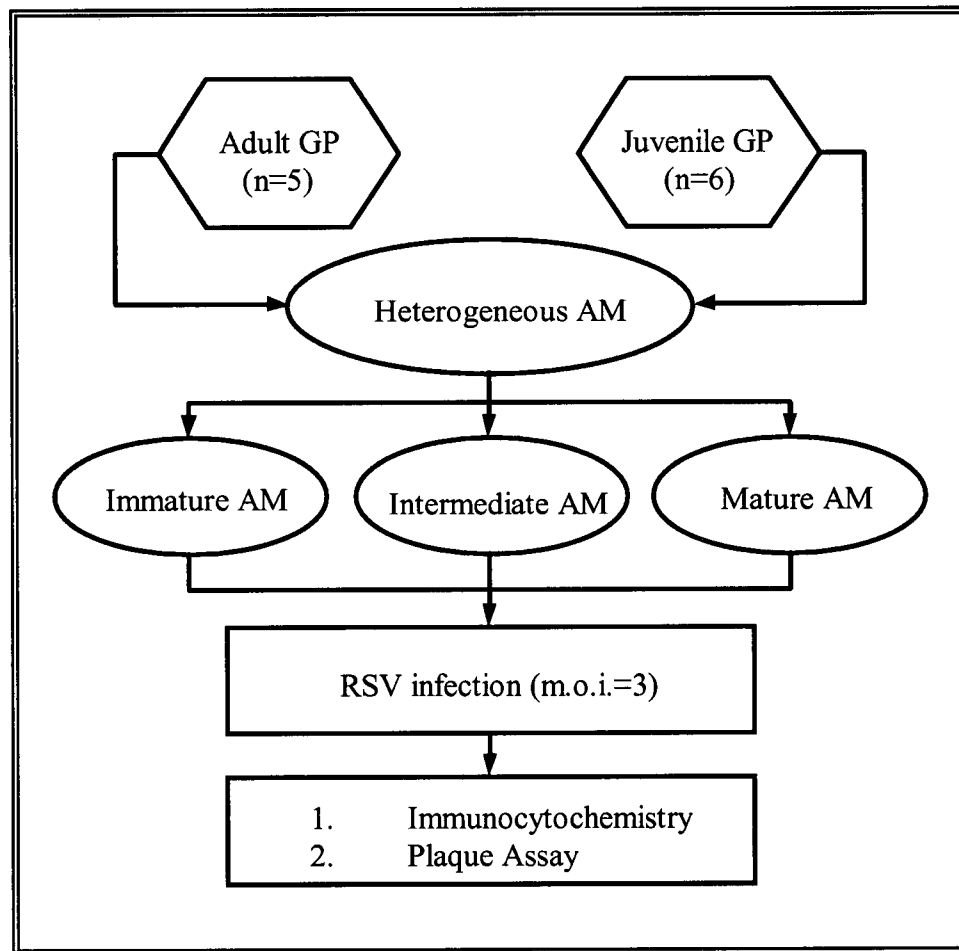


Figure 6.1 Experimental design for study of effect of age of host animal on *in vitro* RSV infection in guinea pig AM.

Cytospin preparation

RSV-exposed AM and control cells (HEp-2 cells) were collected from 6-well plates by scraping off the monolayers using a sterile cell scraper and transferred to 15 mL polypropylene tubes. The cells were collected by centrifugation at $200 \times g$ for 10 minutes in a bench top centrifuge. The resultant cell pellets were re-suspended in MEM supplemented media plus 1% FBS. The cell density was adjusted to 0.5×10^6 cells/mL. 100 μ L of each sample was applied to the cytospin chamber that had been assembled with a blotter (Shandon Inc, Pittsburgh, PA) and a labeled adhesion microscope slide (Histobond[®], Marienfeld, Germany). At this cell density, a target of 50,000 to 100,000 cells per cytospin spot was obtained. The assembled cytospin chambers were spun at $200 \times g$ for 5 minutes at room temperature. The prepared slides were air-dried and fixed in methanol (BDH Chemicals) for 5 minutes.

Immunocytochemistry

RSV Immunostaining

RSV antigens in cytospin preparations were detected by immunostaining using RSV mouse monoclonal antibody (NCL-RSV2, Novocastra Laboratories, New Castle-upon-Tyne, UK) in conjunction with the Vectastain[®] Avidin-Biotin Complex-alkaline phosphatase (ABC-AP) kit (Vector Laboratories, Burlingame, CA). NCL-RSV2 is made up of a pool of monoclonal antibodies with specificities for RSV fusion protein, phosphoprotein and M2 protein. The staining protocol as recommended by the manufacturers has been modified for cytospin preparations as follows. Slides were boiled in 0.01 M sodium citrate buffer (pH 6.0, BDH Chemicals) for 10 minutes, cooled and rinsed in dH₂O. The slides were incubated for 20 minutes with diluted normal blocking serum⁴. Excess serum was blotted off, and the NCL-RSV2 antibody solution at 10 μ g/mL was applied to each section and incubated for one hour. The

⁴ Normal blocking serum: 3 drops of stock to 10 mL TBS (10 mM sodium phosphate, pH 7.5, 0.9% saline).

slides were washed thrice in TBS and incubated with the biotinylated secondary antibody⁵ for 30 minutes. After another 3 x 5 minute washes, the slides were incubated with VECTASTAIN® ABC-AP Reagent⁶ for 30 minutes. Following that, the slides were washed again and incubated with Vector® Red Alkaline Phosphatase Substrate⁷ (Vector Laboratories) for 30 minutes. A final wash in tap water was carried out before mounting in VECTASHIELD® mounting medium and viewed under light microscope. For every cytopsin sample tested, control slides using IgG₁ of equivalent protein concentration to substitute the primary antibody were carried out in parallel. All incubations were performed at room temperature.

Scoring and Statistical Analysis

A total of 300 AM were scored and the proportion of RSV-positive cells were reported as a percentage of cells counted. The data were reported as the means of each group ± SEM, analyzed using ANOVA and the Bonferroni procedure was used to correct for multiple comparisons. A two-tailed p value of < 0.05 was considered as statistically significant.

Viral Plaque Assay

Quantification of RSV progeny titer

After the AM had been exposed to RSV for 90 minutes at an m.o.i. of 3 and allowed to incubate overnight, the cells were gently scraped with sterile cell scraper (Fisher Scientific) and the cell suspensions collected into 2 mL sterile eppendorf tubes. Sterile glass beads (Fisher Scientific) were added and the tubes were vortexed for 5 minutes to release cell-associated virus. Ten-fold serial dilutions (10^{-1} to 10^{-3}) of each sample were prepared using culture medium. 1 mL of each dilution was applied onto a monolayer of HEp-2 cells in 6-well plates. All samples

⁵ Biotinylated secondary antibody: working concentration is 1 drop of stock in 10 mL TBS.

⁶ ABC-AP Reagent: 2 drops of Reagent A + 2 drops of Reagent B in 10 mL TBS. Mix and stand for 30 minutes before use.

⁷ Vector Red Substrate: Working solution is prepared immediately before use – 2 drops of Reagent 1 + 2 drops of Reagent 2 + 2 drops of Reagent 3 in 5 mL of 100 mM Tris-HCl buffer, pH 8.2-8.5

were plated in duplicate. Subsequent steps for this assay involved washing of virus-exposed cells with PBS, agarose overlay followed by incubation over a period of 7 to 10 days of incubation and syncytia scoring. Full details of these methods are described in the section for RSV titer determination (Chapter 4, General Materials & Methods).

Scoring and Statistical Analysis

The number of syncytia formed in the different serial dilutions of sample applied was scored. The dilution, which yields 25-75 syncytia, was used to determine the number of plaque forming units (pfu) per 10^6 cells. The data, reported as the means \pm SEM, were analyzed using ANOVA and the Bonferroni method was used to correct for multiple comparisons. A value of $p<0.05$ (two-tailed) was considered as statistically significant.

RESULTS

Distribution of AM subpopulations

The distribution of AM subpopulations from juvenile and adult guinea pigs was examined and is presented in Table 6.1. There were no significant differences in the distribution of AM subpopulations between adult and juvenile guinea pigs.

Table 6.1 Distribution of AM subpopulations in adult and juvenile guinea pigs.

| | Adult | Juvenile |
|-----------------|----------------|----------------|
| Mature AM | 38.8 ± 5.9 | 46.6 ± 1.9 |
| Intermediate AM | 31.5 ± 1.4 | 29.8 ± 4.4 |
| Immature AM | 29.7 ± 5.0 | 23.6 ± 4.8 |

Data represent the proportion (mean \pm SEM) of mature, intermediate and immature AM.

Effect of Age on RSV Immunopositivity

Figure 6.2 shows the staining pattern of RSV-infected subpopulations of AM in comparison to the IgG₁ non-specific staining control. RSV antigens were localized in the cytoplasm of RSV-infected AM. Control slides incubated with immunoglobulin (IgG₁) did not exhibit any immunostaining. Figure 6.3 shows results of the percentage of RSV-immunopositive cells, determined by scoring at least 300 cells per specimen under the light microscope. The proportion of RSV-immunopositive cells in juvenile guinea pigs are significantly higher compared to their respective maturation stages in adult guinea pigs ($p<0.0001$).

In juvenile animals, the percentage RSV-immunopositive AM from the mature subpopulation was significantly less than those in the intermediate (mature vs. intermediate (mean \pm SEM): $10.6 \pm 0.7\%$ vs. $18.6 \pm 0.9\%$, $p<0.0002$) as well as immature (mature vs. immature: $10.6 \pm 0.7\%$ vs. $20.6 \pm 1.3\%$, $p<0.002$) subpopulations. There were no significant differences in the proportion of RSV-immunopositive cells between intermediate and immature AM subpopulations from juvenile animals. In contrast, there were no significant differences among the three subpopulations of AM from adult guinea pigs.

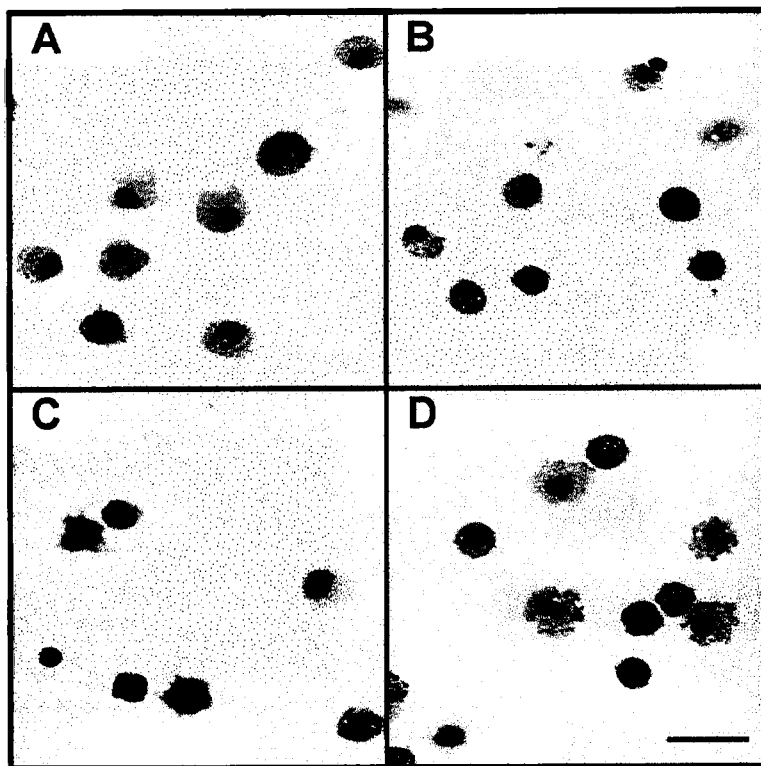


Figure 6.2 Immunostaining of mature (A), intermediate (B), and immature (C) subpopulations of guinea pig AM with anti-RSV antibody. The negative control (D) was an irrelevant isotype-matched IgG1. Hematoxylin counterstained. Scale bar represents 50 μ m.

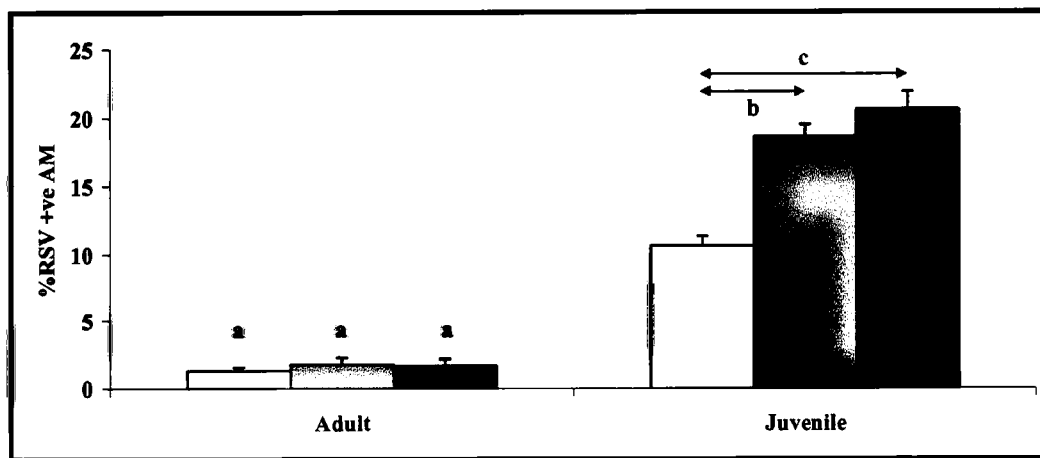


Figure 6.3 Effect of age of host animal on RSV immunopositivity.

Data represent percentage of RSV immunopositive AM (mean \pm SEM) in mature (white bars), intermediate (gray bars) and immature (black bars) subpopulations from adult and juvenile guinea pigs.

'a' p<0.0001 adult vs. juvenile guinea pigs in respective AM subpopulations.

'b' p<0.0002 mature AM vs. intermediate AM in juvenile guinea pigs.

'c' p<0.002 mature AM vs. immature AM in juvenile guinea pigs.

Effect of Age on RSV Replication

Infectious, replicating RSV within AM was released by mechanical disruption with sterile glass beads. Ten-fold serial dilutions of the virus were used to infect HEp-2 cells which form large syncytia when exposed to RSV (Figure 6.4). The number of RSV progeny from AM was determined as the product of the number of syncytia observed and the reciprocal of the dilution factor in which the syncytia were scored. Figure 6.5 shows the RSV progeny in different AM subpopulations from adult and juvenile guinea pigs. The RSV progeny in all three subpopulations of AM from juvenile guinea pigs was significantly greater than their respective counterparts from adult animals ($p<0.002$).

As shown in Figure 6.5, the immature subpopulation of AM from juvenile animals had significantly more RSV progeny compared to the intermediate ((mean \pm SEM) 4554 ± 751 vs. 975 ± 257 , $p<0.006$) and mature (4554 ± 751 vs. 252 ± 27 , $p<0.003$) subpopulations. In addition, intermediate AM contained more RSV progeny than the mature AM in juvenile animals (975 ± 257 vs. 252 ± 27 , $p<0.03$). In contrast, there were no significant differences in the RSV progeny from the three AM subpopulations isolated from adult animals.

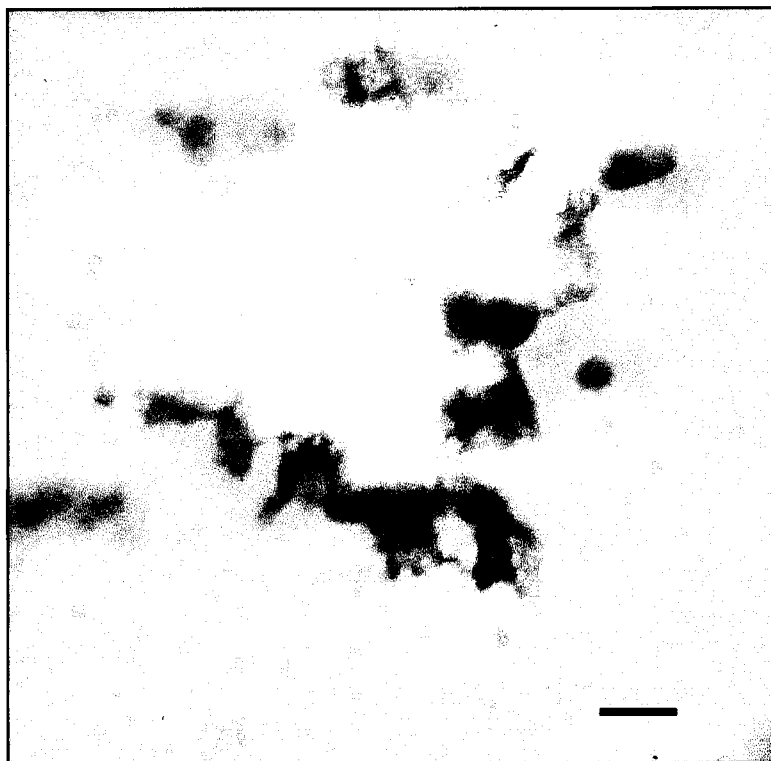


Figure 6.4 Formation of syncytium as a result of infection and fusion with neighboring cells on a monolayer of HEp-2 cells stained with neutral red (0.1%). Scale bar represents 50 μ m.

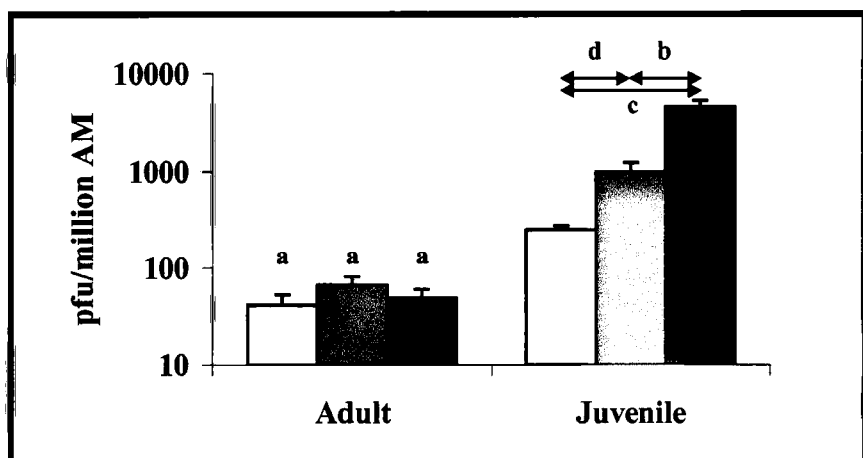


Figure 6.5 Effect of age of host animal on RSV replication.

Data represent RSV progeny per million AM exposed to RSV in mature (white bars), intermediate (grey bars) and immature (black bars) subpopulations from adult and juvenile guinea pigs.

'a' p<0.002 adult vs. juvenile guinea pigs in respective subpopulations.

'b' p<0.006 immature AM vs. intermediate AM from juvenile guinea pigs.

'c' p<0.003 immature AM vs. mature AM from juvenile guinea pigs.

'd' p<0.03 intermediate AM vs. mature AM from juvenile guinea pigs.

Effect of Age on RSV Yield

The RSV Yield in AM from adult and juvenile guinea pigs is presented in Table 6.2. The data show that RSV Yield of immature AM from juvenile guinea pigs was 5 times greater than that from adult guinea pigs (Immature AM, juvenile vs. adult: 228 ± 45 vs. 45 ± 13 , p<0.002). Comparison of RSV Yield on intermediate AM between adult and juvenile did not reveal significant differences and there was a trend (p=0.08) for higher RSV Yield in mature AM from adult versus juvenile animals.

In juvenile guinea pigs, the data indicate that RSV Yield of immature AM was significantly higher than the intermediate (228 ± 45 vs. 52 ± 13 , p<0.008) or mature (228 ± 45 vs. 24 ± 3 , p<0.008) AM subpopulations. In contrast, there were no significant differences in RSV Yield among the AM subpopulations from adult guinea pigs.

Table 6.2 RSV Yield in subpopulations of AM from adult and juvenile female guinea pigs.

| | Adult | Juvenile |
|-----------------|-------------|----------------|
| Mature AM | 40 ± 9 | 24 ± 3^c |
| Intermediate AM | 86 ± 58 | 52 ± 13^b |
| Immature AM | 45 ± 13 | 228 ± 45^a |

Data represent the RSV Yield (mean \pm SEM) of subpopulations of guinea pig AM.

'a' p<0.002, Immature AM: adult vs. juvenile animals.

'b' p<0.01, Juvenile animals: immature AM vs. intermediate AM.

'c' p<0.01, Juvenile animals: immature AM vs. mature AM.

Summary of Results

In summary, the data in this study showed that there were no differences in the distribution of AM subpopulations between adult and juvenile guinea pigs. However, in juvenile animals, the uptake of RSV by immature AM and the corresponding RSV progeny titer was significantly greater than mature AM. By contrast, there were no differences in the RSV Yield (neither in uptake of RSV nor in RSV progeny titer) in AM subpopulations from adult guinea pigs. Immature AM from juvenile guinea pigs had by far the highest RSV Yield of the AM subpopulations examined.

DISCUSSION

The working hypothesis for this study is that susceptibility of guinea pig AM to RSV infection depends on 2 intrinsic host factors, namely, the age of the host animal and the state of cell maturation. The main objective of this study was to determine and compare the *in vitro* RSV infection of AM subpopulations from adult and juvenile guinea pigs in terms of RSV Yield, defined as the RSV progeny per RSV-immunopositive cell.

Distribution of AM subpopulations

Due to difficulties in obtaining clinical samples from the lower respiratory tract of infants and young children, examination and analyses of subpopulations of AM from children have not been investigated. To my knowledge, the distribution of AM subpopulations between different age groups or sexes (see Chapter 7) has not been investigated in animal models. The data obtained in this study showed that the distribution of mature, intermediate and immature AM between adult and juvenile guinea pigs is similar. In Chapter 5, based on the localization of RSV antigens in the lysosomes of mature AM as opposed to the cytoplasm in intermediate and immature AM, it was speculated that perhaps the propensity of children to severe RSV disease

may be explained by a proportionately greater distribution of AM towards the immature subpopulation. Although data from the studies of Ferro *et al.* (201) suggest that the majority of AM from the normal adult lung is composed mainly of the mature subpopulation, this phenomenon is not observed in the guinea pig. The observations in this animal model do not support the hypothesis that young children are more prone to severe RSV disease because of having a higher proportion of immature AM. As there is little or no published literature on the interaction of age of the host animal and AM subpopulations, it is presently unclear whether the data obtained are specific to guinea pigs or whether they can be extrapolated to other species.

RSV Yield between Adult and Juvenile guinea pigs

In this thesis, the term “RSV Yield” was introduced and defined as the ability of a cell to internalize RSV and its ability to support viral replication. By this definition, the measures of viral uptake (as determined by RSV immunostaining) and replication (as determined by plaque assay) in the AM are correlated and incorporated into one entity. Therefore RSV Yield is a reflection of viral replication within RSV-immunopositive AM based on immunostaining of RSV antigens. In this experiment, the RSV Yield was greatest in immature AM from juvenile animals, suggesting that this subpopulation of AM is particularly conducive to RSV propagation. The data obtained in this study are consistent with and extend the findings of previous investigators who documented increased viral replication in macrophages from young animals (83, 108, 113).

Together with these previous findings by others, the data presented in this study demonstrate that as monocytes and the relatively immature AM differentiate and mature, they lose their tropism for RSV. Immature AM are more susceptible to RSV infection compared to the more mature cells in juvenile guinea pigs and also when compared to immature AM from adult animals, but this increased susceptibility does not appear to be related to differences in

distribution of AM subpopulations between the ages. Furthermore, these *in vitro* findings, when considered in the context of the *in vivo* observations by Hegele *et al.* (207), suggest that young animals may be highly susceptible to RSV infection of AM, with potential effects on more extensive viral replication, suppression of host lung defenses, and production of more severe lung injury.

CHAPTER 7

EFFECT OF SEX OF HOST ANIMAL

INTRODUCTION

There are many risk factors known to predispose young children to RSV bronchiolitis. Children born prematurely, with underlying cardiac and/or pulmonary disease seem to be particularly susceptible to clinically severe RSV infections. In addition, the absence of breastfeeding, low levels of maternal antibodies, sex (male), crowding and being in daycare also increases the prevalence and severity of illness during the epidemic months (1). This study examines the effect of sex of the host animal on *in vitro* RSV infection in guinea pig AM.

Epidemiological data of RSV-infected children indicates that male infants have a higher risk of RSV bronchiolitis compared to females with a ratio ranging from 1.4:1 to 1.9:1 (31-33). Furthermore, the more severe forms of RSV-bronchiolitis seen more frequently in male infants than female infants may be associated with eosinophilia during illness (209). The reasons and mechanisms responsible for these apparent sex-related disparities are not understood. Speculations include sex-related differences in fetal lung development that result in earlier maturation of the female lung than in males (210) and differences in pulmonary surfactant production between the sexes (211). The investigations in this study examined the issue of sex differences observed in RSV-bronchiolitis from 2 perspectives: the RSV Yield and the cytokine profile of infected AM. First, based on our earlier findings that immature AM are more susceptible to RSV infection than mature AM, the following questions were addressed: Do male guinea pigs have more immature AM than females? Do AM from male guinea pigs have a greater RSV Yield than females? Secondly, because a major role for cytokines has been implicated in RSV-induced inflammation (95, 116), the production of these pro-inflammatory cytokines by AM due to RSV infection was examined: TNF α which has anti-viral activity (212,

213), IL-6 which plays a major role in the initiation of the humoral arm of immunosurveillance, and IL-8, a major chemoattractant for neutrophils (69).

HYPOTHESIS AND SPECIFIC AIMS

Therefore the **Working Hypothesis** of this study is:

AM from male guinea pigs are more susceptible to RSV infection and produce more inflammatory cytokines than AM from female guinea pigs.

The **Specific Aims** of this study are:

1. To determine and compare the uptake of RSV in AM subpopulations between male and female guinea pigs.
2. To determine and compare viral replication of RSV in AM subpopulations between male and female guinea pigs.
3. To determine and compare RSV Yield in AM subpopulations between male and female guinea pigs.
4. To examine the secretion of IL-6, IL-8 and TNF α in subpopulations of AM from male and female guinea pigs.

EXPERIMENTAL PROTOCOLS

Study Design

The design of this study is shown in Figure 7.1. Based on the data obtained in the EM study and the age effect study, it was apparent that the intermediate and immature subpopulations of AM responded in a similar manner to RSV. Therefore, for this experiment, intermediate AM were isolated together with the immature cells by omitting the 20% metrizamide layer in the density gradient column. Juvenile female (n=4) and male (n=4) guinea pigs were sacrificed and heterogeneous AM were harvested by bronchoalveolar lavage. The heterogeneous AM were fractionated into mature and immature subpopulations and were exposed to RSV (m.o.i.=3). At 24 hours post-infection, the cell supernatants were used for cytokine assays and the cells were used for immunostaining for proportion of RSV-immunopositive AM and plaque assay for RSV progeny.

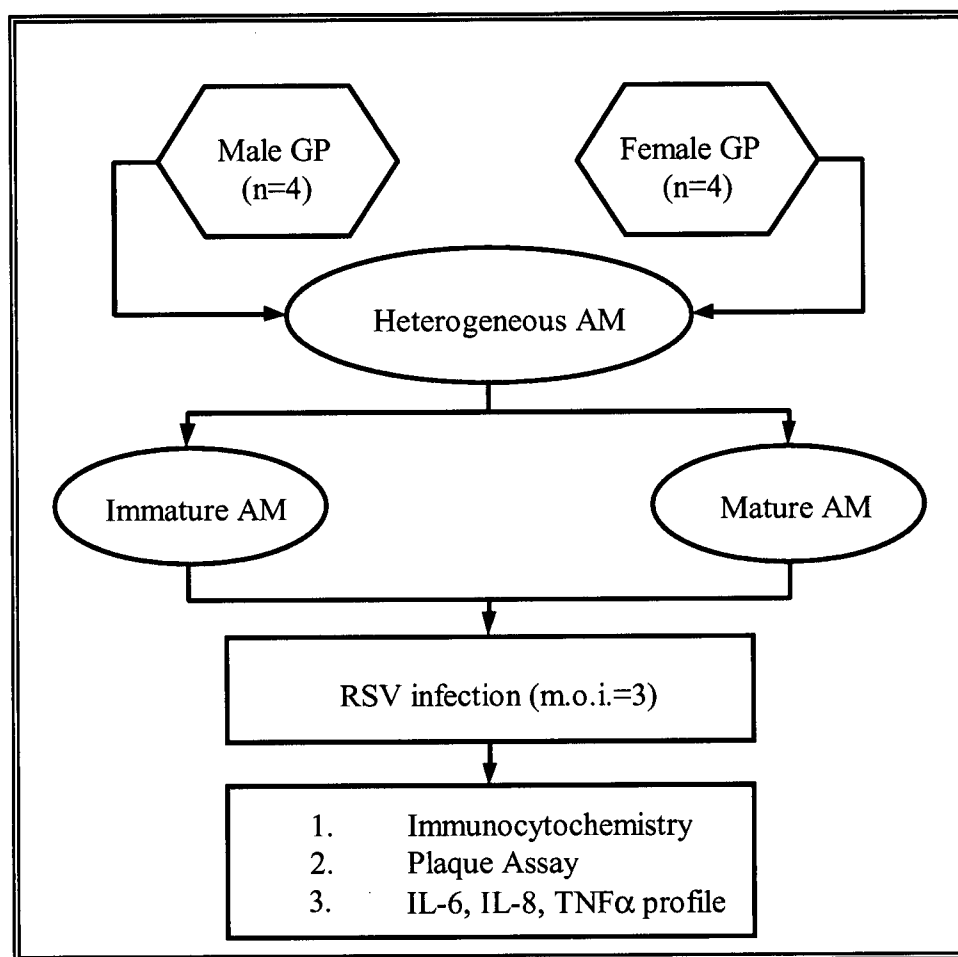


Figure 7.1 Experimental design for study of effect of gender of host animal on *in vitro* RSV infection in guinea pig AM.

Detection of IL-6 & IL-8 by ELISA

A protocol established by Dr. T.R. Bai and associates (McDonald Research Laboratories) was utilized for the analyses of IL-6-like and IL-8-like proteins in supernatants from guinea pig AM. For IL-6 ELISA assay, monoclonal anti-human IL-6 antibody (4 μ g/mL) was used as a capture antibody with biotinylated polyclonal anti-human IL-6 antibody (25ng/mL) as the detection antibody. Likewise, a monoclonal anti-human IL-8 antibody (4 μ g/mL) was used in conjunction with a biotinylated polyclonal anti-human IL-8 antibody (20 ng/mL) for the IL-8 ELISA assays. Recombinant human IL-6 and IL-8 were used in the respective assays for calculation of standard curves that were generated for each set of samples assayed. All antibodies and recombinant proteins for ELISA assays were obtained from R&D Systems.

Plate Preparation

High binding polyvinyl chloride plates (Corning Costar, Corning, NY) were coated with 100 μ L/well of the capture antibody overnight. Using a multi-channel pipettor, the plates were washed thrice with Wash Buffer⁸ to remove unadsorbed excess capture antibodies. 300 μ L of Blocking Solution⁹ were added to each well and incubated for one hour to minimize non-specific binding of cytokines to the plates. Again the plates were washed thrice using Wash Buffer, dried under vacuum and stored at 4°C until used.

Assay Procedure

Dilutions of standards were carried out in polypropylene tubes. Samples of culture supernatant from guinea pig AM (2 x 2x10⁶ AM per well per animal) and standards (100 μ L/well) were added and mixed gently by tapping the plate frame. The plates were sealed and

⁸ Wash Buffer: 0.05% Tween-20 (Sigma-Aldrich) in PBS, pH 7.4

⁹ Blocking Solution: 1% BSA (Sigma-Aldrich), 5% sucrose (Fisher Scientific), 0.05% NaN₃ (Sigma-Aldrich) in PBS, pH 7.4

incubated for 2 hours. Washing, as described above, was carried out and the biotinylated detection antibody (100 µL/well) was added and incubated for 2 hours. The aspiration/washing step was repeated and 100 µL/well of streptavidin HRP (Zymed, South San Francisco, CA) was added and incubated for 20 minutes. A final aspiration/wash procedure was performed and 100 µL/well of Substrate Solution¹⁰ was added to each well and incubated for 20-30 minutes, protected from direct light. The reaction was stopped by the addition of 50 µL/well of Stop Solution¹¹. The absorbance (A_{405}) of each well was read within 30 minutes using a microplate reader set to a wavelength of 405 nm.

Calculation of Results

To calculate assay results, the zero standard absorbance was subtracted from the mean of the sample duplicate readings. A standard curve from each set of experiments was obtained by plotting the A_{405} against the concentrations of the standards. The equation of the best-fit line was determined and the concentration of the cytokine measured can be calculated based on its A_{405} reading and the best-fit equation.

Statistical Analysis

The data were presented as means ± SEM of values. Data were analyzed using an ANOVA and the Bonferroni method was used for correcting multiple comparisons. A value of $p<0.05$ (two-tailed) was considered statistically significant.

¹⁰ Substrate Solution: 1:1 mixture of H₂O₂: Tetramethylbenzidine (Medix Biotech, San Carlos, CA)

¹¹ Stop Solution: 1 M H₂SO₄ (BDH Chemicals)

Detection of TNF α by Bioassay

In our laboratory, Dr. R.R. Schellenberg and colleagues have used this protocol for the detection of TNF α released by AM from guinea pigs (214). The protocol, also known as L929 cell cytotoxicity assay, is a modified version of that described in Current Protocols. The proportion of lysis in the TNF-sensitive L929 cells indicates the level of bioactive TNF in the culture supernatant from guinea pig AM. To confirm the expression of bioactive TNF by guinea pig AM, a neutralization test was performed by using polyclonal rabbit anti-mouse TNF α neutralizing antibody (Genzyme, Cambridge, MA).

Preparation of L929 fibroblasts

A large batch of L929 fibroblasts was cultured in several T75 flasks until confluent. The cells were pooled together by trypsinization and washed in RPMI medium supplemented with 10% FBS. After washing by centrifugation (10-minute centrifugation at 400 \times g, room temperature), the cell pellet was resuspended in supplemented RPMI. A cell count was performed and cell viability was evaluated by the trypan blue exclusion test. The cell density was adjusted to a final concentration of 4×10^5 cells/mL. The fibroblast suspension was added to each well of a 96-well flat-bottom microtiter plate, at 100 μ L/well and incubated overnight at 37°C in a 5% CO₂ humidified incubator. In general, the L929 fibroblasts plated at this density yielded confluence the next day.

Assay Procedure

The confluence of the L929 cells in 96-well microtiter plates were checked the following day before proceeding with the assay as this is important for reproducible assays. The culture media was aspirated from each well of the microtiter plate using an 8-well aspirator with extra

care so as not to damage the monolayers with the aspirator tips. Recombinant human TNF α (rhTNFR α ; R&D Systems) was used as a standard for calibration. Using an 8-channel pipettor, 2-fold serial dilutions of standards (ranging from 5 pg/mL to 5 ng/mL rhTNFR α) and culture supernatants from guinea pig AM (neat to 1:32 dilutions) were performed in the 96-well microtiter plates such that the final volume in each well contained 50 μ L. All standards and samples were plated in duplicate. One set of standards was prepared for every assay performed. The plates were incubated overnight (18 hours) in a 37°C, 5% CO₂ humidified incubator in the presence of the metabolic inhibitor actinomycin D (2.5 μ g per well, Sigma). Following overnight incubation, supernatant from each well was aspirated off and the L929 cells were washed with 200 μ L of PBS. The wells were stained with 50 μ L of Crystal Violet solution¹² for 10 minutes at room temperature. The wells were washed using cold tap water and excess water was removed by a sharp flicking of the plate. Care was taken so as not to hit the plates against any hard surfaces and thereby dislodging the adherent cells. The microtiter plates were inverted over absorbent paper and allowed to dry.

Scoring for TNF α activity

The Crystal Violet stains from the L929 fibroblasts were eluted by the addition of 100 μ L of 100% ethanol. The plates were read immediately with a microtiter plate reader at an absorbance of 595 nm. The mean absorbance reading of the negative control values was subtracted from each well. The resulting data of the standards were graphed by plotting the cellular response values (Y-axis) versus the TNF α concentrations. This calibration graph was used to determine the saturating maximal response value and the linear portion of the dose-response curve. The amount of TNF α required to stimulate a half-maximal response normally

¹² Crystal Violet solution: 0.05% Crystal Violet in 20% Ethanol

falls within the linear portion of the dose-response curve and was used to define a unit of activity. The saturating maximal response value and linear portion of the dose-response curve for each set of serially diluted samples were obtained similarly by graphing the cellular response versus the reciprocal dilution. The half maximal response and the corresponding reciprocal dilution were calculated from the equation of the linear portion of the dose-response curve. The amount of TNF α present in the sample supernatant is equivalent to the product of its reciprocal dilution at half-maximal response and the corresponding amount of TNF α from the standard controls.

Statistical Analysis

The data were presented as means \pm SEM within the same animal in each experiment. Data were analyzed by ANOVA and the Bonferroni method was used for correcting multiple comparisons. A value of $p < 0.05$ (two-tailed) was considered as statistically significant.

RESULTS

Distribution of AM subpopulations between the Sexes

The distribution of AM subpopulations from young male and female guinea pigs was examined and is presented in Table 7.1. There were no significant differences in the distribution of AM subpopulations between the sexes.

Table 7.1 Distribution of AM subpopulations in juvenile male and female guinea pigs.

| | Female | Male |
|-------------|----------------|----------------|
| Mature AM | 47.9 ± 4.3 | 47.3 ± 4.8 |
| Immature AM | 52.1 ± 4.3 | 52.7 ± 4.8 |

Data represent the proportion (mean \pm SEM) of mature and immature AM from young male (n=4) and female (n=4) guinea pigs.

Effect of Sex on RSV Immunopositivity

The data describing the impact of sex on RSV infection are presented in Figure 7.2. In comparison to AM obtained from male guinea pigs, these results indicated that female guinea pigs had a higher proportion of RSV-immunopositive AM in both mature (female vs. male: $13.4 \pm 0.6\%$ vs. $9.9 \pm 0.4\%$, $p < 0.004$) and immature (female vs. male: $25.1 \pm 0.8\%$ vs. $21.2 \pm 0.9\%$; $p < 0.04$) subpopulations. Moreover, regardless of the sex of the host animal, the proportion of RSV-immunopositive cells within the immature subpopulation was significantly higher than those in the mature subpopulation ($p < 0.002$).

Effect of Sex on RSV replication

Quantification of viable RSV progeny from RSV-exposed AM was determined using viral plaque assay. These data are presented in Figure 7.3. There were no significant differences in RSV progeny cultured in AM between male and female guinea pigs. Despite a significantly lower proportion of RSV-immunopositive cells from male guinea pigs, these cells contained similar amounts of RSV progeny as compared to the female cells. A significantly greater number of RSV progeny were isolated by viral plaque assay in immature AM compared to mature AM from both male and female guinea pigs ($p < 0.0003$).

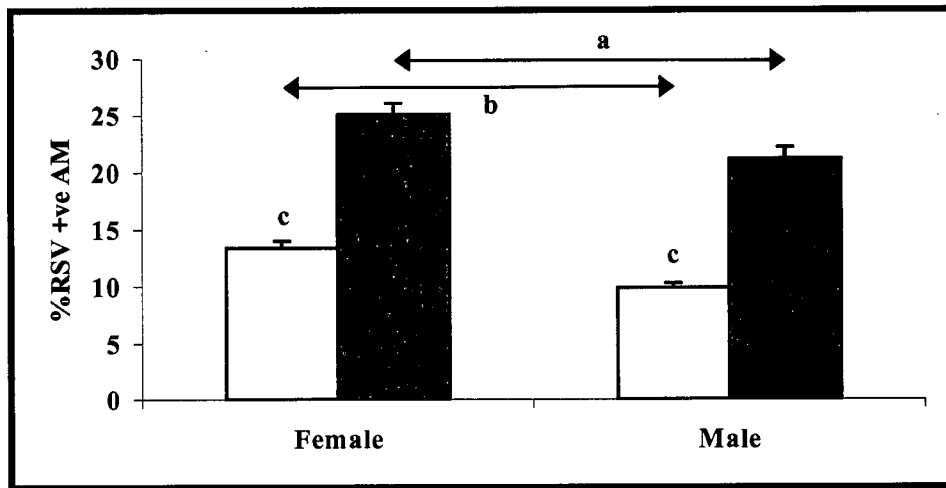


Figure 7.2. Effect of sex of host animal on RSV immunopositivity.

Data represent percentage of RSV immunopositive AM (mean \pm SEM) in mature (white bars) and immature (black bars) subpopulations from juvenile male and female guinea pigs.

'a' p<0.04 immature AM: female vs. male

'b' p<0.004 mature AM: female vs. male

'c' p<0.002 mature vs. immature AM from both male and female guinea pigs.

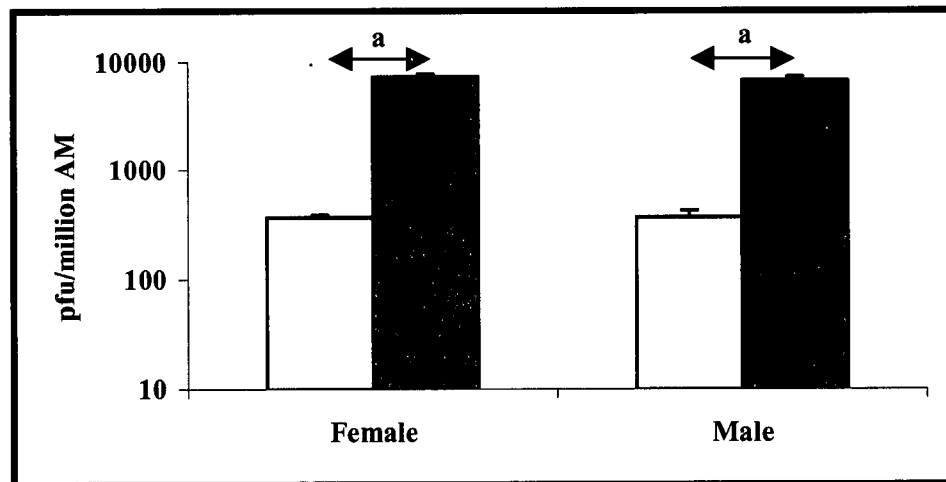


Figure 7.3 Effect of sex of host animal on RSV replication.

Data represent RSV progeny per million AM exposed to RSV in mature (white bars) and immature (black bars) subpopulations from juvenile female and male guinea pigs.

'a' p<0.002 mature vs. immature AM from both male and female guinea pigs.

Effect of Sex on RSV Yield

The RSV Yield of AM between the sexes is presented in Table 7.2. These data indicate that immature AM were significantly more susceptible to RSV than mature cells. In the mature subpopulation, AM from male guinea pigs were significantly more susceptible to RSV than those from female guinea pigs (male vs. female: 41.3 ± 2.9 vs. 28.0 ± 2.8 , p<0.009). By contrast, there were no significant differences between the sexes in the subpopulation of immature AM.

Table 7.2 RSV Yield in AM from male and female guinea pigs.

| | Female | Male |
|-------------|--------------------|--------------------|
| Mature AM | 28.0 ± 2.8 | 41.3 ± 2.9^b |
| Immature AM | 292.9 ± 11.7^a | 313.0 ± 32.2^a |

Data represent the RSV yield (mean \pm SEM) of AM subpopulations from young guinea pigs.

'a' p<0.002 mature AM vs. immature AM from both male and female animals.

'b' p<0.009 female vs. male in mature subpopulation of AM.

Effect of Sex on Cytokine Production

Cytokines released into cell supernatants following *in vitro* RSV infection were detected by ELISA (IL-6 and IL-8) and bioassay (TNF α). The levels of IL-6-like proteins, IL-8-like proteins and TNF α produced by subpopulations of AM from male and female guinea pigs are presented in Table 7.3. All 3 cytokines were upregulated in RSV-infected cells compared to sham-infected cells (see Appendix). However, there were no differences in the levels of cytokines released between AM subpopulations or between the sexes.

Table 7.3 Cytokine profile of guinea pig AM following RSV exposure.

| Cytokine | AM | Female | Male |
|---------------------------------------|----------|------------|------------|
| IL-6 (pg/mL) | Mature | 349 ± 67 | 378 ± 68 |
| | Immature | 331 ± 68 | 350 ± 82 |
| IL-8 (pg/mL) | Mature | 627 ± 160 | 730 ± 59 |
| | Immature | 863 ± 206 | 871 ± 108 |
| TNFα (ng/mL) | Mature | 8.7 ± 2.1 | 8.5 ± 2.5 |
| | Immature | 10.4 ± 3.7 | 13.1 ± 4.6 |

Data represent the amounts of IL-6, IL-8 and TNF α (mean ± SEM) produced by RSV-exposed AM from male and female guinea pigs.

Summary of Results

The data obtained in this study are summarized as follows. The distribution of AM subpopulations in juvenile guinea pigs is similar between the sexes. Regardless of the sex of the host animal, immature AM are more susceptible to RSV infection and manifest a higher RSV Yield than mature AM. Although cells from female guinea pigs appear to be more susceptible to RSV infection than male guinea pigs, the quantity of viable RSV progeny isolated from these cells are similar between the sexes. Finally, examination of the cytokine profile revealed similar levels of RSV-induced IL-6, IL-8 or TNF α produced by different AM subpopulations from male and female guinea pigs.

DISCUSSION

The working hypothesis in this study is that AM from male guinea pigs are more susceptible to RSV infection and produce more inflammatory cytokines than AM from female animals. This study was an attempt to determine if there was any disparity between the sexes of the guinea pig AM response to RSV, as a possible mechanism of the apparent propensity for boys to develop more clinically severe RSV infections than girls. This was achieved by examining the distribution of AM subpopulations between the sexes, the susceptibility of AM subpopulations to RSV (as reflected by RSV Yield) and the cytokine response of AM to RSV.

Effect of sex on distribution of AM subpopulations

Analysis of the distribution of AM subpopulations from male versus female guinea pigs did not indicate any statistically significant differences. These findings do not support the possibility that males are more at risk for RSV-bronchiolitis because of an increased proportion of immature AM which are relatively more susceptible to *in vitro* RSV infection. There are no published data on similar analysis of AM subpopulations between the sexes in humans or other animal models. While epidemiological data suggest that young males are more at risk to RSV-bronchiolitis, such differences have not been reported in animal studies. Microscopic examination comparing histological changes in the lungs of RSV-infected male versus female guinea pigs may provide further information concerning the risk differences observed in male versus female infants. Regardless, the data in this study do not show any differences in the distribution of AM subpopulations between male and female guinea pigs.

Effect of sex on RSV Yield in AM subpopulations

While the immunostaining data indicated a higher proportion of RSV-immunopositive cells from female versus male guinea pigs, the plaque assay data showed that the quantities of

RSV progeny from both sexes were similar. Therefore, the RSV yield, defined as the quantity of RSV progeny per million AM that were exposed to RSV, was higher in the subpopulation of mature AM from young male guinea pigs compared to the respective cells from the female guinea pigs. Contrary to the initial speculation that male guinea pigs may have a greater uptake of RSV (based on expression of RSV antigens determined by immunostaining), these data showed that mature AM from male guinea pigs are capable of an enhanced support of RSV replication rather than increased viral uptake. These findings suggest that male guinea pigs may not be as efficient as female guinea pigs in restricting viral replication or inactivating RSV, presumably due to differences in fetal lung development between the sexes. It is conceivable that differences between male and female guinea pigs may involve cellular mechanisms of virus clearance. Whether a similar phenomenon occurs in humans remains to be elucidated.

Effect of sex on RSV-induced cytokine production by AM subpopulations

Cytokines play major roles in the modulation of inflammatory and immune responses. These molecules are often referred to as a “two-edged sword” because of their roles in protection as well as pathogenicity and the subsequent structural damage brought about by increased production. The relationship between RSV-induced cytokine production and the sex of the host animal has not been previously investigated. Examination of the cytokine response of juvenile male and female guinea pigs infected by RSV may aid in the understanding of increased severity of RSV-bronchiolitis seen in infant boys compared to infant girls. IL-6, IL-8 and TNF α were chosen to be analyzed in this study because of their major roles in the complex network of cell-cell communication, the activation of AM and previous reports describing RSV-induced increases in secretion of these cytokines by AM (114, 116). In this study, the expression of these cytokines by guinea pig AM was upregulated in a similar manner when exposed to RSV; however, the results showed no differences in these cytokine levels between the sexes in guinea

pigs. This observation implies that the differential susceptibility of AM to RSV between the sexes has no effect on viral-induced production of these cytokines. A major limitation of the *in vitro* system used in this study is the lack of cell-cell interaction and the interaction between cytokines. Therefore, an experimental system that enables such interactions to be examined would be highly valuable in the understanding of the complex and dynamic network of cytokines involved over the course of an episode of RSV-bronchiolitis.

Despite limitations, the data in this study show that the guinea pig is a useful animal model for studying human RSV infection. In conclusion, mature AM from male guinea pigs are more susceptible to RSV infection and support more viral replication compared to AM from female guinea pigs. However, these differences observed between the sexes were not associated with differences in distribution of AM subpopulations or differences in the cellular production of IL-6, IL-8 or TNF α induced by RSV infection.

CHAPTER 8

RSV INTERACTION WITH PM10

INTRODUCTION

Over the last 2 decades, there has been a remarkable increase in the prevalence of allergic respiratory diseases and it is hypothesized that environmental, and not genetic, factors are responsible (70). At the same time, for unexplained reasons, the prevalence of RSV bronchiolitis has increased 2.4-fold within 16 years (4). To obtain an improved understanding about the potential contribution of environmental factors in these marked increases in the prevalence of respiratory diseases, scientists have examined the role of air pollution, as one environmental factor. In some studies (215, 216), air pollution has been implicated as a possible protective factor in preventing development of atopy and asthma in later life. On the other hand, data from epidemiological studies indicated that air particulates caused adverse pulmonary health effects (217) as well as increased the susceptibility of children to RSV and other airway infections (218, 219).

One plausible explanation for the increase in the prevalence of allergic respiratory diseases over the last twenty years is known as the “Hygiene Hypothesis”. This term was coined by David P. Strachan (72) who proposed that improved household amenities and the higher standards of personal cleanliness have significantly reduced the incidence of various childhood infections. This in turn led to increased susceptibility to become sensitized to harmless allergens in later life. The basis for this hypothesis is that childhood viral or bacterial infections, which induce Th1 type response and long-lasting immunological memory, could potentially prevent the Th2 immune responses in individuals susceptible to atopy and asthma. Hence common childhood infections are implicated as a protective factor against sensitization to allergens later in life.

Numerous reports appear to support the possibility that common childhood infections could play a protective role in development of allergic diseases. Results from various cohort studies (220-222) showed that young children who attend daycare or have older siblings are at a lower risk of atopic diseases. Other studies carried out in Guinea-Bissau (223) and in Scotland (224) provided epidemiological evidence that measles infection could reduce the risk of allergies. von Mutius and colleagues studied children from East and West Germany (considered a reasonably genetically homogeneous population) soon after the Reunification of 1989 and found that East German children had a higher frequency of respiratory disease but a lower prevalence of asthma compared to their West German peers (215). In a highly influential paper, Shirakawa *et al.* (225) showed that a positive tuberculin response in BCG-vaccinated schoolchildren in Japan correlated with a lower incidence of atopic conditions. Moreover, a similar inverse relationship was proposed between hepatitis virus infection and atopy (226). Taken together, the implication of these studies is that viral and bacterial infections during childhood might afford protection against allergic sensitization.

However, there are others (227, 228) who dispute the apparent protective effects of childhood infections against atopic diseases. In contradiction to earlier studies (223, 224), data from Paunio *et al.* (227) showed that naturally acquired measles infection in Finnish children was associated with *increased* prevalence of atopic conditions. Furthermore, investigations on tuberculin response by Strannegard *et al.* (229) did not confirm the findings of Shirakawa and coworkers (225).

Air pollution has been incriminated as an important health risk factor. For example, acute episodes of air pollution have been associated with increased mortality due to cardiovascular disease (230, 231). Epidemiological studies have reported that air particulates cause adverse cardiopulmonary effects especially in those with pre-existing lung diseases and are also associated with increased incidence of pneumonia and airway hyperreactivity (217). Other

studies have also suggested that pollution may influence the incidence of viral infections in children living in rural versus urban environment (218, 219).

While the evidence for the pathogenic role of air pollution in lung disease is compelling, there have been numerous published studies that suggest a possible *protective* role for air pollution. The Reunification of Germany provided a unique opportunity to study the effects of air pollution on the development of allergic disorders in two genetically similar populations that had been exposed to different environmental conditions over four decades. Several studies of children and adults have demonstrated a significantly lower prevalence of bronchial hyperresponsiveness, hay fever and atopy in the more polluted East German cities compared to the relatively cleaner West German cities (215, 232, 233). Similar evidence was also obtained in studies performed in the Baltic region where schoolchildren living in the more polluted Poland demonstrated a lower prevalence of atopic sensitization and asthma compared to those in relatively less polluted western Sweden (234, 235).

The goal of the current study was to examine the interactive effects of RSV infection and air pollution (using PM10) on guinea pig AM functions. Recent studies by Becker *et al.* (193) showed that PM10 inhibits the ability of human AM to take up RSV. However, earlier studies demonstrated that RSV infection severely diminished the phagocytic ability of mouse AM (114). To understand how RSV and PM10 might interact and affect AM functions, we proposed that the AM response to RSV and PM10 is dependent on the sequence in which AM were exposed to these agents. The following specific questions were considered: Does PM10 exposure protect AM against RSV infection? Does RSV infection exacerbate a pre-existing PM10-induced cytokine response of AM? Does RSV protect against effects of acute PM10 exposure? Does exposure to PM10 exacerbate a pre-existing RSV-induced inflammation? Based on these considerations, *in vitro* experiments using guinea pig AM were designed to simulate 2 scenarios: RSV infection of individuals in high pollution areas (PM10+RSV) and RSV-infected individuals

exposed to an acute episode of air pollution (RSV+PM10). This was achieved by sequential exposure of AM to 2 environmental agents, RSV and PM10. In the former case, experiments were performed on AM that had been pre-treated with PM10. In the latter case, RSV-infected AM were subjected to a subsequent treatment of PM10. These 2 situations were analyzed in 3 aspects: (1) ability of AM to phagocytose PM10, (2) the RSV Yield based on ability of the AM to take up virus and support viral replication and (3) cytokine response of the AM to these stimuli.

HYPOTHESIS AND SPECIFIC AIMS

On the basis of the rationale presented above, the **Working Hypothesis** of this study is:

The outcome of the interaction of RSV and environmental particulates in AM is dependent on the sequence in which the cells were exposed to these agents.

The **Specific Aims** of this study are:

1. To compare the effect of sequential PM10 and RSV exposure, and vice versa, on the phagocytic function of AM using flow cytometric analysis.
2. To compare the effect of sequential PM10 and RSV exposure, and vice versa, on RSV uptake by AM.
3. To compare the effect of sequential PM10 and RSV exposure, and vice versa, on RSV replication.
4. To compare the effect of sequential PM10 and RSV exposure, and vice versa, on RSV Yield.
5. To measure cytokine production (IL-6, IL-8 and TNF α) of AM in response to sequential PM10 and RSV exposure, and vice versa.

EXPERIMENTAL PROTOCOLS

Study Design

The design of this study is shown in Figure 8.1. In this study, heterogeneous AM were obtained by bronchoalveolar lavage from female juvenile guinea pigs ($n=4$). Data from the previous study (Chapter 7) has indicated that neither the gender of the host animal nor the maturation stage of the AM influenced the cytokine profile of RSV-infected AM. Therefore in this experiment, AM were used and examined as a heterogeneous population.

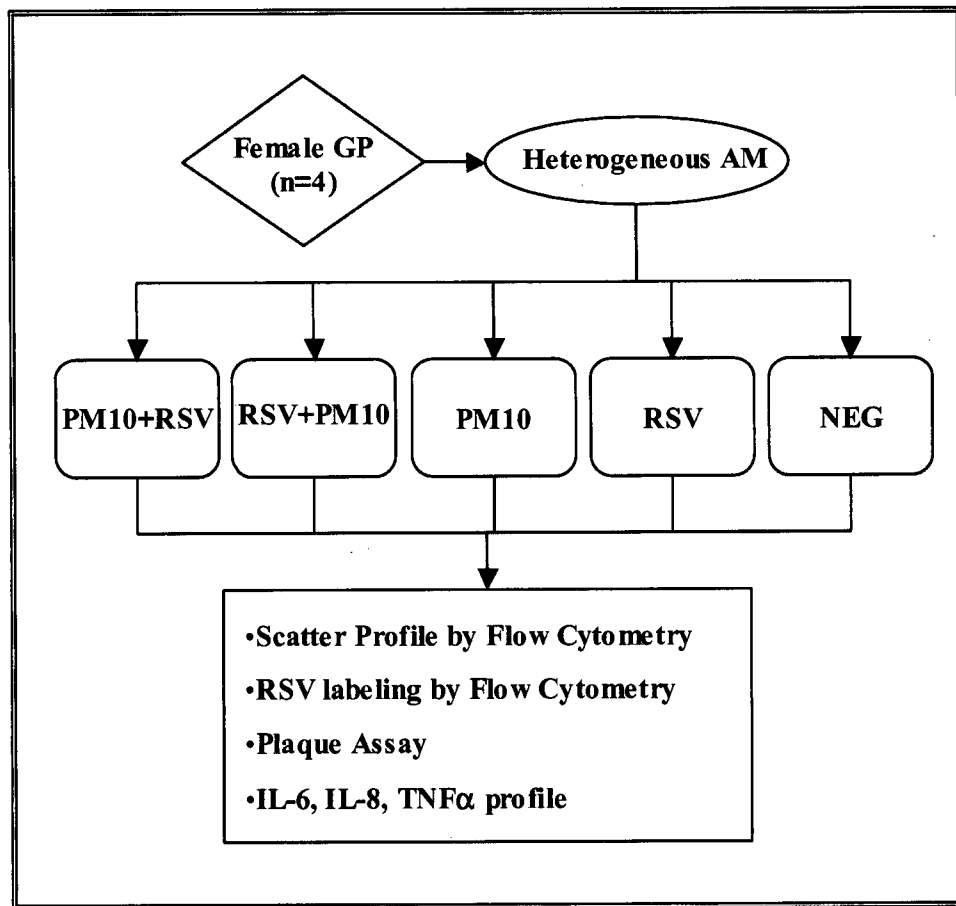


Figure 8.1 Experimental design for study of PM10-RSV interactions in guinea pig AM.

Heterogeneous AM from each guinea pig were subjected to five different treatments: exposure to PM10 followed by RSV infection (PM10+RSV), RSV infection followed by PM10 exposure (RSV+PM10), exposure to PM10 only (PM10), exposure to RSV only (RSV) and the negative control (i.e., exposure to neither PM10 nor RSV) (NEG). At 24 hours post-treatment, the AM were used for plaque assay to quantify RSV progeny and flow cytometric analysis of proportion of RSV-infected cells and cell scatter properties while the cell supernatants were used for ELISA (IL-6 and IL-8 detection) and bioassay (TNF α).

Several reports have demonstrated that the cytokine response of AM to environmental particulates might be due to the presence of endotoxin on particles (193, 236). Results from preliminary experiments indicated trace amounts of endotoxin (0.05 EU/100 μ g PM10) in the batch of particulates used in this study and this amount of endotoxin is unable to provoke a cytokine response in guinea pig AM by using a similar method of *in vitro* exposure (237). In addition, the dose response and viability of AM subpopulations to various concentrations of PM10 was examined. These results showed a minimal toxic effect on the AM (>90% cell viability by trypan blue exclusion test) and a maximal cytokine response with 100 μ g/mL PM10 (238). Consequently, a PM10 concentration of 100 μ g/mL was selected for use in the present study. Furthermore, the association of PM10 with AM was examined using both light and electron microscopes. Light microscopic examination of cytopsin preparations (method is as described in Chapter 6) of AM exposed to PM10 localized the particles within the cytoplasm (Figure 8.2). Using techniques as described in Chapter 5, PM10-exposed AM were embedded in Epon and examination under transmission electron microscope revealed PM10 within lysosomal compartments of AM (Figure 8.3).

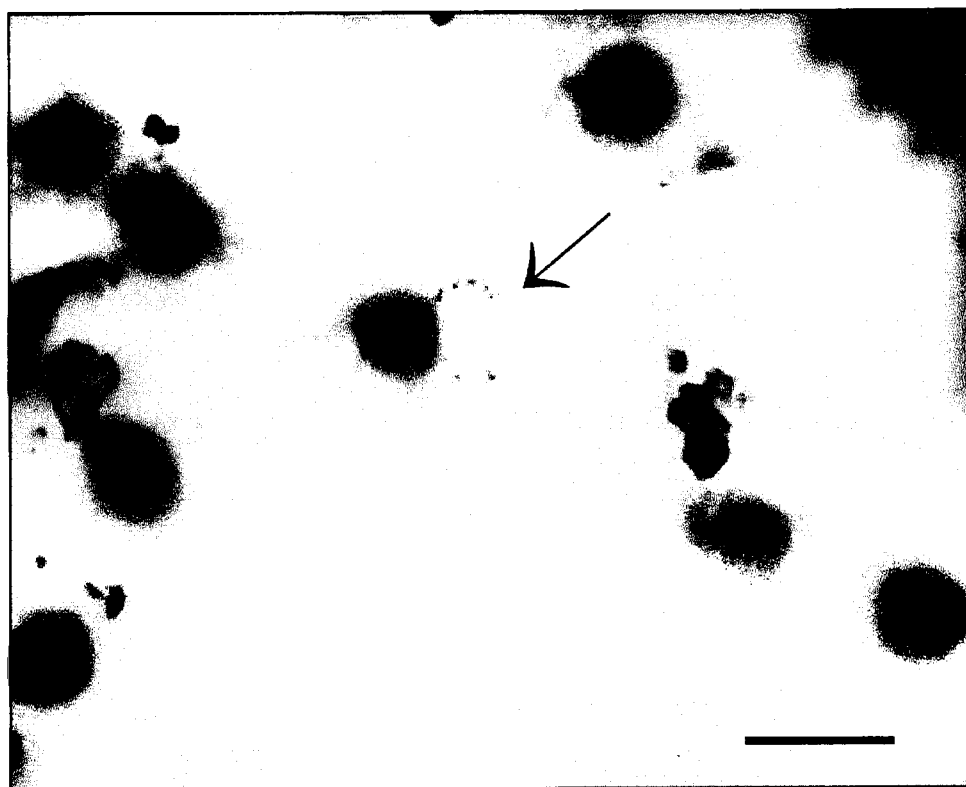


Figure 8.2 PM10-exposed AM in hematoxylin-eosin stain. Particulates (arrow) are located within cytoplasmic regions of AM. Bar represents 25 μm .



Figure 8.3 Electron micrograph of an AM containing PM10 (arrow) within a lysosome. Bar represents 100 nm.

Particulate Matter (PM10)

The PM10 used in this thesis work was obtained from Environmental Health Canada, Ottawa (EHC-93, kindly provided by Dr. R. Vincent of Health Canada). Airborne urban particles were collected from the outdoors using a single-pass air-purifier by vacuum and were sieved through a 36- μm mesh filter before using for experimental purposes. The median diameter of this preparation of fine particles is 0.35 μm but also retained a coarse component (approximately 7 to 15 μm). The chemical components of EHC-93 consisted mainly of polycyclic aromatic hydrocarbons, ions and metals and are listed in Table 8.1 (239). The individual components of this complex mixture of organic and inorganic compounds responsible for adverse health effects have not been identified. However, the soluble metal components in ambient PM10 have been proposed as the major contributor in stimulating the production of cytokines by AM (240). In addition, it has been suggested that the PM10-associated metals with redox potential (for example, iron, vanadium or copper) play significant roles in contributing to the toxicity of particulate matter (241-243).

Table 8.1 Chemical components of EHC-93Extracted and modified from Vincent *et al.* (239), with permission.

| Polycyclic Aromatic Hydrocarbons | µg/g particle |
|---|--|
| Anthracene | 0.54 |
| Benzo(a)anthracene | 1.10 |
| Benzo(b)fluoranthene | 2.78 |
| Benzo(ghi)perylene | 1.52 |
| Benzo(a)pyrene | 0.95 |
| Fluoranthene | 2.47 |
| Phenanthrene | 1.83 |
| Pyrene | 2.11 |
| Ions | µg/g particle |
| Hydrogen ion | 0 |
| Sulfate ion | 45×10^3 |
| Metals | µg/g particle (% solubility in water) |
| Aluminum | 10×10^3 (2%) |
| Chromium | 42 (3%) |
| Copper | 845 (17%) |
| Iron | 15×10^3 (1%) |
| Lead | 7×10^3 (4%) |
| Magnesium | 7×10^3 (14%) |
| Nickel | 67(7%) |
| Vanadium | 90(0%) |
| Zinc | 10×10^3 (46%) |

PM10-RSV Exposure

The EHC-93 particles were prepared fresh as 100 µg/mL particulate suspensions using RPMI media supplemented with 2% FBS and gentamycin. To minimize aggregates of particles, the PM10 suspensions were sonicated using a probe sonicator (VibraCell™, Sonics & Materials, Danbury, CT) 3 times at 5 minutes intervals prior to use. 500 µL of PM10 particulate suspensions were added to 6-well plates containing approximately 2×10^6 adherent AM per well. The cells were exposed to PM10 particulates for 60 minutes in a 5% CO₂ incubator at 37°C. Following exposure, the excess PM10 suspensions were removed by washing twice with PBS and 1 mL of fresh medium was added to wells with no RSV infection. In wells where AM were subjected to both agents, the cells were treated with the first agent (PM10 or RSV) and washed

twice with PBS before being treated with the second agent (RSV or PM10) immediately following the first treatment. Each treatment was carried out for 60 minutes, with intermittent agitation to ensure even exposure, in a 37°C 5% CO₂ incubator. After removal of the second agent, 1 mL of fresh medium was added to each well and the cells were allowed to incubate in a 37°C 5% CO₂ incubator overnight.

Flow Cytometry

Flow cytometry was used to analyze the cells because of the ability of this technique to measure multiple parameters in large number of cells simultaneously. In this thesis, flow cytometry was utilized for the measurement of cell parameters (such as cell size and granularity) and the expression of RSV antigens defined by fluorescent antibodies. The samples were analyzed using the FACScan flow cytometer (UBC Biomedical Research Center, Flow Cytometry Facility). The term “FACS” is Becton-Dickinson’s registered trademark and is an acronym for “Fluorescence-Activated Cell Sorter”. The FACScan uses an air-cooled argon gas laser with a fixed wavelength emission of 488 nm. It has fluorescence detectors that detect green, yellow-orange and red light. For the purpose of this thesis, fluorescein was used extensively for the green channel. The FACScan analyzes cells at the rate of several hundreds per second and 5,000 to 10,000 cells were acquired per sample. The samples were in mono-disperse suspensions whereby the cells passed single-file through a laser beam by continuous flow of a fine stream of the suspension.

The measurement of the side scatter intensity, which is proportional to the granularity of the cell and reflection of particle ingestion, was obtained simultaneously with the fluorescence intensity of the fluorescent-labeled RSV-infected cells. The photomultiplier tube (PMT) voltage and compensation were set using cell surface staining controls (i.e., IgG of equivalent protein concentration) and the same quadrant markers were used for all experiments to facilitate inter-

experiment comparisons. Data were saved to zip disks and analyzed with WinMDI (version 2.8), a graphics software. WinMDI is a freeware obtained from the World Wide Web (<http://facs.scripps.edu>). Using WinMDI, histograms and bivariate dot plots were generated upon data reanalysis to display the mean fluorescence intensity (MFI) frequency of AM with expression of surface and intracellular RSV antigens.

Immunofluorescent staining of RSV antigens

The protocol described below was established empirically and optimized for combined surface and intracellular labeling of RSV antigens in guinea pig AM. Following treatment, the AM were scraped off 6-well plates using disposable sterile cell scrapers (Fisher Scientific). The wells were rinsed with 1 mL PBS and collected into the respective tubes. Since the anti-RSV antibodies (NCL-RSV3-FITC, Novocastra, UK) used in this protocol is a pool of monoclonal antibodies that detect both surface and intracellular antigens, a two-step immunostaining procedure was devised. The cells were washed in PBS and underwent centrifugation for 8 minutes at 1000 $\times g$. A cell pellet was obtained by rapid decanting and was resuspended in 100 μ L PBS. 10 μ L of FITC conjugated anti-RSV antibody (NCL-RSV3-FITC) was added to the cells and incubated for 30 minutes. Excess antibodies were washed off and the cells were fixed in 4% paraformaldehyde (Ted Pella) in PBS for 5 minutes. After washing, the cells were incubated in 0.5% Triton-X 100 (Sigma) for 10 minutes. Intracellular RSV antigens were labeled by a second incubation with the NCL-RSV3-FITC antibody for 30 minutes. The cells were washed in PBS and 0.2 mL crystal violet (2mg/mL PBS, BDH Chemical) was added to quench auto-fluorescence (244). After 5 minutes, a final wash with PBS was carried out and the cells were resuspended in 500 μ L PBS and stored on ice. All incubations were performed at room temperature unless otherwise stated. Flow cytometry was performed within 2 hours at the UBC Biomedical Research Center, Flow Cytometry Facility. The proportion of RSV-

immunopositive cells was determined by the amount of green fluorescence emitted by the FITC conjugated anti-RSV antibody.

Statistical Analyses

Data were expressed as the mean value \pm SD. ANOVA analysis was performed with a Bonferroni correction for multiple comparisons. A value of $p<0.05$ (two-tailed) was considered as statistically significant.

RESULTS

The effects of sequential exposure of AM to PM10 and/or RSV were examined in this study. The objectives were to examine the impact of sequential PM10-RSV interaction with respect to the phagocytic ability of AM, ability of AM to take up RSV and support viral replication as well as the cytokine response of these cells.

Effect of PM10-RSV interaction on the phagocytic ability of AM

The ability of AM to phagocytose PM10 was determined indirectly by the measurement of side scatter that is proportional to the granularity of the cell and a reflection of particle ingestion. The effect of PM10-RSV interaction on AM granularity is summarized and presented in Figure 8.2. AM that were exposed to PM10 showed a significant increase in mean side scatter in comparison to the negative control AM ($p<0.05$) and in comparison to RSV-infected AM ($p<0.04$). There were no significant differences in mean side scatter between negative control AM and RSV-infected AM. In addition, there were no significant differences in mean side scatter between AM that were exposed only to PM10 and AM that were exposed to both agents.

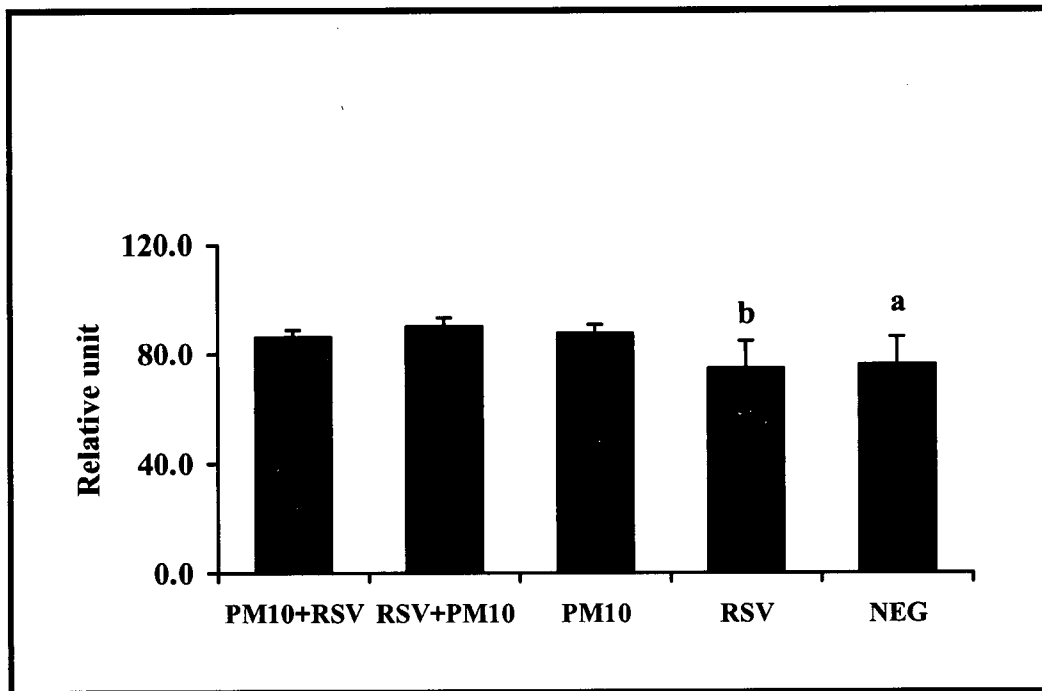


Figure 8.4. Effect of PM10-RSV interaction on AM granularity.

Data represent side scatter (mean \pm SD) of guinea pig AM subjected to different treatments.

'a' p<0.05 NEG vs. PM10+RSV, NEG vs. RSV+PM10, NEG vs. PM10

'b' p<0.04 RSV vs. PM10+RSV, RSV vs. RSV+PM10, RSV vs. PM10

Effect of PM10-RSV interaction on RSV Immunopositivity

Typical histograms of RSV labeling by flow cytometry on HEp-2 cells and guinea pig AM with and without RSV infection are presented in Figure 8.5. The mean fluorescence of uninfected HEp-2 cells (Top Left) and guinea pig AM (Top Right) labeled with anti-RSV antibodies and IgG1 (equivalent isotype control) are very similar. The population of RSV-immunopositive HEp-2 cells (>85%) is indicated by a right shift increase in mean fluorescence intensity (MFI, Bottom Left, anti-RSV vs. IgG1: 53.2 vs. 4.3). The spread of this cell population indicates that some HEp-2 cells are more heavily infected than others. Bottom right panel in Figure 8.3 shows a right shift of a minor proportion (>25%) of RSV-immunopositive guinea pig AM when labeled with anti-RSV antibodies (MFI anti-RSV vs. IgG1: 17.9 vs. 1.6).

The data describing the effect of PM10-RSV interaction on RSV infection are summarized and presented in Figure 8.6. All four treated groups showed a significantly greater proportion of RSV-immunopositive cells compared to negative control AM ($p<0.007$). The low proportion ($1.98\% \pm 0.37\%$ (mean \pm SD)) of RSV-immunopositive cells in the PM10 group may be attributed to non-specific staining. In comparison to AM in the RSV group, AM that were initially exposed to RSV followed by exposure to PM10 (i.e., RSV+PM10 group) showed a similar proportion of RSV-immunopositive AM. By contrast, AM that were initially exposed to PM10 followed by exposure to RSV (i.e. PM10+RSV group) showed a significantly smaller proportion of RSV-immunopositive AM (PM10+RSV vs. RSV: $(4.5\% \pm 0.84\%)$ vs. $(10.5\% \pm 5.11\%)$, $p<0.05$). In addition, for cells that were subjected to both treatments, the RSV-immunopositivity of AM is influenced by the sequence of exposure to these agents. The data indicated that RSV uptake by AM is suppressed if these cells had been exposed to PM10 prior to RSV (PM10+RSV vs. RSV+PM10: $(4.5\% \pm 0.8\%)$ vs. $(12.6\% \pm 0.9\%)$, $p<2 \times 10^{-5}$).

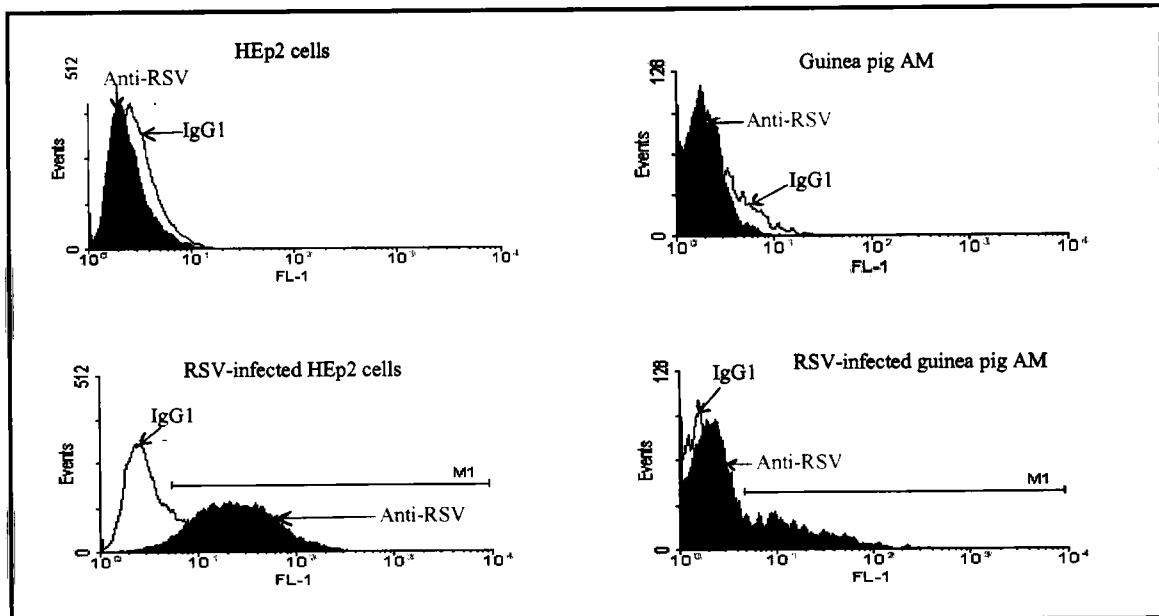


Figure 8.5 Representative histograms of HEp-2 cells and guinea pig AM with and without RSV infection.

Top Left: HEp-2 cells labeled with anti-RSV antibodies (Red) and IgG1 (Black line, no fill).
Bottom Left: RSV-exposed HEp-2 cells labeled with anti-RSV antibodies ($>85\%$ RSV immunopositive cells, MFI=53.2) and control IgG1 (MFI=4.3).

Top Right: Guinea pig AM labeled with anti-RSV antibodies and IgG1.

Bottom Right: RSV-exposed guinea pig AM labeled with anti-RSV antibodies ($>25\%$ RSV immunopositive cells, MFI=17.9) and control IgG1 (MFI=1.6).

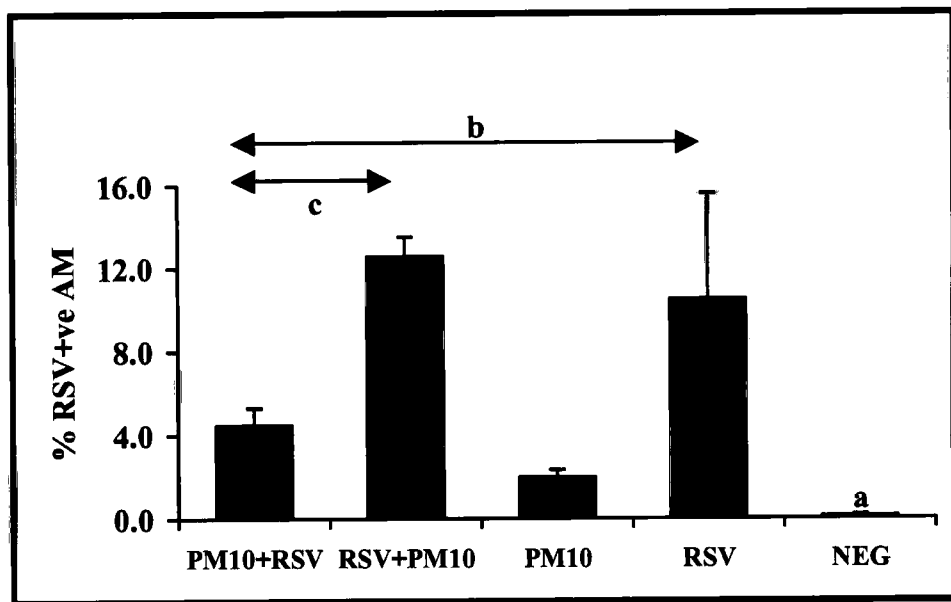


Figure 8.6 Effect of PM10-RSV interactions on RSV immunopositivity.

Data represent percentage of RSV-immunopositive AM (mean \pm SD) as determined by flow cytometric measurement of FITC-linked RSV antibodies.

'a' $p<0.007$ NEG vs. all other groups

'b' $p<0.05$ PM10+RSV vs. RSV

'c' $p<2 \times 10^{-5}$ PM10+RSV vs. RSV+PM10

Effect of PM10-RSV interaction on RSV replication

The quantity of RSV progeny isolated from AM, as determined by plaque assay, is shown in Figure 8.7. Negative control AM and those that were exposed to PM10 alone did not propagate RSV progeny. AM that were exposed to both agents produced 3- to 9-fold less RSV progeny compared to AM that were exposed to RSV alone (PM10+RSV vs. RSV (mean \pm SD): (390.6 \pm 205) vs. (3534 \pm 1457), p<0.005; RSV+PM10 vs. RSV: (1009.4 \pm 449) vs. (3534 \pm 1457), p<0.02). However, the quantity of RSV progeny was not significantly affected by the sequence of exposure to RSV and PM10.

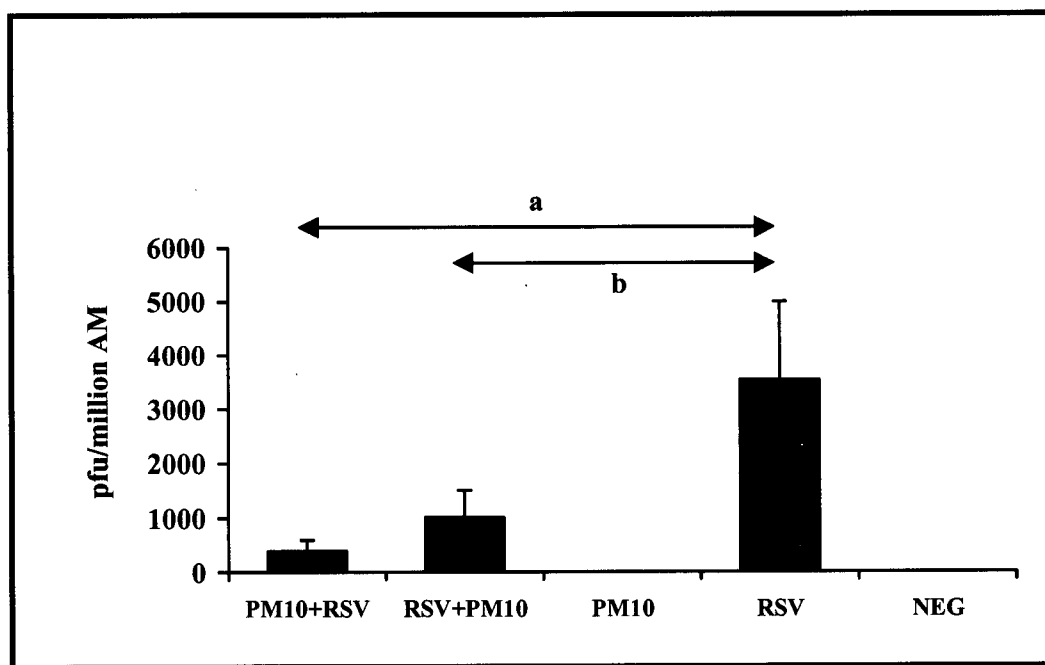


Figure 8.7 Effect of PM10-RSV interaction on RSV replication.

Data represent quantity of RSV progeny scored per million AM (mean \pm SD).

'a' p<0.005 PM10+RSV vs. RSV

'b' p<0.02 RSV+PM10 vs. RSV

Effect of PM10-RSV interaction on RSV Yield

RSV Yield, as explained in earlier studies, is a measurement of the amount of replicating virus per RSV-immunopositive AM as determined by immunolabeling of RSV antigens. RSV Yield can therefore be considered as a reflection of the robustness of viral replication within an infected cell. These data are summarized and presented in Table 8.2. AM that were exposed to RSV alone produced the highest RSV Yield ($p<0.04$). When AM were exposed to both RSV and PM10, a 5-fold decrease in RSV Yield was observed. This reduction in RSV Yield was independent of the sequence by which AM were exposed to both RSV and PM10.

Table 8.2 Effect of PM10-RSV interaction on RSV Yield.

| 1 st Exposure | 2 nd Exposure | RSV Yield |
|--------------------------|--------------------------|-----------------|
| RSV | - | 463 ± 346^a |
| PM10 | RSV | 88 ± 40 |
| RSV | PM10 | 79 ± 37 |

Data represent RSV Yield (mean \pm SD) of AM in different treatments.
 'a' $p<0.04$ PM10+RSV vs. RSV, RSV+PM10 vs. RSV

Effect of PM10-RSV interaction on IL-6 production

IL-6-like proteins released into cell supernatants following various treatments were detected by ELISA. The levels of IL-6-like proteins produced by AM are summarized and presented in Figure 8.8. Of the different treatments, AM that were exposed to RSV alone produced the most IL-6-like proteins ($p<0.0002$). Negative control AM and PM10-exposed AM released similar amounts of IL-6-like proteins. Exposure of AM to PM10 significantly suppressed RSV-induced IL-6 production (PM10+RSV vs. RSV (mean \pm SD): (69.3 ± 6.4) vs. (327.9 ± 31.7), $p<4 \times 10^{-6}$; RSV+PM10 vs. RSV: (11.3 ± 2.2) vs. (327.9 ± 31.7), $p<1 \times 10^{-6}$). Furthermore, IL-6 expression by guinea pig AM was dependent on the sequence of exposure to PM10 and RSV (PM10+RSV vs. RSV+PM10: (69.3 ± 6.4) vs. (11.3 ± 2.2), $p<3 \times 10^{-6}$).

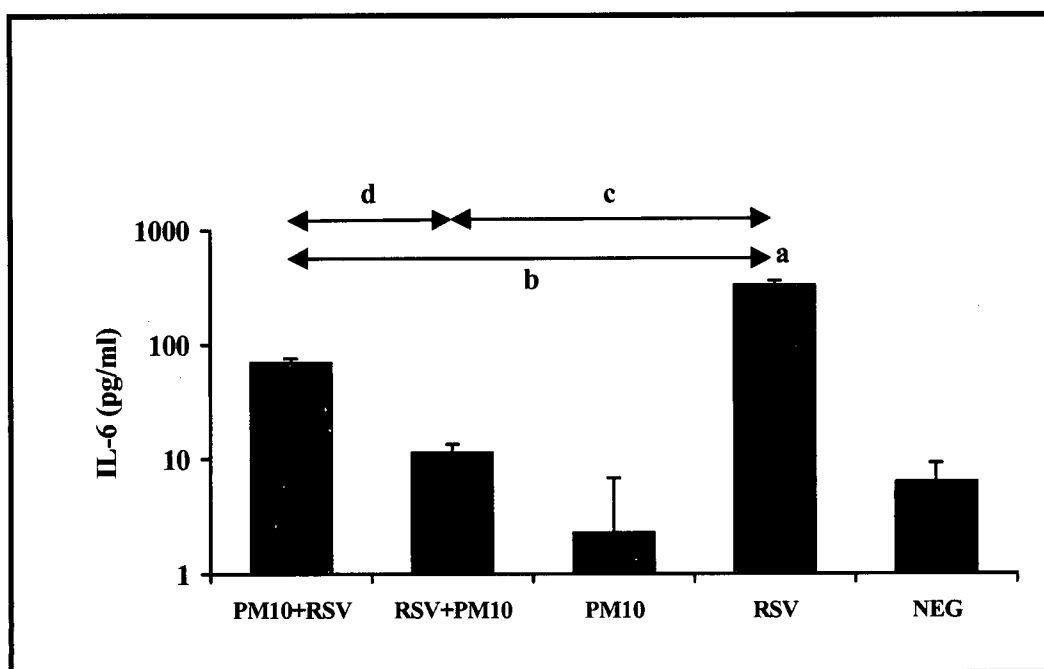


Figure 8.8 Effect of PM10-RSV interaction on IL-6 production by AM.

Data represent IL-6-like protein (mean \pm SD) released by AM subjected to different treatments.

'a' $p<0.0002$ RSV vs. all other groups

'b' $p<4 \times 10^{-6}$ PM10+RSV vs. RSV

'c' $p<1 \times 10^{-6}$ RSV+PM10 vs. RSV

'd' $p<3 \times 10^{-6}$ PM10+RSV vs. RSV+PM10

Effect of PM10-RSV interaction on IL-8 production

IL-8-like proteins released into cell supernatants were detected by ELISA. The levels of IL-8-like proteins produced by AM are summarized and presented in Figure 8.9. As in the production of IL-6-like proteins, AM that were exposed to RSV alone produced the most IL-8-like proteins compared to all other groups ($p<0.009$). Negative control AM produced a mean baseline level of 256.2 pg/mL IL-8-like proteins per million AM. Exposure of AM to PM10 significantly suppressed baseline IL-8 production (PM10 vs. NEG: (45.4 ± 14.5) vs. (256.2 ± 66.7) , $p<0.009$) as well as that of RSV-induced IL-8 production ($p<0.003$). In contrast to IL-6 expression, IL-8 expression by guinea pig AM was not influenced by the sequence of exposure to PM10 and RSV.

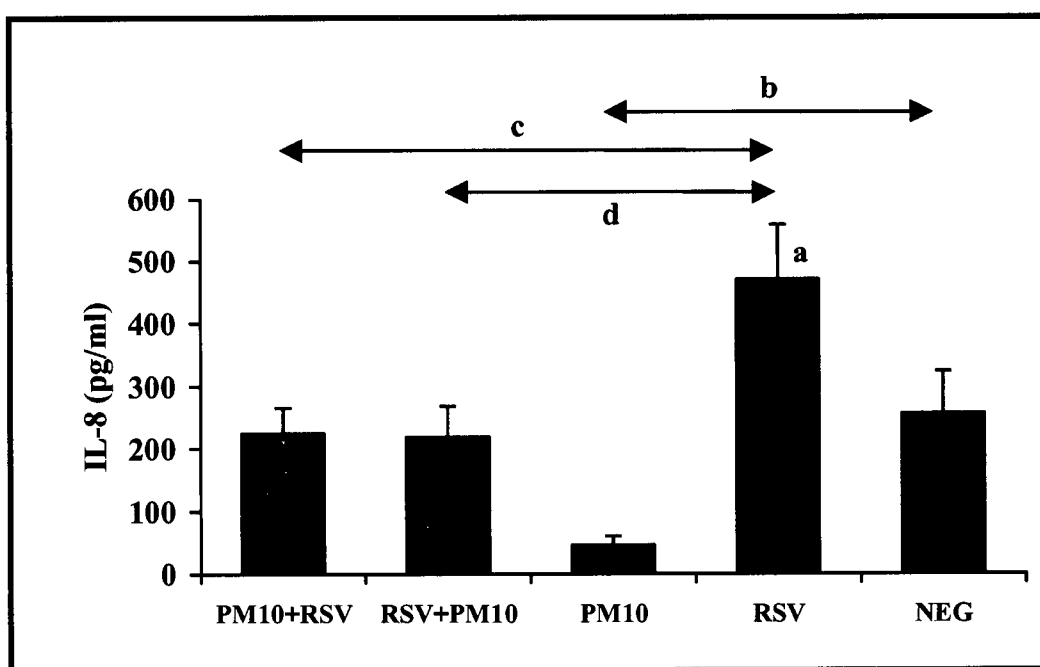


Figure 8.9 Effect of PM10-RSV interaction on IL-8 production by AM.

Data represent IL-8-like protein (mean \pm SD) released by AM subjected to different treatments.

'a' $p<0.009$ RSV vs. all other groups

'b' $p<0.009$ PM10 vs. NEG

'c' $p<0.003$ PM10+RSV vs. RSV

'd' $p<0.003$ RSV+PM10 vs. RSV

Effect of PM10-RSV interaction on TNF α production

TNF α released into cell supernatants were detected by bioassay of L929 cells. The levels of TNF α produced by AM are summarized and presented in Figure 8.10. The data showed that AM production of TNF α was significantly upregulated when these cells were exposed to RSV, PM10 or a combination of both agents ($p<0.02$). There were no differences in the production of TNF α by AM among different treatments. AM exposed to both RSV and PM10 did not exhibit synergistic or inhibitory effect on TNF α levels from interaction of the two agents.

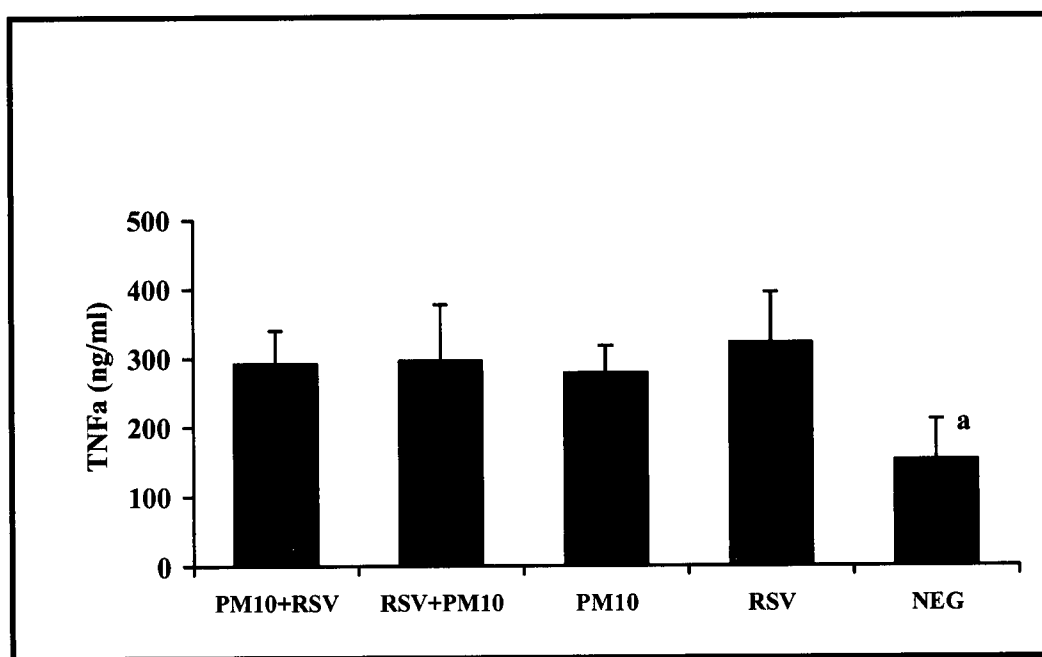


Figure 8.10 Effect of PM10-RSV interaction on TNF α production by AM.
Data represent TNF α (mean \pm SD) released by AM subjected to different treatments.
'a' $p<0.02$ NEG vs. all other groups.

Summary of Results

The results obtained in this study are summarized thus: Pre-exposure of AM to PM10 significantly reduced the proportion of RSV-immunopositive cells, inhibited RSV replication within infected cells and suppressed the expression of RSV-induced IL-6 and IL-8 proteins. As for RSV-infected AM that were subsequently treated with PM10, RSV replication, RSV Yield and RSV-induced IL-6 and IL-8 production was similarly reduced despite the relatively higher proportion of RSV-immunopositive cells which indicate that synthesis of viral proteins has been initiated.

DISCUSSION

The working hypothesis of this study is that the AM response to the interaction of RSV and environmental particulates is dependent on the sequence in which the cells are exposed to these agents. Specifically, we postulated that initial exposure of AM to PM10 results in cytokine secretion that may decrease the ability of AM to fend off RSV infection. In contrast, the initial exposure of AM to RSV may potentiate the secretion of cytokines in response to subsequent exposure to PM10. The experiments in this study represent a direct and sequential exposure of 2 environmental agents, RSV and PM10, to isolated AM in an *in vitro* system. An initial exposure of AM to PM10 followed by RSV infection performed in *in vitro* experiments represent the study of AM (obtained by bronchoalveolar lavage) from individuals who live in high pollution environment and subsequently contracting RSV disease. On the other hand, an initial exposure of AM to RSV followed by PM10 in an *in vitro* system may be analogous to the study of AM from RSV-infected individuals who are subsequently exposed to an acute episode of high particle concentration.

*PM10+RSV: Model of RSV infection of individuals living in high pollution areas**Does PM10 protect against RSV infection?*

Epidemiological studies have indicated that the prevalence of RSV infection and atopy is higher in urban compared to rural areas (218, 219). The experimental design of this study, specifically the sequential exposure of PM10 and RSV, allows the comparison of the PM10+RSV group (modeling RSV infection of individuals in high pollution areas) to the RSV group (modeling RSV infection in rural dwellers). Comparison of data obtained between the PM10+RSV versus RSV groups indicate that the pre-exposure of AM to PM10 prior to RSV infection results in reduction of RSV uptake, replication and yield as well as decrease in IL-6 and IL-8 production.

The ability of AM to support RSV infection was studied on the basis of its ability to synthesize viral proteins and support intracellular viral replication. The apparently lower RSV Yield and quantity of RSV progeny in the PM10+RSV group compared to the RSV group may be consequences of a lower proportion of RSV-immunopositive AM. Although the mechanisms responsible for reduced immunofluorescent staining of RSV antigens in PM10+RSV versus RSV are unclear, it has been suggested that exposure of AM to PM10 causes impairment of phagocytosis of RSV by these cells (193). Ingestion of environmental particles by human and rat AM have been demonstrated to impair phagocytosis of silica particles specifically at the attachment and internalization steps (245, 246). Similar impairment of phagocytosis by ultrafine particles has also been demonstrated in a macrophage cell line (247). In retrospect, additional experiments involving the examination of RSV mRNA and protein expression in AM at earlier time points (e.g. T=0, 2, 4, 8 and 12 hours after exposure of AM to both agents) might provide more insight on the phagocytosis of RSV following PM10 exposure.

We studied the cytokine response of AM following exposures to PM10 and RSV by examining the production of proinflammatory cytokines IL-6, IL-8 and TNF α . Stimulation of

these cytokines by environmental particulates had been reported in AM from humans and rats (193, 236). However, the presence of endotoxin in the particulate preparations used by these investigators was demonstrated by a partial inhibition using polymyxin B. In this study, guinea pig AM responded to PM10 by production of TNF α but not IL-6 or IL-8. As indicated earlier, the batch of PM10 in our hands contained minute traces of endotoxin (0.05 EU/100 μ g PM10) that was not sufficient to induce a cytokine response. Hence the TNF α response of guinea pig AM to particulate stimulation must be due to components of PM10 other than contaminating endotoxins. It is not clear whether the different particulate-induced cytokine response observed in this study, when compared to results of previous studies (193, 236), is due to species differences and/or increased concentration of endotoxin in the preparation of environmental particulates.

In vitro studies by Li and colleagues (248) demonstrated that bronchoalveolar lavage leukocytes from rats following intratracheal instillation of PM10 produced greater amounts of NO and TNF α than BAL leukocytes from control animals. Although the production of NO has not been investigated in the present study, the production of bioactive TNF α release from AM in the two groups, PM10+RSV and RSV, are increased in similar amounts compared to unexposed AM (NEG group). Recent studies demonstrate that NO functions in an anti-inflammatory capacity to modulate inflammatory response in human AM (196). RSV induction of the inducible nitric oxide synthase (iNOS) gene has been demonstrated in epithelial cells (249). Cytokines such as IFN γ , IL-1 β and TNF α have been shown to enhance iNOS induction in both untreated and RSV-treated A549 cells (249, 250). Enhanced iNOS gene expression and NO production have been reported in an *in vitro* Hepatitis B virus infection model (251). Many studies now suggest an anti-viral role for NO (252). Activation of cellular NOS activity has been associated with inhibition of viral replication in *in vitro* models of poliovirus (253), vaccinia

virus (254), coxsackievirus (255), and rhinovirus infections (256). However, the possible anti-viral role of NO induced by PM10 on RSV infection and replication in AM requires further investigation.

Besides reduction in viral replication, analysis of the data for PM10+RSV versus RSV groups also indicated a suppression of RSV-induced IL-6 and IL-8 in AM that were pretreated with PM10. The results in this study demonstrated RSV stimulation of IL-6, IL-8 and TNF α in guinea pig AM and are consistent with previously reported studies (114, 116, 117). RSV infection of PM10-treated AM stimulated equivalent amounts of bioactive TNF α as in untreated AM. However, the levels of IL-6 and IL-8 proteins were significantly downregulated in the PM10-treated AM than untreated cells. Reduced expression of IL-6 and IL-8 is likely a consequence of reduced load of infectious virus, as reflected by decreased RSV Yield. While reduced production of these mediators could potentially minimize structural damage in the lung, it is not certain if recruitment of granulocytes and lymphocytes to the sites of infection and consequently virus clearance could be hindered. Data from *in vivo* experiments are required to provide further insights on this issue.

Since suppression of RSV-induced proinflammatory cytokines could potentially minimize destruction of surrounding tissue *in vivo*, and reduction in virus yield suggest decreased virus activity and virus load, PM10 may play a protective role against *in vitro* RSV infection in AM. On the other hand, in the complexities of an *in vivo* system, the suppression of RSV-induced proinflammatory cytokines and reduction in RSV Yield may reflect a hindered recruitment of second line of defense as well as virus clearance. Therefore the possibility of a protective role of PM10 in RSV infection *in vivo* requires further elucidation.

Does RSV infection exacerbate a pre-existing PM10-induced inflammation?

Comparison of results between PM10+RSV and PM10 groups indicates that the presence of the second stimulus, RSV, stimulated increased IL-6 and IL-8 expression. These findings suggest a pathogenic role for RSV in our *in vitro* model. Future animal studies using a similar experimental design are needed to provide clues to explain the observed differences in the prevalence of RSV infection and atopy between communities of different pollution levels.

RSV+PM10: Model of RSV-infected individuals subjected to acute pollution

Does RSV protect against effects of acute PM10 exposure?

The ability of AM to phagocytose PM10 was measured indirectly by the granularity (side scatter) of the cell. Cell granularity data in the PM10 group versus RSV+PM10 group indicate that phagocytosis of PM10 by AM is not affected by a pre-existing RSV infection. Previous studies have shown that RSV infection in AM can inhibit the ability of the cell to phagocytose *Saccharomyces cerevisiae* (114). Species specificities of AM and the type of particulate matter being phagocytosed are two factors that might explain the differences between the present data and the previous reports (114). Exposure of RSV-infected AM to PM10 resulted in higher levels of IL-6 and IL-8 in comparison to PM10-exposed AM. These data suggest a pathogenic role for *in vitro* RSV infection in AM.

Does exposure to PM10 exacerbate a pre-existing RSV-induced inflammation?

The present data show that PM10+RSV (i.e. Model of RSV infection of individuals in high pollution areas), the RSV Yield and quantity of RSV progeny in the RSV+PM10 group was significantly reduced compared to RSV-infected AM. In contrast to the PM10+RSV group, the proportion of RSV-immunopositive in RSV+PM10 group is similar to AM that were exposed to RSV alone. While PM10 treatment of RSV-infected AM has no inhibitory effect on cellular

synthesis of viral proteins, it has the potential to suppress viral propagation. Although the mechanisms for this effect are uncertain, others have postulated that particulate-induced immune response may constitute an antiviral effect (85).

As mentioned previously, this reduced cytokine expression is likely a reflection of the viral load. Studies examining cytokine production by RSV-infected AM indicate that transcription of RSV induced IL-6, IL-8 and TNF α occurs within 1 hour after interaction with RSV (116). PM10 treatment of RSV-infected AM resulted in suppression of IL-6 and IL-8 production, suggesting that PM10 inhibition of these proteins may target the translational stage of cellular protein synthesis.

Overall, the exposure of RSV-infected AM to PM10 reduced the expression of inflammatory cytokines (IL-6 and IL-8) as well as the propagation of RSV progeny and viral load, all of which implicate a protective role for PM10. Although the manipulation of the order of stimuli to guinea pig AM in an *in vitro* system may represent an oversimplified analogy to the biological system, this study began by the examination of 2 different scenarios: RSV infection of individuals living in high pollution areas (PM10+RSV) and RSV-infected individuals exposed to an episode of acute pollution (RSV+PM10). Interestingly, the results from both scenarios suggest a pathogenic role for RSV and a protective role for PM10.

CHAPTER 9

EXPRESSION OF PROTEIN KINASES IN RSV INFECTION

INTRODUCTION

Like many other viruses, RSV could cause dysfunction in the immune system through activation of cytokine genes and consequently these cytokines cause inflammation and injury in the lung (257). We have been interested in IL-6, IL-8 and TNF α and current evidence have indicated that these proinflammatory cytokines could regulate macrophage gene expression (258). While research in signal transduction has been extensively investigated in epithelial cells, it is a relatively new avenue in RSV research. The intention of this introduction is to review current knowledge of signal transduction in RSV research, provide an overview of potentially related pathways and controversial issues.

RSV activation of NF κ B

The regulation of numerous RSV-induced mediators including the cytokines IL-6, IL-8 (89, 259), IL-11 (260), the chemokine RANTES (261) as well as the adhesion molecule ICAM-1 (262) has been shown to be modulated by activation of the transcription factor NF κ B. NF κ B was originally identified in 1986 as a nuclear factor that bound to the enhancer element of the immunoglobulin (Ig) κ light chain gene (263). In unstimulated cells, NF κ B is bound to its inhibitor I κ B and is maintained in the cytosol in an inactive form (264, 265). Upon cellular stimulation, phosphorylation and degradation of I κ B results in the release of NF κ B and its translocation to the nucleus where it may interact with specific binding sites in the promoter region of a number of genes. The activated NF κ B participates in a variety of cellular processes, such as activation of cytokine genes, stress response and apoptosis (266). NF κ B consists of 2

subunits of 50 kDa (p50) and 65 kDa (p65) and can function as homodimers or heterodimers (267). In the IL-8 promoter, NF κ B activates gene transcription by binding to its specific binding site as a p65 homodimer (268). On the other hand, activation of TNF α (269, 270) and IL-6 (271, 272) genes requires that NF κ B bind as a p50/p65 heterodimer. The role of NF κ B in apoptosis is an interesting one and depends on the cell and the signaling pathway. Studies by Baichwal *et al.* (273) showed that NF κ B suppressed TNF-mediated apoptosis. In contrast, activation of NF κ B was demonstrated to induce apoptotic cell death in Dengue virus-infected hepatoma cells (274). Currently, whether RSV induces or inhibits apoptosis remains controversial (see section on RSV and apoptosis below).

Using alveolar epithelial cells Garofalo *et al.* demonstrated that RSV infection induced transcriptional activation of the IL-8 gene and that translocation of the p65 component of NF κ B (also known as Rel A) from the cytosol to the nucleus was necessary for gene expression (275). Fiedler *et al.* (262) and Mastronarde *et al.* (276) independently demonstrated that viral replication is required for NF κ B activation in RSV-induced cytokine expression. These findings led to the proposal that activation of IL-8 gene may be a mechanism involved in the production of airway mucosal inflammation (275). Subsequently, other investigators demonstrated that the transcription factors NF κ B and NF-IL6 were essential in the regulation of IL-8 gene activation following RSV infection (259, 262, 277). In addition, subsequent studies demonstrated that the cooperative interaction between NF κ B and either AP-1 (89) or NF-IL-6 (278) was important in the activation of IL-8 after RSV infection. In a recent study (279) using promoter deletion and mutagenesis experiments, a novel upstream response element (termed as RSV response element (RSVRE) by the authors) was identified as a requirement for RSV-induced IL-8 transcription; however, the identity and source of the protein binding to this RSVRE remains unknown. Moreover, a role for the RSV P protein has been suggested in the long term activation of NF κ B

(280). Several upstream activators of NF κ B have been identified. These include the ring-finger interacting protein (RIP – a death domain containing serine/threonine kinase) and members of the TNF-receptor associated factors (TRAF) family of proteins (TRAF-2, -5, -6, which mediate responses associated with TNF-receptor family members) and the IL-1 type I receptor (281, 282). Furthermore, NF κ B activation has been associated with a few major signaling pathways including the mitogen-activated protein kinase (MAPK), protein kinase B (PKB/Akt) (283, 284) and the Toll receptor (285, 286) signaling pathways. In the existence of the numerous combinations of multiple stimuli and divergent signaling pathways, the mechanisms involved in activation of NF κ B induced by RSV infection remains to be characterized.

Activation of MAPK pathway by RSV

Viral infections of cells have been associated with activities of MAPKs. Examples include activation of ERK2 (extracellular signal-regulated kinase) during Hepatitis B virus infection of Chang liver cells (287, 288) and during adenovirus infection of HeLa cells (289). Chen *et al.* (290) were the first to demonstrate that activation of ERK2 by RSV infection may be one of the mechanisms that result in the production of IL-8. ERK belongs to the family of MAPKs signal transduction pathways that mediate effects of various extracellular stimuli on signaling pathways in the cells (291, 292). Other members of the MAPK pathway family, p38 and JNK (c-jun N-terminal kinases), are not activated by RSV infection of A549 cells (290, 293). There are multiple levels of control in MAPK cascades: MAPKs are activated by upstream kinases (known as MAPK/Erk Kinases or MAPKK or MEK) which are in turn activated by additional upstream kinases (known as MAPKK kinases or MAP3K) such as the oncogene product Raf (294). Recent studies (295) from the laboratory of Hunninghake focused on upstream events involved in ERK activation by RSV. Monick *et al.* (295) found that RSV infection activated MEK through multiple isoforms of PKC in epithelial cells in a biphasic

pattern: immediately following RSV binding and later during active viral replication. RSV binding was demonstrated to induce early activation but transient expression of ERK via PKC ζ activation of MEK. During RSV replication, the activation of ERK was more sustained and was activated through Raf-1 activation of MEK via multiple Ca²⁺-dependent isoforms of PKC (α , β 1, β 2, and γ). Although the concerted efforts and results of various research laboratories have clearly indicated the crucial role of the PKC-Raf-MEK-ERK MAPK signal transduction pathway during RSV infection of epithelial cells, events upstream of PKC, events downstream of ERK and the association (or lack thereof) with NF κ B have yet to be determined.

RSV and Apoptosis

Apoptosis is thought to be a major defense mechanism by the mammalian immune system for virally infected cells to eliminate viral proteins and nucleic acids without inducing an inflammatory response (296). While the evidence for induction of apoptosis by certain viruses exists, other viruses have acquired the ability to evade apoptotic destruction. For example, apoptosis is a major mode of cell death due to HIV-1 (297, 298) and influenza virus infections (299, 300). However, since cell survival is advantageous to the virus whose replication and survival is dependent on host cell viability, many viruses have elaborate strategies to evade apoptosis. DNA viruses, such as herpesvirus, poxvirus and insect baculoviruses encode viral proteins to prevent apoptosis triggered by p53 activation (301, 302). The EBV and Adenovirus encode viral gene products, BHRF1 and E1B/19kDa respectively, that are homologues of the Bcl-2 protein, a major inhibitory molecule that blocks the apoptotic pathway (303, 304). The myxomavirus-encoded TNF-receptor homologue, M-T2, functions as a secreted glycoprotein that blocks the activity of TNF and also functions as an intracellular effector that inhibits apoptosis in myxomavirus-infected cells (305).

The evidence on RSV regulation of apoptosis in lung epithelial cells has been somewhat conflicting. The work by O'Donnell *et al.* (306) demonstrated that RSV infection directly resulted in cellular apoptosis of A549 cells through upregulation of Fas mRNA as well as protein. Subsequent studies by Bitko *et al.* (307) confirmed RSV-induced apoptosis in A549 cells. Furthermore, they showed that RSV-induced apoptosis is independent of NF κ B activation and is associated with increased expression of caspase-12, an endoplasmic reticulum-specific stress-activated caspase (307, 308). By contrast, there is also mounting evidence that RSV inhibits cellular apoptosis. Takeuchi *et al.* (309) demonstrated that RSV infection induced mRNA and protein expressions of IL-1 β converting enzyme (ICE) and its transcriptional activator interferon regulatory factor (IRF-1). However, despite enhanced expression of CPP32 (caspase-3, a key protein that stimulates apoptosis (310)), Takeuchi *et al.* were not able to demonstrate apoptosis in the RSV-infected cells (309). Further evidence for RSV inhibition of TNF α -induced apoptosis came from the laboratory of Domachowske *et al.* (311). By means of differential display reverse-transcriptase polymerase chain reaction, Domachowske *et al.* demonstrated that RSV-mediated inhibition of apoptosis is associated with increased expression of the IEX-1L gene. The IEX-1L gene was originally cloned as a radiation-inducible early response gene (312). The IEX-1L protein is now recognized as an apoptosis inhibitor involved in NF κ B-mediated cell survival (313). Since induction of the IEX-1L gene is dependent on RSV replication and is not a universal response to viral infections, it was postulated that RSV proteins might participate in transactivation of the IEX-1L gene (311). In addition, others have used methods such as TUNEL assay and immunophenotyping to quantify apoptosis, and demonstrated that RSV-infected peripheral blood mononuclear cells isolated from cord blood and from adults are protected from apoptosis (314). Whether this inhibition of apoptosis by RSV is specific for mononuclear cells requires further investigations. Both laboratories, that of O'Donnell and coworkers as well as Bitko and associates, have attempted to explain the differences in ability to

demonstrate RSV-induced apoptosis in A549 cells compared to that of Takeuchi *et al.*(309); suggestions offered included differences in virus virulence, cell line used and methodology used in detection of apoptosis. Regardless of these plausible explanations, the controversy regarding the role of RSV in the regulation of apoptosis in A549 cells remains unresolved.

Summary

The current data on signal transduction in RSV infection indicate a strong association between RSV infection and activation of the transcription factor NF κ B, a significant role in the PKC-Raf-MEK-ERK MAPK cascade and a controversial role of RSV in the regulation of cellular apoptosis. Much more investigation will be required to understand the complex network of signaling molecules involved in RSV infection. The purpose of this study was to utilize a megascreening technique (KinetworksTM Protein Kinase Screen (PKS-1.0)) to examine the signal transduction pathway(s) involved in RSV infection of guinea pig AM.

HYPOTHESIS AND SPECIFIC AIMS

On the basis of the rationale presented, the **Working Hypothesis** of this study is:

RSV infection of guinea pig AM results in differential expression of intracellular protein kinases that may be involved in molecular mechanisms of virus-cell interaction.

The **Specific Aims** of this study are:

1. To determine and compare the expression of protein kinases in guinea pig AM in response to *in vitro* RSV infection by the PKS-1.0.
2. To delineate potential pathway(s) regulating the activation of guinea pig AM in response to *in vitro* RSV infection.

EXPERIMENTAL PROTOCOLS

Study Design

The design of this study is depicted in Figure 9.1. Briefly, female guinea pigs (n=4) were euthanized by an overdose of sodium pentobarbital (i.p.) and heterogeneous AM were obtained by *in situ* bronchoalveolar lavage. The cells from all 4 animals were pooled together and plated onto 15 cm tissue culture plates (Corning) in RPMI containing antibiotics. The cells were allowed to adhere to the plastic for 30 minutes and excess floating cells were washed off. The AM were exposed to RSV at an m.o.i. of 3 for 90 minutes and after washing off unadsorbed virus, the cells were incubated overnight at 37°C, 5% CO₂. An equal proportion of AM was set aside as sham-infected control in which RPMI medium was used instead of the virus.

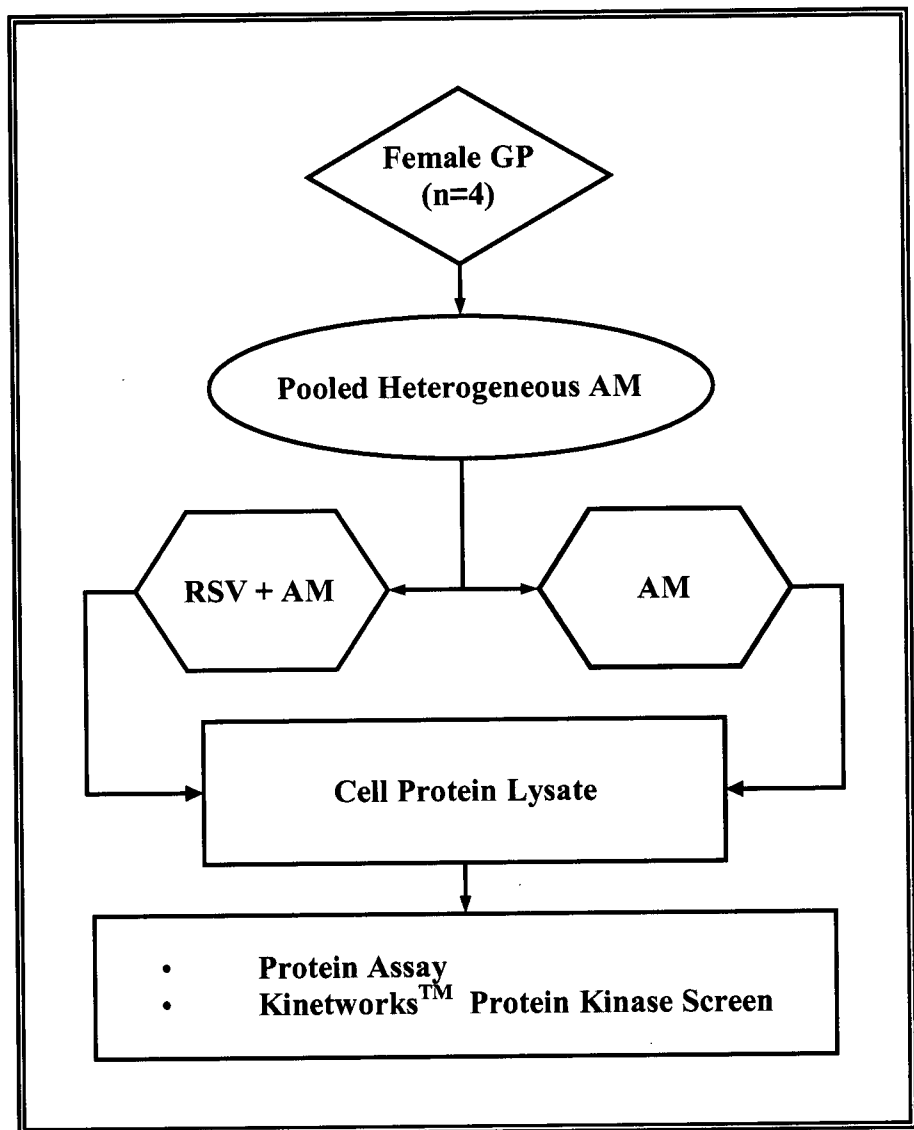


Figure 9.1 Experimental design for detection of protein kinase expression in RSV-infected guinea pig AM.

Cell Lysate Preparation

Eighteen hours following RSV infection, the AM were scraped and pooled into a pellet in a 50 mL Falcon tube by refrigerated centrifugation at 5,000 $\times g$ for 5 minutes. Excess medium was decanted and the cells were lysed in 0.5 mL of ice-cold lysis buffer¹³ was added to each sample. The cells were sonicated twice for 15 seconds each time using the VibraCell™ probe sonicator set at 80% of maximum output. The resultant homogenate was subjected to ultracentrifugation for 30 minutes at 100,000 $\times g$ using the Optima™ TL ultracentrifuge (Beckman Instruments Inc., Palo Alto, CA). The resulting supernatant fraction was removed and the protein concentration was assayed immediately. As per Kinexus protocol, the protein concentration of each sample was adjusted to 1 mg/mL in SDS-PAGE Sample buffer¹⁴ and boiled for four minutes at 100°C prior to shipping to Kinexus Bioinformatics Corporation.

Additional controls using the human epithelial cell line, HEp-2 cells (RSV-infected and sham-infected), were included in this study. HEp-2 cells were used because of the high rate of RSV infection and to ensure specific detection of protein kinases by the KPKS-1.0.

Protein Assay

The protein concentrations of cell extract samples were determined using the DC Protein Assay kit (Bio-Rad Laboratories, Mississauga, ON, Canada) with bovine serum albumin (BSA) as a protein standard. This is a colorimetric assay for protein concentration following detergent solubilization and is modified from that of Lowry *et al.* (316). The assay is based on the reaction between protein and copper in an alkaline medium whose product is responsible for reduction of

¹³ The lysis buffer as recommended by Kinexus Bioinformatics Corporation contained 20 mM MOPS (pH7.2), 5 mM EGTA, 2 mM EDTA, 5 mM sodium fluoride, 40 mM β-glycerophosphate (pH 7.2), 1 mM sodium orthovanadate, 1 mM phenylmethylsulfonylfluoride, 3 mM benzamidine, 5 μM pepstatin A, 10 μM leupeptin and 0.5% Nonidet P-40.

¹⁴ The SDS-PAGE Sample buffer as recommended by Kinexus Bioinformatics Corporation contains 50mM Tris-HCl (pH 6.8), 2% SDS (w/v), 25% glycerol (v/v), 0.7 M (5%) β-mercaptoethanol and 0.1%bromophenol blue (w/v) (315).

the Folin reagent. The protein concentration of the sample can be measured by its correlation to the quantity of reduced Folin species that have a characteristic blue color with maximum absorbance at 750 nm (317).

A microplate assay protocol was used for quantification of protein concentration in the cell extract samples. Six dilutions of the BSA standard (0, 62.5, 125, 250, 500 and 1000 µg/mL) and three dilutions of samples (Undiluted, 1:2, 1:4) were prepared using a 0.1% SDS solution. Five µL of each protein standard and sample were pipetted into individual wells of a clean, dry 96-well microtiter plate. Reagent A was used at a working concentration of 1:50 and 25 µL were added into each well. Finally 200 µL of Reagent B was added into each well and the microtiter plate was gently agitated to mix the reagents. The reagents were incubated at room temperature for 15 minutes. The absorbance was read at 750 nm using a microplate reader. A standard curve was obtained by plotting the A_{750} against the concentrations of the BSA standards. The equation of the best-fit line was determined mathematically and the concentration of each sample can be calculated based on its A_{750} reading measured and the best-fit equation.

Western blot

Expression of protein kinases was assessed by Western blots. This part of the study was contracted out and performed by Kinexus Bioinformatics Corporation (Vancouver, BC, Canada) using the Kinetworks™ Protein Kinase Screen (KPKS-1.0) which tracks the expression of 86 protein kinases. Briefly, the cell lysate of each sample was separated on 12.5% SDS-PAGE gels and the proteins were transferred onto nitrocellulose membranes. The blots were blocked against non-specific binding with 5% (w/v) non-fat dried milk and probed with cocktails of multiple primary antibodies against specific protein kinases. (The source of antibodies used in KPKS-1.0 is considered as intellectual property of Kinexus and is not revealed by the Company.) After washing, antigen-antibody immune complexes were detected with goat anti-rabbit IgG

conjugated with horseradish peroxidase for an hour. Signals due to specific binding were detected using the enhanced chemiluminescence (ECL) detection system (Amersham, Arlington Heights, IL). Images from ECL autoradiograms were captured using Adobe software. The relative abundance of protein kinases present in a sample is measured using a high-resolution scanner that detects chemiluminescence. Finally, the relative abundance of each detected immunoreactive protein is quantified and this information is provided by Kinexus to the customer in an Excel spreadsheet.

RESULTS

The KPKS-1.0 measures a total of 86 protein kinases. Cell lysates were prepared (as per Kinexus protocol) from control and RSV-infected cells (HEp-2 and guinea pig AM) and were sent for analysis. The data resulting from the screen are summarized in Table 9.1. Of the 86 protein kinases tracked, 61 were detected in cell lysates from guinea pig AM. Similarly 42 protein kinases were detectable in the preparation from HEp-2 cells. Of the protein kinases detected, 32 from guinea pig AM and 30 from HEp-2 cells were modulated. All 30 detectable protein kinases in HEp-2 cell lysates were downregulated. As for the detectable protein kinases from guinea pig AM lysates, 19 of them demonstrated a reduction in expression and the expression of the remaining 13 protein kinases were enhanced. A representative blot scan of RSV-infected guinea pig AM is shown in Figure 9.2. The intensity of each band of protein kinase detected in lysates from guinea pig AM was measured as relative counts and are presented in the Appendix. Table 9.2 summarizes the relative expression of protein kinases detected in guinea pig AM lysates following RSV infection.

Table 9.1 Summary of data from KPKS-1.0

| Changes in Expression | No. of Protein Kinases (& isoforms) in AM | No. of Protein Kinases (& isoforms) in HEp-2 cells |
|-----------------------|---|--|
| Downregulation⊗ | 19 | 30 |
| Upregulation⊗ | 13 | 0 |
| Insignificant changes | 29 | 12 |
| No signal☒ | 25 | 44 |
| Total | 86 | 86 |

⊗, ⊖ By a difference of at least 30% in comparison to control cells.

☒ Expression of protein kinases not detected in control cells.

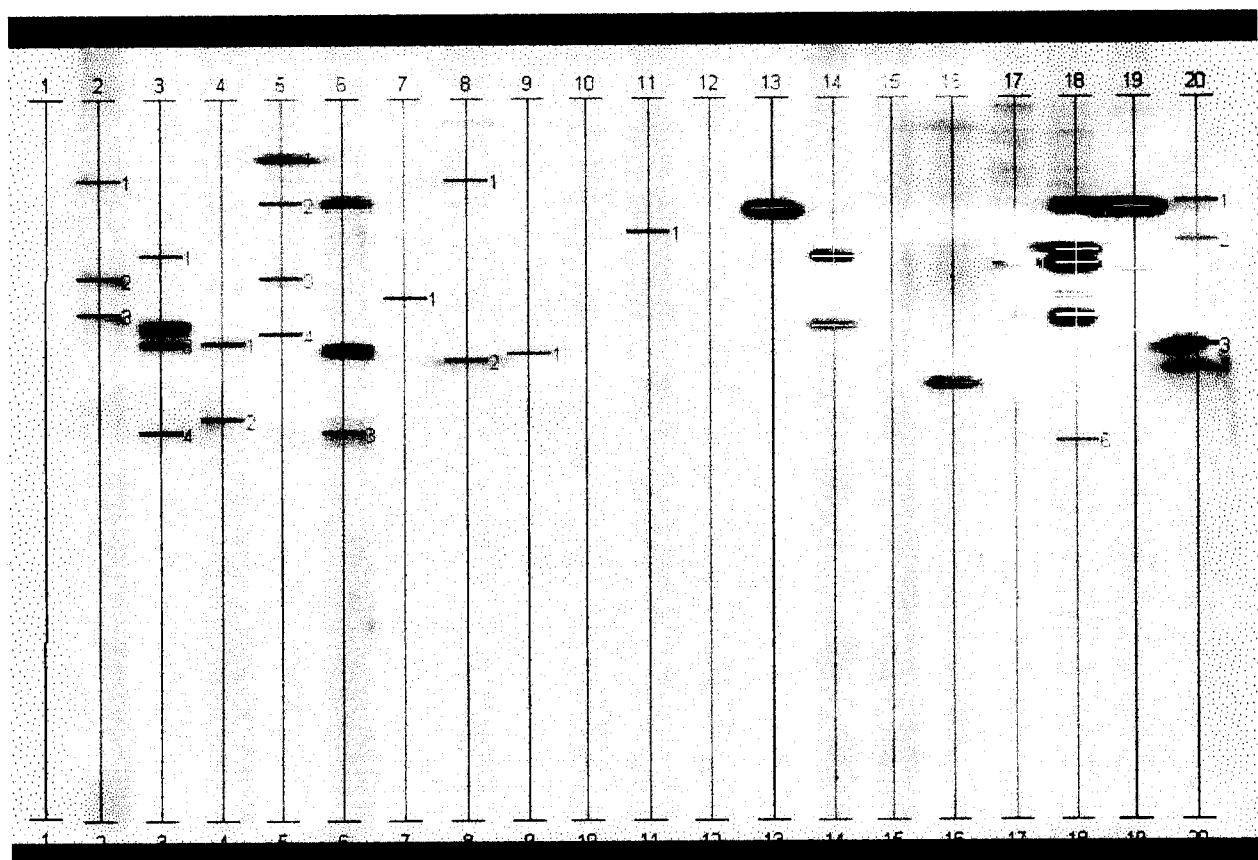
**Figure 9.2** Representative autoradiogram of the KPKS-1.0.

Table 9.2 Protein kinases detected in guinea pig AM following RSV infection.

| Downregulation | | | Upregulation | | |
|----------------|---------|---------|--------------|---------|-----------|
| <30% | 30-50% | >50% | <30% | 30-50% | >50% |
| Lyn | ERK1-B1 | Cdk2 | ♣ERK1-A2 | ERK2-B1 | Ck4 |
| PKCζ | GRK2 | Cdk7 | ERK2-A3 | | Ck2α |
| | p38α | Ck2α' | Fyn-U | | ♣ERK2-A2 |
| | p90 S6K | Fyn-L | p43 | | FAK |
| | | Hpk | | | MEK1 |
| | | ♣JAK1 | | | p70 S6K L |
| | | ♣MEK6 | | | PKBα |
| | | p52 S6K | | | Rsk2 |
| | | PAKα | | | |
| | | PKC β1 | | | |
| | | RAF1 | | | |
| | | Rsk1 | | | |
| | | ZIPK | | | |

♣ Data confirmed by a different vendor using similarly treated cells.

DISCUSSION

The working hypothesis for this study is that RSV infection of guinea pig AM affects intracellular protein kinases involved in molecular mechanisms of virus-cell interactions. The objectives of this study were to determine which kinases are expressed in guinea pig AM and to determine changes in the expression of the protein in response to *in vitro* RSV infection by a "blast" screen method. As a first step, these studies may help to delineate potential pathway(s) involved in the activation of these cells as a consequence of the viral infection.

The data in this "blast" screen were obtained for one time point, at 18 hours post-infection, when late signals and/or signals that were activated and sustained over long periods could be detected. Therefore early and transient events were not examined in this analysis. Expressions of protein kinases were detected in RSV-infected AM and the control cell line, HEp-2 cells. Protein kinases in RSV-infected HEp-2 cells at 18 hours post-infection were predominantly downregulated. Trypan blue exclusion test on these cells indicated viability of over 95%, suggesting that while most of the cells are viable, 18 hours post-infection is not a suitable time point to detect upregulation of protein kinases induced by RSV infection. Since activation of protein kinases could occur very fast (seconds to minutes) following receptor-ligand binding, future studies of protein kinases in RSV infected HEp-2 cells should be carried out at earlier time points. In addition, it would be useful to test for the activities of kinases that show changes in expression. Protein kinases with phosphorylation activities at earlier times may act as key regulators in signaling cascades. Nonetheless, in this study, the HEp-2 cells indicated that the KPKS 1.0 is a feasible method for detecting expression of protein kinases in RSV-infected guinea pig AM.

Both upregulation as well as downregulation of protein kinases were detected in RSV-infected AM. This suggests that the kinetics of RSV infection in guinea pig AM versus HEp-2 cells is quite different. From the data summarized in Table 9.2, several important pathways and

cross-talk between these pathways could be indicated. In this discussion, I would like to focus on 2 major pathways: (1) Mitogen-activated protein kinase (MAPK), and (2) Protein kinase B (PKB/Akt).

(1) The MAPK pathway

The data in this study clearly indicated RSV-induced changes in components of the MAPK pathway. The amount of MEK increased by 3.5 fold and that of ERK2 increased by approximately 3.0 fold following RSV infection of AM. These data are interesting in light of the studies by Chen *et al.* (290), who demonstrated activation of MEK in RSV-infected A549 cells. In addition, these data confirmed the upregulation of MEK as demonstrated by Monick *et al.* (295) and emphasized the significance of the MEK-ERK MAPK pathway as proposed by them. However, in this “blast” screen, the two upstream components in the MEK-ERK pathway – PKC and Raf, that were activated by RSV infection (295) appear to be downregulated. This discrepancy could be due to an intended “feedback” mechanism that downregulates the upstream elements of the pathway. Alternatively, it may be due to a time factor in the design of the experiment and future studies with early time points might ascertain temporal consequences. In macrophages, TNF α plays an important role in initiating activation of the MAPK cascade by binding to the p55 TNF receptor (CD120) (318). Although a specific RSV response element has been identified in the IL-8 promoter (279), it is unclear whether MAPK expression is mediated directly by RSV or if a synergistic role of TNF-induced MAPK activation is implicated. Furthermore, whether the RSV G protein, which has structural homology to the TNF receptor (20), plays a role in this pathway remains to be elucidated.

In addition, the data in this study indicated that levels of Rsk, a substrate for ERK activation also increased. RSV-mediated activation of Rsk has not been reported (as of February 2002), an increase in the level of Rsk expression suggests that the potential involvement of this

kinase should be considered. Rsk belongs to a family of 90 kDa ribosomal S6 kinases and being a substrate of ERK, mediates MAPK signal transduction. The role of Rsk has been implicated in proliferation, differentiation and cell survival (319, 320). More specifically, and interestingly, Rsk is involved in regulation of gene expression via association and phosphorylation of numerous transcriptional regulators including NF κ B/I κ B α (321, 322). Shouten *et al.* demonstrated that I κ B α is a target for Rsk and phosphorylation of Rsk is essential for subsequent degradation of I κ B α (321). The role and the mechanisms of Rsk in regulation of RSV-induced expression of IL-6 and IL-8 via the MAPK pathway and activation of NF κ B require further investigation.

RSV interaction with host cells has been described as biphasic: viral binding which induces a transient activation of ERK through PKC ζ activation of MEK and viral replication which causes a more sustained activation of ERK through Raf activation of MEK (280, 295). Biphasic activation of host cell is not restricted to RSV. A similar phenomenon has been observed in Coxsackievirus B3 infection of HeLa cells; Luo *et al.* (323) demonstrated that the inhibition of MEK and ERK resulted in suppression of viral protein and replication as well as reduced cell apoptosis. As the protein lysates were prepared 18 hours post-infection, it is conceivable that the increased expressions of MEK, ERK and Rsk may be associated with late activation of AM by RSV. Future studies to inhibit RSV progeny release and determination of viral gene/protein involved in the facilitation of sustained activation of intracellular signal transduction will enhance the understanding of RSV-AM interaction and may contribute to therapies in RSV disease.

(2) The PKB pathway

In this study, RSV infection of AM induced increased expression of the protein kinases PKB α and p70 S6K. The activities of both these kinases were not detectable in control cells. So far neither the roles of PKB α and p70 S6K nor any signaling pathways involving these 2 protein kinases have been implicated in RSV-cell interaction.

PKB α , a multifunctional serine/threonine kinase (324, 325), plays a key role in insulin metabolism (326, 327), in cell survival mechanisms (328, 329) as well as in various forms of human cancers (330-333). Activation of the phosphatidyl 3-OH kinase (PI3K) has been utilized as a survival strategy by various forms of cancer cells; consequently this survival signal pathway is a major target for the development of inhibitors used in drug interventions (334, 335).

PKB was identified as the cellular homologue of the viral oncogene v-Akt from AKT8, a retrovirus found in rodent T-cell lymphoma (336). PKB is activated by various growth and survival factors and is a target of PI3K (337, 338). Following stimulation of growth factor receptors, PI3K is activated and generates phosphorylated phosphatidyl inositides (PI-3,4-P₂ and PI-3,4,5-P₃). These phosphoinositides bind with high affinity to the amino-terminal pleckstrin homology (PH) domain of PKB and recruits PKB to the plasma membrane (339). To fully activate PKB, subsequent phosphorylation of Thr308 in the activation loop and Ser473 in the carboxyl terminal hydrophobic site are required. The conformational change, as the result of the binding between the PH domain of PKB and PI-3,4-P₂/PI-3,4,5-P₃, unmasks the activation loop site and allows phosphoinositide-dependent kinase (PDK-1) phosphorylation at Thr308 (340, 341). While phosphorylation at Ser473 is essential for activation of PKB, despite extensive biochemical analyses, the upstream kinase for this hydrophobic site remains to be identified (342).

Cellular substrates downstream of PKB have been identified. These include the metabolic regulators glycogen synthase kinase 3 (GSK3) (326) and 6-phosphofructo 2-kinase

(PFK-2) (343), the Bcl-2 related apoptosis regulatory protein BAD (344, 345) as well as the ribosomal protein S6 kinase (p70 S6K) (338). These identified PKB substrates contain the sequence motif RxRyz(S/T)(hy) where x is any amino acid, y and z are small residues other than glycine and hy is a hydrophobic residue (346). The consequences of these activated PKB substrates include control of glycogen metabolism and suppression of apoptosis (347).

As alluded to earlier (see Introduction), apoptosis is a contentious issue in RSV research. The potential role of PKB in preventing apoptosis may provide insights to regulatory role of RSV in cellular apoptosis. Activated PKB promotes cell survival through various distinct pathways. PKB inhibits apoptosis by phosphorylating the pro-apoptotic Bcl-2 family member BAD. Uncoupling of BAD from the BAD/Bcl-X_L complex inhibits the apoptotic pathway. In addition, PKB can also suppress apoptosis via several other mechanisms such as phosphorylation of Caspase-9 (348), CREB (349), GSK-3 β (350), the Forkhead transcription factor FKHLR 1 (351) and I κ B kinase (352). Although it has been suggested that RSV-mediated apoptosis is independent of NF κ B (280) and unrelated to Caspase-9 (307), whether PKB can promote cell survival in RSV-infected cells via any of the other aforementioned mechanisms remains to be tested. Furthermore, whether a RSV protein can directly activate PKB via PI3K as seen in other viruses (353, 354) has yet to be determined. Therefore, examining the phosphorylation activity of PKB, particularly at the residues Thr308 and Ser473, may provide useful information.

The protein kinase p70 S6K deserves some attention in this study. *In vivo*, p70 S6K phosphorylates ribosomal protein S6 which plays a major role in the translation of mRNA transcripts encoding ribosomal proteins and protein synthesis elongation factors (355). p70 S6K is shown to be phosphorylated by PDK in a manner similar to PDK phosphorylation of PKB (356). Burgering *et al.* have demonstrated that p70 S6K is a target for PKB; however, other protein kinase(s) upstream of p70 S6K and downstream of PKB may be involved (338). More interestingly, p70 S6K has been found in complexes with protein phosphatase 2A (PP2A) (357).

Recent studies have indicated that the RSV P protein may play an important role in the persistent activation of NF κ B via its association with PP2A (280). Taken together, these data suggest that the role of the RSV P protein may have a more extensive role in virus-cell interaction than previously thought.

Summary

This “blast” screen has identified numerous protein kinases and potential signaling pathways that may be pertinent to the intracellular signal transduction activities during RSV infection of guinea pig AM. For the purpose of this thesis, the discussion focused on 2 major and distinct pathways (MAPK and PKB) and 3 protein kinases (Rsk, PKB and p70 S6K) whose potential involvements in RSV-mediated signal transduction are novel. The significance of the MEK-ERK MAPK pathway in RSV-infected cells was reiterated and a potential role for Rsk in this pathway and the regulation of NF κ B activation is implicated. It is conceivable that the PKB-p70 S6K pathway may provide further insights to the role of RSV in cellular apoptosis. Through the analysis of expressions of protein kinases, this discussion has highlighted the roles of a limited number of protein kinases; that of many other potential candidates (for instance PDK, FAK, CK2 etc.) have not been reviewed. It should be emphasized here that this study utilized the KPKS-1.0 which measured the relative abundance of protein kinases present in a sample. Although some of the protein kinases in SDS-PAGE gels indicated mobility shifts (changes in mobility due to phosphorylation are often correlated with changes in activity states), KPKS-1.0 does not measure kinase activity. Future experiments designed to examine the phosphorylation activities of these candidate protein kinases could improve our understanding of RSV-AM interaction. The availability of the completely sequenced RSV genome, comprehensive databases of signaling information, peptide libraries, protein-RNA, protein-DNA and protein-protein interaction systems, suggest a bright future for RSV research.

CHAPTER 10

CONCLUDING REMARKS

RSV infections represent a major source of morbidity in young children. Despite 46 years of research since its discovery, the numerous issues of controversies concerning the mechanisms of RSV-induced disease remain uncertain. Moreover, recent trends of the increasing incidence of RSV bronchiolitis are alarming. This thesis examines the interaction of RSV and guinea pig AM *in vitro*, where the conditions can be well controlled. The results confirm that RSV causes a productive infection in AM. On the basis of these experiments, several major findings were obtained and are summarized below.

1. Preferential RSV replication depends on the stage of cell maturation and age and sex of the host animal in our guinea pig model. These results reflect a similar phenomenon observed in humans, demonstrate the relevance of the guinea pig model and provide new insights at a cellular level. Further EM studies are needed to provide quantitative information on the abundance of lysosomes in AM subpopulations from animals of different age and sex groups. Additional studies examining the mechanisms by which RSV might evade host immunity will yield relevant information on persistence of RSV infection in guinea pig lung and probable persistence in humans.

2. The interaction of PM10 and RSV in guinea pig AM resulted in suppression of RSV replication, and RSV-induced cytokine production. The mechanisms involved in the uptake of PM10 resulting in the aforementioned AM response to RSV are unclear. Future studies to determine the potential antiviral role of NO, for example, may provide insights to the mechanisms involved in the interaction between PM10 and RSV. In addition, *in vivo* studies of sequential exposure of these agents will be valuable in

determining the significance of reduction of viral replication and RSV-induced cytokine expression in the complexity of the host organism and their effects on virus clearance mechanisms and lung pathology. Cell signaling studies may also provide valuable information on the activation of AM by RSV-PM10 interaction.

3. The MEK-ERK MAPK and PKB pathways, as indicated by expression of the corresponding protein kinase members play crucial roles in the response of AM to RSV infection. Future studies on activation of protein kinases in these pathways (in particular Rsk, PKB and p70 S6K) are needed to ascertain their significance in RSV-mediated signaling in AM and elucidate the mechanisms involved in RSV-induced cytokine production and the controversies of apoptosis in RSV-infected cells.

In conclusion, the studies in this thesis demonstrated that the AM response to RSV infection is dependent on intrinsic properties of the cell (i.e. maturation stage), host factors (i.e., age and sex) and environmental factors (for example, air pollution). The findings in this thesis, which form a basis for further studies on mechanisms of susceptibility to RSV infection, have provided new insights on RSV-AM interaction and the potential effects of these interactions on the pathogenesis of RSV disease in young children.

BIBLIOGRAPHY

1. Wohl MEB. Bronchiolitis in children. In: Epler GR, editor. Diseases of the Bronchioles. New York: Raven Press Ltd; 1994. p. 397-407.
2. Falsey AR, Walsh EE. Respiratory syncytial virus infection in adults. Clin Microbiol Rev 2000; 13(3):371-84.
3. Institute of Medicine. Prospect for immunizing against respiratory syncytial virus. In: Institute of Medicine. New vaccine development: establishing priorities. Washington, DC: National Academy Press; 1986. p. 299-307.
4. Shay DK, Holman RC, Newman RD, Liu LL, Stout JW, Anderson LJ. Bronchiolitis-associated hospitalizations among US children, 1980-1996. JAMA 1999; 282(15):1440-6.
5. Boyce TG, Mellen BG, Mitchel EF, Jr., Wright PF, Griffin MR. Rates of hospitalization for respiratory syncytial virus infection among children in medicaid. J Pediatr 2000; 137(6):865-70.
6. Stang P, Brandenburg N, Carter B. The economic burden of respiratory syncytial virus-associated bronchiolitis hospitalizations. Arch Pediatr Adolesc Med 2001; 155(1):95-6.
7. Officer. BCPH. A report on the health of British Columbians: Provincial Health Officer's annual report 1997. Feature report: The health and well-being of British Columbia's children. Victoria, B.C.: Minsitry of Health and Ministry Responsible for Seniors; 1998.
8. Sigurs N, Bjarnason R, Sigurbergsson F, Kjellman B. Respiratory syncytial virus bronchiolitis in infancy is an important risk factor for asthma and allergy at age 7. Am J Respir Crit Care Med 2000; 161(5):1501-7.
9. Sigurs N. Epidemiologic and clinical evidence of a respiratory syncytial virus-reactive airway disease link. Am J Respir Crit Care Med 2001; 163(3 Pt 2):S2-6.
10. Morris JAJ, Blount RE, Savage RE. Recovery of cytopathogenic agent from chimpanzees with coryza. Proc Soc Exp Biol Med 1956; 92:544-550.
11. Chanock RM, Finberg L. Recovery from infants with respiratory illness of a virus related to chimpanzee coryza agent. II. Epidemiological aspects of infection in infants and young children. Am J Hygiene 1957; 66:291-300.
12. Chanock RM, Roizman B, Myers R. Recovery from infants with respiratory illness of a virus related to chimpanzee coryza agent. I. Isolation, properties and characterization. Am J Hygiene 1957; 66:281-290.
13. Collins P, McIntosh K, Chanock R. Respiratory Syncytial Virus. In: Fields B, Knipe D, Howley P, *et al.*, editors. Fields Virology. Third ed. Philadelphia: Lippincott-Raven; 1996. p. 1313-1351.

14. Sullender WM. Respiratory syncytial virus genetic and antigenic diversity. *Clin Microbiol Rev* 2000; 13(1):1-15, table of contents.
15. McConnochie KM, Hall CB, Walsh EE, Roghmann KJ. Variation in severity of respiratory syncytial virus infections with subtype. *J Pediatr* 1990; 117(1 Pt 1):52-62.
16. McIntosh ED, De Silva LM, Oates RK. Clinical severity of respiratory syncytial virus group A and B infection in Sydney, Australia. *Pediatr Infect Dis J* 1993; 12(10):815-9.
17. Wang EE, Law BJ, Stephens D. Pediatric Investigators Collaborative Network on Infections in Canada (PICNIC) prospective study of risk factors and outcomes in patients hospitalized with respiratory syncytial viral lower respiratory tract infection. *J Pediatr* 1995; 126(2):212-9.
18. Arslanagic E, Matsumoto M, Suzuki K, Nerome K, Tsutsumi H, Hung T. Maturation of respiratory syncytial virus within HEp-2 cell cytoplasm. *Acta Virol* 1996; 40(4):209-14.
19. Collins PL, Hill MG, Camargo E, Grosfeld H, Chanock RM, Murphy BR. Production of infectious human respiratory syncytial virus from cloned cDNA confirms an essential role for the transcription elongation factor from the 5' proximal open reading frame of the M2 mRNA in gene expression and provides a capability for vaccine development. *PNAS* 1995; 92(25):11563-7.
20. Langedijk JP, de Groot BL, Berendsen HJ, van Oirschot JT. Structural homology of the central conserved region of the attachment protein G of respiratory syncytial virus with the fourth subdomain of 55-kDa tumor necrosis factor receptor. *Virology* 1998; 243(2):293-302.
21. Zhao X, Singh M, Malashkevich VN, Kim PS. Structural characterization of the human respiratory syncytial virus fusion protein core. *PNAS* 2000; 97(26):14172-7.
22. Garcia J, Garcia-Barreno B, Vivo A, Melero JA. Cytoplasmic inclusions of respiratory syncytial virus-infected cells: formation of inclusion bodies in transfected cells that coexpress the nucleoprotein, the phosphoprotein, and the 22K protein. *Virology* 1993; 195(1):243-7.
23. Ruuskanen O, Ogra PL. Respiratory syncytial virus. *Curr Probl Pediatr* 1993; 23(2):50-79.
24. Simoes EA. Respiratory syncytial virus infection. *Lancet* 1999; 354(9181):847-52.
25. Domachowske JB, Rosenberg HF. Respiratory Syncytial Virus infection: immune response, immunopathogenesis, and treatment. *Clin Microbiol Rev* 1999; 12:298-309.
26. Hall CB. Respiratory syncytial virus and parainfluenza virus. *N Engl J Med* 2001; 344(25):1917-28.

27. McConnochie KM, Hall CB, Barker WH. Lower respiratory tract illness in the first two years of life: epidemiologic patterns and costs in a suburban pediatric practice. Am J Public Health 1988; 78(1):34-9.
28. Bozzola M, Comoli P, Marchi A, Capra E, Percivalle E, et al. Chromosomal breaks in lymphocytes from respiratory syncytial virus-infected infants. Intl J Med Biol Environ 1999; 27(2):147-150.
29. Hull J, Ackerman H, Isles K, Usen S, Pinder M, et al. Unusual haplotypic structure of IL8, a susceptibility locus for a common respiratory virus. Am J Hum Genet 2001; 69(2):413-9.
30. Holberg CJ, Wright AL, Martinez FD, Ray CG, Taussig LM, Lebowitz MD. Risk factors for respiratory syncytial virus-associated lower respiratory illnesses in the first year of life. Am J Epidemiol 1991; 133(11):1135-51.
31. Colocho Zelaya EA, Pettersson CA, Forsgren M, Orvell C, Strannegard O. Respiratory syncytial virus infection in hospitalized patients and healthy children in El Salvador. Am J Trop Med Hyg 1994; 51(5):577-584.
32. La Via WV, Grant SW, Stutman HR, Marks MI. Clinical profile of pediatric patients hospitalized with respiratory syncytial virus infection. Clin Pediatr 1993; 32(8):450-454.
33. Huq F, Rahman M, Nahar N, Alam A, Haque M, et al. Acute lower respiratory tract infection due to virus among hospitalized children in Dhaka, Bangladesh. Rev Infect Dis 1990; 12(Suppl 8):S982-987.
34. Glezen WP, Paredes A, Allison JE, Taber LH, Frank AL. Risk of respiratory syncytial virus infection for infants from low-income families in relationship to age, sex, ethnic group, and maternal antibody level. J Pediatr 1981; 98(5):708-15.
35. Hogg JC. Chronic bronchitis: the role of viruses. Semin Respir Infect 2000; 15(1):32-40.
36. Wohl MEB, Chernick V. State of the art: bronchiolitis. Am Rev Respir Dis 1978; 118(4):759-81.
37. van Schaik SM, Welliver RC, Kimpen JL. Novel pathways in the pathogenesis of respiratory syncytial virus disease. Pediatr Pulmonol 2000; 30(2):131-8.
38. Murphy BR, Prince GA, Walsh EE, Kim HW, Parrott RH, et al. Dissociation between serum neutralizing and glycoprotein antibody responses of infants and children who received inactivated respiratory syncytial virus vaccine. J Clin Microbiol 1986; 24(2):197-202.
39. Kimpen JL. Respiratory syncytial virus immunology. Pediatr Allergy Immunol 1996; 7(9 Suppl):86-90.

40. Hogg JC, Williams J, Richardson JB, Macklem PT, Thurlbeck WM. Age as a factor in the distribution of lower-airway conductance and in the pathologic anatomy of obstructive lung disease. *N Engl J Med* 1970; 282(23):1283-7.
41. Martinez FD, Morgan WJ, Wright AL, Holberg CJ, Taussig LM. Diminished lung function as a predisposing factor for wheezing respiratory illness in infants. *N Engl J Med* 1988; 319(17):1112-7.
42. Dargaville PA, South M, McDougall PN. Surfactant abnormalities in infants with severe viral bronchiolitis. *Arch Dis Child* 1996; 75(2):133-6.
43. Welliver RC, Sun M, Rinaldo D, Ogra PL. Predictive value of respiratory syncytial virus-specific IgE responses for recurrent wheezing following bronchiolitis. *J Pediatr* 1986; 109(5):776-80.
44. Welliver RC, Wong DT, Sun M, Middleton E, Jr., Vaughan RS, Ogra PL. The development of respiratory syncytial virus-specific IgE and the release of histamine in nasopharyngeal secretions after infection. *N Engl J Med* 1981; 305(15):841-6.
45. Welliver RC, Kaul TN, Ogra PL. The appearance of cell-bound IgE in respiratory-tract epithelium after respiratory-syncytial-virus infection. *N Engl J Med* 1980; 303(21):1198-202.
46. Welliver RC, Kaul TN, Sun M, Ogra PL. Defective regulation of immune responses in respiratory syncytial virus infection. *J Immunol* 1984; 133(4):1925-30.
47. Garofalo R, Kimpen JL, Welliver RC, Ogra PL. Eosinophil degranulation in the respiratory tract during naturally acquired respiratory syncytial virus infection. *J Pediatr* 1992; 120(1):28-32.
48. Harrison AM, Bonville CA, Rosenberg HF, Domachowske JB. Respiratory syncytical virus-induced chemokine expression in the lower airways: eosinophil recruitment and degranulation. *Am J Respir Crit Care Med* 1999; 159(6):1918-24.
49. Ogra PL. From chimpanzee coryza to palivizumab: changing times for respiratory syncytial virus. *Pediatr Infect Dis J* 2000; 19(8):774-9; discussion 811-3.
50. Law BJ, Wang EE, MacDonald N, McDonald J, Dobson S, *et al.* Does ribavirin impact on the hospital course of children with respiratory syncytial virus (RSV) infection? An analysis using the pediatric investigators collaborative network on infections in Canada (PICNIC) RSV database. *Pediatrics* 1997; 99(3):E7.
51. Welliver RC. Respiratory syncytial virus immunoglobulin and monoclonal antibodies in the prevention and treatment of respiratory syncytial virus infection. *Semin Perinatol* 1998; 22(1):87-95.
52. Groothuis JR, Simoes EA, Levin MJ, Hall CB, Long CE, *et al.* Prophylactic administration of respiratory syncytial virus immune globulin to high-risk infants and

- young children. The Respiratory Syncytial Virus Immune Globulin Study Group. N Engl J Med 1993; 329(21):1524-30.
53. Kim HW, Canchola JG, Brandt CD, Pyles G, Chanock RM, *et al.* Respiratory syncytial virus disease in infants despite prior administration of antigenic inactivated vaccine. Am J Epidemiol 1969; 89(4):422-34.
 54. Chin J, Magoffin RL, Shearer LA, Schieble JH, Lennette EH. Field evaluation of a respiratory syncytial virus vaccine and a trivalent parainfluenza virus vaccine in a pediatric population. Am J Epidemiol 1969; 89(4):449-63.
 55. Graham BS, Henderson GS, Tang YW, Lu X, Neuzil KM, Colley DG. Priming immunization determines T helper cytokine mRNA expression patterns in lungs of mice challenged with respiratory syncytial virus. J Immunol 1993; 151(4):2032-40.
 56. Hall CB, Powell KR, MacDonald NE, Gala CL, Menegus ME, *et al.* Respiratory syncytial viral infection in children with compromised immune function. N Engl J Med 1986; 315(2):77-81.
 57. Englund JA, Sullivan CJ, Jordan MC, Dehner LP, Vercellotti GM, Balfour HH, Jr. Respiratory syncytial virus infection in immunocompromised adults. Ann Intern Med 1988; 109(3):203-8.
 58. Whimbey E, Couch RB, Englund JA, Andreeff M, Goodrich JM, *et al.* Respiratory syncytial virus pneumonia in hospitalized adult patients with leukemia. Clin Infect Dis 1995; 21(2):376-9.
 59. Bangham CR, Openshaw PJ, Ball LA, King AM, Wertz GW, Askonas BA. Human and murine cytotoxic T cells specific to respiratory syncytial virus recognize the viral nucleoprotein (N), but not the major glycoprotein (G), expressed by vaccinia virus recombinants. J Immunol 1986; 137(12):3973-7.
 60. Isaacs D. Viral subunit vaccines. Lancet 1991; 337(8751):1223-4.
 61. Renzi PM, Turgeon JP, Yang JP, Drblik SP, Marcotte JE, *et al.* Cellular immunity is activated and a TH-2 response is associated with early wheezing in infants after bronchiolitis. J Pediatr 1997; 130(4):584-93.
 62. Enhoring G, Duffy LC, Welliver RC. Pulmonary surfactant maintains patency of conducting airways in the rat. Am J Respir Crit Care Med 1995; 151(2 Pt 1):554-6.
 63. Enhoring G, Holm BA. Disruption of pulmonary surfactant's ability to maintain openness of a narrow tube. J Appl Physiol 1993; 74(6):2922-7.
 64. LeVine AM, Gwozdz J, Stark J, Bruno M, Whitsett J, Korfhagen T. Surfactant protein-A enhances respiratory syncytial virus clearance *in vivo*. J Clin Invest 1999; 103(7):1015-21.

65. Vos GD, Rijtema MN, Blanco CE. Treatment of respiratory failure due to respiratory syncytial virus pneumonia with natural surfactant. *Pediatr Pulmonol* 1996; 22(6):412-5.
66. Luchetti M, Casiraghi G, Valsecchi R, Galassini E, Marraro G. Porcine-derived surfactant treatment of severe bronchiolitis. *Acta Anaesthesiol Scand* 1998; 42(7):805-10.
67. Graham BS, Johnson TR, Peebles RS. Immune-mediated disease pathogenesis in respiratory syncytial virus infection. *Immunopharmacology* 2000; 48(3):237-47.
68. Mosmann TR, Coffman RL. TH1 and TH2 cells: different patterns of lymphokine secretion lead to different functional properties. *Annu Rev Immunol* 1989; 7:145-73.
69. Roitt I. Essential Immunology. 7th ed. Oxford, UK: Blackwell Scientific Publications; 1991.
70. Woolcock AJ, Peat JK. Evidence for the increase in asthma worldwide. *Ciba Found Symp* 1997; 206:122-34.
71. Steerenberg PA, Van Amsterdam JG, Vandebriel RJ, Vos JG, Van Bree L, Van Loveren H. Environmental and lifestyle factors may act in concert to increase the prevalence of respiratory allergy including asthma. *Clin Exp Allergy* 1999; 29(10):1303-8.
72. Strachan DP. Hay fever, hygiene, and household size. *BMJ* 1989; 299(6710):1259-60.
73. Byrd LG, Prince GA. Animal models of respiratory syncytial virus infection. *Clin Infect Dis* 1997; 25:1363-1368.
74. Piedimonte G, Rodriguez MM, King KA, McLean S, Jiang X. Respiratory syncytial virus upregulates expression of the substance P receptor in rat lungs. *Am J Physiol* 1999; 277(4 Pt 1):L831-40.
75. Wagner MH, Evermann JF, Gaskin J, McNicol K, Small P, Stecenko AA. Subacute effects of respiratory syncytial virus infection on lung function in lambs. *Pediatr Pulmonol* 1991; 11(1):56-64.
76. Openshaw P. Immunity and immunopathology to respiratory syncytial virus. The mouse model. *Am J Respir Crit Care Med* 1995; 152:S59-S62.
77. Graham BS, Bunton LA, Wright PF, Karzon DT. Role of T lymphocyte subsets in the pathogenesis of primary infection and rechallenge with respiratory syncytial virus in mice. *J Clin Invest* 1991; 88(3):1026-33.
78. Cannon MJ, Openshaw PJ, Askonas BA. Cytotoxic T cells clear virus but augment lung pathology in mice infected with respiratory syncytial virus. *J Exp Med* 1988; 168(3):1163-8.
79. Alwan WH, Record FM, Openshaw PJ. CD4+ T cells clear virus but augment disease in mice infected with respiratory syncytial virus. Comparison with the effects of CD8+ T cells. *Clin Exp Immunol* 1992; 88(3):527-36.

80. Hegele RG, Robinson PJ, Gonzalez S, Hogg JC. Production of acute bronchiolitis in guinea pigs by human respiratory syncytial virus. *Eur Respir J* 1993; 6(9):1324-31.
81. Hegele RG, Hayashi S, Bramley AM, Hogg JC. Persistence of respiratory syncytial virus genome and protein after acute bronchiolitis in guinea pigs. *Chest* 1994; 105(6):1848-54.
82. Riedel F, Oberdieck B, Streckert HJ, Philippou S, Krusat T, Marek W. Persistence of airway hyperresponsiveness and viral antigen following respiratory syncytial virus bronchiolitis in young guinea-pigs. *Eur Respir J* 1997; 10(3):639-45.
83. Dakhama A, Kaan PM, Hegele RG. Permissiveness of guinea pig alveolar macrophage subpopulations to acute respiratory syncytial virus infection *in vitro*. *Chest* 1998; 114(6):1681-1688.
84. Welliver R. Chemokines, cytokines and inflammatory cells in Respiratory Syncytial Virus infection: similarities to allergic responses. *Ped Asthma Allergy Immunol* 2000; 14(2):93-100.
85. Gern JE, Busse WW. The role of viral infections in the natural history of asthma. *J Allergy Clin Immunol* 2000; 106(2):201-12.
86. Zhu Z, Tang W, Ray A, Wu Y, Einarsson O, *et al*. Rhinovirus stimulation of interleukin-6 *in vivo* and *in vitro*. Evidence for nuclear factor kappa B-dependent transcriptional activation. *J Clin Invest* 1996; 97(2):421-30.
87. Zhu Z, Tang W, Gwaltney JM, Jr., Wu Y, Elias JA. Rhinovirus stimulation of interleukin-8 *in vivo* and *in vitro*: role of NF-kappaB. *Am J Physiol* 1997; 273(4 Pt 1):L814-24.
88. Jamaluddin M, Casola A, Garofalo RP, Han Y, Elliott T, *et al*. The major component of IkappaBalpha proteolysis occurs independently of the proteasome pathway in respiratory syncytial virus-infected pulmonary epithelial cells. *J Virol* 1998; 72(6):4849-57.
89. Mastronarde JG, Monick MM, Mukaida N, Matsushima K, Hunninghake GW. Activator protein-1 is the preferred transcription factor for cooperative interaction with nuclear factor-kappaB in respiratory syncytial virus-induced interleukin-8 gene expression in airway epithelium. *J Infect Dis* 1998; 177(5):1275-81.
90. Chini BA, Fiedler MA, Milligan L, Hopkins T, Stark JM. Essential roles of NF-kappaB and C/EBP in the regulation of intercellular adhesion molecule-1 after respiratory syncytial virus infection of human respiratory epithelial cell cultures. *J Virol* 1998; 72(2):1623-6.
91. Becker S, Koren HS, Henke DC. Interleukin-8 expression in normal nasal epithelium and its modulation by infection with respiratory syncytial virus and cytokines tumor necrosis factor, interleukin-1, and interleukin-6. *Am J Respir Cell Mol Biol* 1993; 8(1):20-7.

92. Jiang Z, Kunimoto M, Patel JA. Autocrine regulation and experimental modulation of interleukin-6 expression by human pulmonary epithelial cells infected with respiratory syncytial virus. *J Virol* 1998; 72(3):2496-9.
93. Kunkel SL, Standiford T, Kasahara K, Strieter RM. Interleukin-8 (IL-8): the major neutrophil chemotactic factor in the lung. *Exp Lung Res* 1991; 17(1):17-23.
94. Everard ML, Swarbrick A, Wrightham M, McIntyre J, Dunkley C, *et al.* Analysis of cells obtained by bronchial lavage of infants with respiratory syncytial virus infection. *Arch Dis Child* 1994; 71(5):428-32.
95. Noah TL, Henderson FW, Wortman IA, Devlin RB, Handy J, *et al.* Nasal cytokine production in viral acute upper respiratory infection of childhood. *J Infect Dis* 1995; 171(3):584-92.
96. Arnold R, Werner F, Humbert B, Werchau H, Konig W. Effect of respiratory syncytial virus-antibody complexes on cytokine (IL-8, IL-6, TNF-alpha) release and respiratory burst in human granulocytes. *Immunol* 1994; 82(2):184-91.
97. Cromwell O, Hamid Q, Corrigan CJ, Barkans J, Meng Q, *et al.* Expression and generation of interleukin-8, IL-6 and granulocyte-macrophage colony-stimulating factor by bronchial epithelial cells and enhancement by IL-1 beta and tumour necrosis factor-alpha. *Immunol* 1992; 77(3):330-7.
98. Noah TL, Becker S. Respiratory syncytial virus-induced cytokine production by a human bronchial epithelial cell line. *Am J Physiol* 1993; 265(5 Pt 1):L472-8.
99. Lotz M. Interleukin-6: a comprehensive review. *Cancer Treat Res* 1995; 80:209-33.
100. Wilmott RW, Khurana-Hershey G, Stark JM. Current concepts on pulmonary host defense mechanisms in children. *Curr Opin Pediatr* 2000; 12(3):187-93.
101. Becker S, Reed W, Henderson FW, Noah TL. RSV infection of human airway epithelial cells causes production of the beta-chemokine RANTES. *Am J Physiol* 1997; 272(3 Pt 1):L512-20.
102. Olszewska-Pazdrak B, Casola A, Saito T, Alam R, Crowe SE, *et al.* Cell-specific expression of RANTES, MCP-1, and MIP-1alpha by lower airway epithelial cells and eosinophils infected with respiratory syncytial virus. *J Virol* 1998; 72(6):4756-64.
103. Garofalo R, Mei F, Espejo R, Ye G, Haeberle H, *et al.* Respiratory syncytial virus infection of human respiratory epithelial cells up-regulates class I MHC expression through the induction of IFN-beta and IL-1 alpha. *J Immunol* 1996; 157(6):2506-13.
104. Wang SZ, Hallsworth PG, Dowling KD, Alpers JH, Bowden JJ, Forsyth KD. Adhesion molecule expression on epithelial cells infected with respiratory syncytial virus. *Eur Respir J* 2000; 15(2):358-66.

105. Kimata H, Yoshida A, Ishioka C, Fujimoto M, Lindley I, Furusho K. RANTES and macrophage inflammatory protein 1 alpha selectively enhance immunoglobulin (IgE) and IgG4 production by human B cells. *J Exp Med* 1996; 183(5):2397-402.
106. Taub DD, Sayers TJ, Carter CR, Ortaldo JR. Alpha and beta chemokines induce NK cell migration and enhance NK-mediated cytosis. *J Immunol* 1995; 155(8):3877-88.
107. Panuska JR, Hertz MI, Taraf H, Villani A, Cirino NM. Respiratory syncytial virus infection of alveolar macrophages in adult transplant patients. *Am Rev Resp Dis* 1992; 145(4 Pt 1):934-9.
108. Midulla F, Huang YT, Gilbert IA, Cirino NM, McFadden ER, Jr., Panuska JR. Respiratory syncytial virus infection of human cord and adult blood monocytes and alveolar macrophages. *Am Rev Resp Dis* 1989; 140(3):771-7.
109. Kimpel JL, Garofalo R, Welliver RC, Fujihara K, Ogra PL. An ultrastructural study of the interaction of human eosinophils with respiratory syncytial virus. *Pediatr Allergy Immunol* 1996; 7(1):48-53.
110. Jaovisidha P, Peeples ME, Brees AA, Carpenter LR, Moy JN. Respiratory syncytial virus stimulates neutrophil degranulation and chemokine release. *J Immunol* 1999; 163:2816-2820.
111. Panuska JR, Cirino NM, Midulla F, Despot JE, McFadden ER, Jr., Huang YT. Productive infection of isolated human alveolar macrophages by respiratory syncytial virus. *J Clin Invest* 1990; 86(1):113-9.
112. Becker S, Soukup J, Yankaskas JR. Respiratory syncytial virus infection of human primary nasal and bronchial epithelial cell cultures and bronchoalveolar macrophages. *Am J Respir Cell Mol Biol* 1992; 6(4):369-74.
113. Cirino NM, Panuska JR, Villani A, Taraf H, Rebert NA, *et al.* Restricted replication of respiratory syncytial virus in human alveolar macrophages. *J Gen Virol* 1993; 74(Pt 8):1527-37.
114. Franke-Ullmann G, Pfortner C, Walter P, Steinmuller C, Lohmann-Matthes ML, *et al.* Alteration of pulmonary macrophage function by respiratory syncytial virus infection *in vitro*. *J Immunol* 1995; 154(1):268-80.
115. Trigo E, Liggitt HD, Evermann JF, Breeze RG, Huston LY, Silflow R. Effect of *in vitro* inoculation of bovine respiratory syncytial virus on bovine pulmonary alveolar macrophage function. *Am J Vet Res* 1985; 46(5):1098-103.
116. Becker S, Quay J, Soukup J. Cytokine (tumor necrosis factor, IL-6, and IL-8) production by respiratory syncytial virus-infected human alveolar macrophages. *J Immunol* 1991; 147:4307-4312.

117. Arnold R, Konig B, Galatti H, Werchau H, Konig W. Cytokine (IL-8, IL-6, TNF-alpha) and soluble TNF receptor-I release from human peripheral blood mononuclear cells after respiratory syncytial virus infection. *Immunol* 1995; 85(3):364-72.
118. Gordon S, Hughes D. Macrophages and their origins. In: Lipscomb M, Russell SW, editors. *Lung Macrophages and Dendritic Cells in Health and Disease*. New York, NY: Marcel Dekker Inc.; 1997. p. 3-31.
119. Thomas ED, Ramberg RE, Sale GE, Sparkes RS, Golde DW. Direct evidence for a bone marrow origin of the alveolar macrophage in man. *Science* 1976; 192(4243):1016-8.
120. Metcalf D. Transformation of granulocytes to macrophages in bone marrow colonies *in vitro*. *J Cell Physiol* 1971; 77(2):277-80.
121. Golde DW, Groopman JE. Production, distribution and fate of monocytes and macrophages. In: Williams WJ, Beutler E, Erslev AJ, Lichtman MA, editors. *Haematology*. 4th Ed. New York: McGraw-Hill; 1990.
122. Cannistra SA, Rambaldi A, Spriggs DR, Herrmann F, Kufe D, Griffin JD. Human granulocyte-macrophage colony-stimulating factor induces expression of the tumor necrosis factor gene by the U937 cell line and by normal human monocytes. *J Clin Invest* 1987; 79(6):1720-8.
123. van Furth R. Origin and turnover of monocytes and macrophages. *Curr Top Pathol* 1989; 79:125-50.
124. Matsushima K, Larsen CG, DuBois GC, Oppenheim JJ. Purification and characterization of a novel monocyte chemotactic and activating factor produced by a human myelomonocytic cell line. *J Exp Med* 1989; 169(4):1485-90.
125. Blusse van Oud Ablas A, van Furth R. Origin, Kinetics, and characteristics of pulmonary macrophages in the normal steady state. *J Exp Med* 1979; 149(6):1504-18.
126. Bitterman PB, Saltzman LE, Adelberg S, Ferrans VJ, Crystal RG. Alveolar macrophage replication. One mechanism for the expansion of the mononuclear phagocyte population in the chronically inflamed lung. *J Clin Invest* 1984; 74(2):460-9.
127. Nakata K, Akagawa KS, Fukayama M, Hayashi Y, Kadokura M, Tokunaga T. Granulocyte-macrophage colony-stimulating factor promotes the proliferation of human alveolar macrophages *in vitro*. *J Immunol* 1991; 147(4):1266-72.
128. Lohmann-Matthes ML, Steinmuller C, Franke-Ullmann G. Pulmonary macrophages. *Eur Respir J* 1994; 7(9):1678-89.
129. Dehring DJ, Wismar BL. Intravascular macrophages in pulmonary capillaries of humans. *Am Rev Respir Dis* 1989; 139(4):1027-9.

130. Warner AE, Molina RM, Brain JD. Uptake of bloodborne bacteria by pulmonary intravascular macrophages and consequent inflammatory responses in sheep. *Am Rev Respir Dis* 1987; 136(3):683-90.
131. Sibille Y, Reynolds HY. Macrophages and polymorphonuclear neutrophils in lung defense and injury. *Am Rev Respir Dis* 1990; 141(2):471-501.
132. Hance AJ. Pulmonary immune cells in health and disease: dendritic cells and Langerhans' cells. *Eur Respir J* 1993; 6(8):1213-20.
133. Holt PG, Schon-Hegrad MA, Oliver J. MHC class II antigen-bearing dendritic cells in pulmonary tissues of the rat. Regulation of antigen presentation activity by endogenous macrophage populations. *J Exp Med* 1988; 167(2):262-74.
134. Lehnert BE, Valdez YE, Holland LM. Pulmonary macrophages: alveolar and interstitial populations. *Exp Lung Res* 1985; 9(3-4):177-90.
135. Warren JS, Kunkel RG, Johnson KJ, Ward PA. Comparative O₂- responses of lung macrophages and blood phagocytic cells in the rat. Possible relevance to IgA immune complex induced lung injury. *Lab Invest* 1987; 57(3):311-20.
136. Holian A, Scheule RK. Alveolar macrophage biology. *Hospital Practice* 1990; .
137. Sebring RJ, Lehnert BE. Morphometric comparisons of rat alveolar macrophages, pulmonary interstitial macrophages, and blood monocytes. *Exp Lung Res* 1992; 18(4):479-96.
138. Lehnert BE. Pulmonary and thoracic macrophage subpopulations and clearance of particles from the lung. *Environ Health Perspect* 1992; 97:17-46.
139. Cohen AB, Cline MJ. The human alveolar macrophage: isolation, cultivation *in vitro*, and studies of morphologic and functional characteristics. *J Clin Invest* 1971; 50(7):1390-8.
140. Shellito J, Kaltreider HB. Heterogeneity of immunologic function among subfractions of normal rat alveolar macrophages. II. Activation as a determinant of functional activity. *Am Rev Respir Dis* 1985; 131(5):678-83.
141. Holian A, Dauber JH, Diamond MS, Daniele RP. Separation of bronchoalveolar cells from the guinea pig on continuous gradients of Percoll: functional properties of fractionated lung macrophages. *J Reticuloendothel Soc* 1983; 33(2):157-64.
142. Chandler DB, Fuller WC, Jackson RM, Fulmer JD. Studies of membrane receptors and phagocytosis in subpopulations of rat alveolar macrophages. *Am Rev Respir Dis* 1986; 133:461-467.
143. Dauber JH, Holian A, Rosemiller ME, Daniele RP. Separation of bronchoalveolar cells from the guinea pig on continuous density gradients of Percoll: morphology and cytochemical properties of fractionated lung macrophages. *J Reticuloendothel Soc* 1983; 33(2):119-26.

144. Chandler DB, Fulmer JD. Prostaglandin synthesis and release by subpopulations of rat alveolar macrophages. *J Immunol* 1987; 139(3):893-8.
145. Brannen AL, Chandler DB. Alveolar macrophage subpopulations' responsiveness to chemotactic stimuli. *Am J Pathol* 1988; 132(1):161-6.
146. Douglas SD, Hassan NF. Morphology of monocytes and macrophages. In: Williams WJ, Beutler E, Erslev AJ, Lichtman MA, editors. *Haematology*. 4th ed. New York: McGraw-Hill; 1990.
147. Auger MJ, Ross JA. The biology of the macrophage. In: Lewis CE, McGee JO, editors. *The Macrophage*. Oxford, U.K.: IRL Press; 1992.
148. Reynolds HY. Respiratory infections may reflect deficiencies in host defense mechanisms. *Dis Mon* 1985; 31(2):1-98.
149. Alberts B. *Molecular Biology of the Cell*. 3rd ed. New York: Garland Publishing Inc.; 1994.
150. Kurt-Jones EA, Popova L, Kwinn L, Haynes LM, Jones LP, *et al*. Pattern recognition receptors TLR4 and CD14 mediate response to respiratory syncytial virus. *Nat Immunol* 2000; 1(5):398-401.
151. Tauber AI, Chernyak L. Metchnikoff and the origins of immunology. Oxford: Oxford University Press; 1991.
152. Griffin FM, Jr., Silverstein SC. Segmental response of the macrophage plasma membrane to a phagocytic stimulus. *J Exp Med* 1974; 139(2):323-36.
153. Horwitz MA. Formation of a novel phagosome by the Legionnaires' disease bacterium (*Legionella pneumophila*) in human monocytes. *J Exp Med* 1983; 158(4):1319-31.
154. Sung SS, Nelson RS, Silverstein SC. Yeast mannans inhibit binding and phagocytosis of zymosan by mouse peritoneal macrophages. *J Cell Biol* 1983; 96(1):160-6.
155. Wheater's Functional Histology. 4th ed. New York: Churchill Livingstone; 2000.
156. Nichols BA, Bainton DF, Farquhar MG. Differentiation of monocytes. Origin, nature, and fate of their azurophil granules. *J Cell Biol* 1971; 50(2):498-515.
157. Johnston RB, Jr., Godzik CA, Cohn ZA. Increased superoxide anion production by immunologically activated and chemically elicited macrophages. *J Exp Med* 1978; 148(1):115-27.
158. Rouzer CA, Scott WA, Kempe J, Cohn ZA. Prostaglandin synthesis by macrophages requires a specific receptor-ligand interaction. *PNAS* 1980; 77(7):4279-82.

159. Klebanoff SJ. Phagocytic cells: products of oxygen metabolism. In: Gallin JI, Goldstein IM, Snyderman R, editors. *Inflammation: Basic principles and clinical correlates*. New York: Raven; 1988.
160. Goodman MG, Chenoweth DE, Weigle WO. Induction of interleukin 1 secretion and enhancement of humoral immunity by binding of human C5a to macrophage surface C5a receptors. *J Exp Med* 1982; 156(3):912-7.
161. Shurin SB, Stossel TP. Complement (C3)-activated phagocytosis by lung macrophages. *J Immunol* 1978; 120(4):1305-12.
162. Zeidler R, Eissner G, Meissner P, Uebel S, Tampe R, *et al*. Downregulation of TAP1 in B lymphocytes by cellular and Epstein-Barr virus-encoded interleukin-10. *Blood* 1997; 90(6):2390-7.
163. Panuska JR, Merolla R, Rebert NA, Hoffmann SP, Tsivitse P, *et al*. Respiratory syncytial virus induces interleukin-10 by human alveolar macrophages. Suppression of early cytokine production and implications for incomplete immunity. *J Clin Invest* 1995; 96(5):2445-53.
164. Kimpen JL. Respiratory syncytial virus and asthma. The role of monocytes. *Am J Respir Crit Care Med* 2001; 163(3 Pt 2):S7-9.
165. Fels AO, Pawlowski NA, Cramer EB, King TK, Cohn ZA, Scott WA. Human alveolar macrophages produce leukotriene B4. *PNAS* 1982; 79(24):7866-70.
166. Ming WJ, Bersani L, Mantovani A. Tumor necrosis factor is chemotactic for monocytes and polymorphonuclear leukocytes. *J Immunol* 1987; 138(5):1469-74.
167. Schroder JM, Mrowietz U, Morita E, Christophers E. Purification and partial biochemical characterization of a human monocyte-derived, neutrophil-activating peptide that lacks interleukin 1 activity. *J Immunol* 1987; 139(10):3474-83.
168. Yoshimura T, Matsushima K, Oppenheim JJ, Leonard EJ. Neutrophil chemotactic factor produced by lipopolysaccharide (LPS)-stimulated human blood mononuclear leukocytes: partial characterization and separation from interleukin 1 (IL 1). *J Immunol* 1987; 139(3):788-93.
169. Wolpe SD, Davatelas G, Sherry B, Beutler B, Hesse DG, *et al*. Macrophages secrete a novel heparin-binding protein with inflammatory and neutrophil chemokinetic properties. *J Exp Med* 1988; 167(2):570-81.
170. Goetzl EJ, Pickett WC. Novel structural determinants of the human neutrophil chemotactic activity of leukotriene B. *J Exp Med* 1981; 153(2):482-7.
171. Henderson WR, Jr. Lipid-derived and other chemical mediators of inflammation in the lung. *J Allergy Clin Immunol* 1987; 79(4):543-53.

172. Dahlen SE, Bjork J, Hedqvist P, Arfors KE, Hammarstrom S, *et al.* Leukotrienes promote plasma leakage and leukocyte adhesion in postcapillary venules: *in vivo* effects with relevance to the acute inflammatory response. PNAS 1981; 78(6):3887-91.
173. O'Flaherty JT. Neutrophil degranulation: evidence pertaining to its mediation by the combined effects of leukotriene B₄, platelet-activating factor, and 5-HETE. J Cell Physiol 1985; 122(2):229-39.
174. Martin TR, Raugi G, Merritt TL, Henderson WR, Jr. Relative contribution of leukotriene B₄ to the neutrophil chemotactic activity produced by the resident human alveolar macrophage. J Clin Invest 1987; 80(4):1114-24.
175. Carswell EA, Old LJ, Kassel RL, Green S, Fiore N, Williamson B. An endotoxin-induced serum factor that causes necrosis of tumors. PNAS 1975; 72(9):3666-70.
176. Cerami A, Beutler B. The role of cachectin/TNF in endotoxic shock and cachexia. Immunol Today 1988; 9(1):28-31.
177. Nathan CF. Neutrophil activation on biological surfaces. Massive secretion of hydrogen peroxide in response to products of macrophages and lymphocytes. J Clin Invest 1987; 80(6):1550-60.
178. Shalaby MR, Aggarwal BB, Rinderknecht E, Svedersky LP, Finkle BS, Palladino MA, Jr. Activation of human polymorphonuclear neutrophil functions by interferon-gamma and tumor necrosis factors. J Immunol 1985; 135(3):2069-73.
179. Smith KA, Lachman LB, Oppenheim JJ, Favata MF. The functional relationship of the interleukins. J Exp Med 1980; 151(6):1551-6.
180. Matsuda T, Suematsu S, Kawano M, Yoshizaki K, Tang B, *et al.* IL-6/BSF2 in normal and abnormal regulation of immune responses. PNAS 1989; 557:466-76; discussion 476-7.
181. Baumann H, Richards C, Gauldie J. Interaction among hepatocyte-stimulating factors, interleukin 1, and glucocorticoids for regulation of acute phase plasma proteins in human hepatoma (HepG2) cells. J Immunol 1987; 139(12):4122-8.
182. Tosato G, Seamon KB, Goldman ND, Sehgal PB, May LT, *et al.* Monocyte-derived human B-cell growth factor identified as interferon-beta 2 (BSF-2, IL-6). Science 1988; 239(4839):502-4.
183. Mielke V, Bauman JG, Sticherling M, Ibs T, Zomershoe AG, *et al.* Detection of neutrophil-activating peptide NAP/IL-8 and NAP/IL-8 mRNA in human recombinant IL-1 alpha- and human recombinant tumor necrosis factor-alpha-stimulated human dermal fibroblasts. An immunocytochemical and fluorescent *in situ* hybridization study. J Immunol 1990; 144(1):153-61.

184. Larsen CG, Anderson AO, Appella E, Oppenheim JJ, Matsushima K. The neutrophil-activating protein (NAP-1) is also chemotactic for T lymphocytes. *Science* 1989; 243(4897):1464-6.
185. Baggiolini M, Dewald B, Moser B. Interleukin-8 and related chemotactic cytokines--CXC and CC chemokines. *Adv Immunol* 1994; 55:97-179.
186. Driscoll KE. Macrophage inflammatory proteins: biology and role in pulmonary inflammation. *Exp Lung Res* 1994; 20(6):473-90.
187. Cook DN. The role of MIP-1 alpha in inflammation and hematopoiesis. *J Leukoc Biol* 1996; 59(1):61-6.
188. Driscoll KE, Hassenbein DG, Carter J, Poynter J, Asquith TN, *et al*. Macrophage inflammatory proteins 1 and 2: expression by rat alveolar macrophages, fibroblasts, and epithelial cells and in rat lung after mineral dust exposure. *Am J Respir Cell Mol Biol* 1993; 8(3):311-8.
189. Driscoll KE, Lindenschmidt RC, Maurer JK, Higgins JM, Ridder G. Pulmonary response to silica or titanium dioxide: inflammatory cells, alveolar macrophage-derived cytokines, and histopathology. *Am J Respir Cell Mol Biol* 1990; 2(4):381-90.
190. Koren HS, Devlin RB, Graham DE, Mann R, McGee MP, *et al*. Ozone-induced inflammation in the lower airways of human subjects. *Am Rev Respir Dis* 1989; 139(2):407-15.
191. Alam R, York J, Boyars M, Stafford S, Grant JA, *et al*. Increased MCP-1, RANTES, and MIP-1alpha in bronchoalveolar lavage fluid of allergic asthmatic patients. *Am J Respir Crit Care Med* 1996; 153(4 Pt 1):1398-404.
192. Cruikshank WW, Long A, Tarpy RE, Kornfeld H, Carroll MP, *et al*. Early identification of interleukin-16 (lymphocyte chemoattractant factor) and macrophage inflammatory protein 1 alpha (MIP1 alpha) in bronchoalveolar lavage fluid of antigen-challenged asthmatics. *Am J Respir Cell Mol Biol* 1995; 13(6):738-47.
193. Becker S, Soukup JM. Exposure to urban air particulates alters the macrophage-mediated inflammatory response to respiratory viral infection. *J Toxicol Environ Health* 1999; 57(7):445-57.
194. Garofalo RP, Patti J, Hintz KA, Hill V, Ogra PL, Welliver RC. Macrophage inflammatory protein-1alpha (not T helper type 2 cytokines) is associated with severe forms of respiratory syncytial virus bronchiolitis. *J Infect Dis* 2001; 184(4):393-9.
195. Sible Y, Merrill WW, Naegel GP, Care SB, Cooper JA, Jr., Reynolds HY. Human alveolar macrophages release a factor that inhibits phagocyte function. *Am J Respir Cell Mol Biol* 1989; 1(5):407-16.

196. Thomassen MJ, Buhrow LT, Connors MJ, Kaneko FT, Erzurum SC, Kavuru MS. Nitric oxide inhibits inflammatory cytokine production by human alveolar macrophages. *Am J Respir Cell Mol Biol* 1997; 17(3):279-83.
197. Canadian Council on Animal Care (CCAC). Ottawa: CCAC; 1980.
198. Bendayan M, Zollinger M. Ultrastructural localization of antigenic sites on osmium fixed tissues applying the protein A-gold technique. *J Histochem Cytochem* 1983; 31(1):101-9.
199. Nakstad B, Lyberg T, Skjorten F, Boye NP. Subpopulations of human lung alveolar macrophages: ultrastructural features. *Ultrastructural Pathology* 1989; 13(1):1-13.
200. Phillips MJ, Blendis LM, Poucell S, offterson J, Petric M, *et al.* Syncytial giant-cell hepatitis. Sporadic hepatitis with distinctive pathological features, a severe clinical course, and paramyxoviral features. *N Engl J Med* 1991; 324(7):455-60.
201. Ferro TJ, Kern JA, Elias JA, Kamoun M, Daniele RP, Rossman MD. Alveolar macrophages, blood monocytes, and density-fractionated alveolar macrophages differ in their ability to promote lymphocyte proliferation to mitogen and antigen. *Am Rev Respir Dis* 1987; 135:682-687.
202. Hirsch MS, Zisman B, Allison AC. Macrophages and age-dependent resistance to Herpes simplex virus in mice. *J Immunol* 1970; 104(5):1160-5.
203. Mogensen SC. Macrophages and age-dependent resistance to hepatitis induced by herpes simplex virus type 2 in mice. *Infect Immun* 1978; 19(1):46-50.
204. Turner GS, Ballard R. Interaction of mouse peritoneal macrophages with fixed rabies virus *in vivo* and *in vitro*. *J Gen Virol* 1976; 30(2):223-31.
205. Mogensen SC. Role of macrophages in natural resistance to virus infections. *Microbiol Rev* 1979; 43(1):1-26.
206. Prince GA, Porter DD. The pathogenesis of respiratory syncytial virus infection in infant ferrets. *Am J Pathol* 1976; 82:339-52.
207. Hegele RG, Robinson PJ, Hogg JC. Age susceptibility of guinea pigs to acute bronchiolitis induced by human respiratory syncytial virus. *Am Rev Respir Dis* 1992; 145:A434.
208. Wagner JE, Manning PJ, editors. *The biology of the guinea pig*. London, UK: Academic Press Inc.; 1976.
209. Welliver RC. Immunology of respiratory syncytial virus infection: eosinophils, cytokines, chemokines and asthma. *Pediatr Infect Dis J* 2000; 19(8):780-3; discussion 784-5; 811-3.
210. McMillan EM, King GM, Adamson IYR. Sex hormones influence growth and surfactant production in fetal lung explants. *Exp Lung Res* 1988; 15:167-179.

211. Adamson IYR, King GM. Sex-related differences in cellular composition and surfactant synthesis of developing fetal rat lungs. *Am Rev Respir Dis* 1984; 129:130-134.
212. Mestan J, Digel W, Mittnacht S, Hillen H, Blohm D, *et al.* Antiviral effects of recombinant tumour necrosis factor *in vitro*. *Nature* 1986; 323(6091):816-9.
213. Wong GH, Goeddel DV. Tumour necrosis factors alpha and beta inhibit virus replication and synergize with interferons. *Nature* 1986; 323(6091):819-22.
214. Horiuchi T, Tsang S, Schellenberg RR. Release of Tumor Necrosis Factor alpha from sensitized guinea pig lung by allergen. *Am J Respir Crit Care Med* 1994; 149:A769.
215. von Mutius E, Martinez F, Fritzsch C, Nicolai T, Roell G, Thiemann H. Prevalence of asthma and atopy in two areas of West and East Germany. *Am J Respir Crit Care Med* 1994; 149:358-364.
216. Weiland SK, von Mutius E, Hirsch T, Duhme H, Fritzsch C, *et al.* Prevalence of respiratory and atopic disorders among children in the East and West of Germany five years after unification. *Eur Respir J* 1999; 14(4):862-70.
217. Pope CA, 3rd, Dockery DW. Acute health effects of PM10 pollution on symptomatic and asymptomatic children. *Am Rev Respir Dis* 1992; 145(5):1123-8.
218. French JG, Lowrimore G, Nelson WC, Finklea JF, English T, Hertz M. The effect of sulfur dioxide and suspended sulfates on acute respiratory disease. *Arch Environ Health* 1973; 27(3):129-33.
219. Speizer FE, Ferris B, Jr., Bishop YM, Spengler J. Respiratory disease rates and pulmonary function in children associated with NO₂ exposure. *Am Rev Respir Dis* 1980; 121(1):3-10.
220. Ball TM, Castro-Rodriguez JA, Griffith KA, Holberg CJ, Martinez FD, Wright AL. Siblings, day-care attendance, and the risk of asthma and wheezing during childhood. *N Engl J Med* 2000; 343(8):538-43.
221. Butland BK, Strachan DP, Lewis S, Bynner J, Butler N, Britton J. Investigation into the increase in hay fever and eczema at age 16 observed between the 1958 and 1970 British birth cohorts. *BMJ* 1997; 315(7110):717-21.
222. Strachan DP, Anderson HR, Limb ES, O'Neill A, Wells N. A national survey of asthma prevalence, severity, and treatment in Great Britain. *Arch Dis Child* 1994; 70(3):174-8.
223. Shaheen SO, Aaby P, Hall AJ, Barker DJ, Heyes CB, *et al.* Measles and atopy in Guinea-Bissau. *Lancet* 1996; 347(9018):1792-6.
224. Bodner C, Godden D, Seaton A. Family size, childhood infections and atopic diseases. The Aberdeen WHEASE Group. *Thorax* 1998; 53(1):28-32.

225. Shirakawa T, Enomoto T, Shimazu S, Hopkin JM. The inverse association between tuberculin responses and atopic disorder. *Science* 1997; 275(5296):77-9.
226. Matricardi PM, Rosmini F, Ferrigno L, Nisini R, Rapicetta M, *et al.* Cross sectional retrospective study of prevalence of atopy among Italian military students with antibodies against hepatitis A virus. *BMJ* 1997; 314(7086):999-1003.
227. Paunio M, Heinonen OP, Virtanen M, Leinikki P, Patja A, Peltola H. Measles history and atopic diseases: a population-based cross-sectional study. *JAMA* 2000; 283(3):343-6.
228. Gern JE, Weiss ST. Protection against atopic diseases by measles--a rash conclusion? *JAMA* 2000; 283(3):394-5.
229. Strannegard IL, Larsson LO, Wennergren G, Strannegard O. Prevalence of allergy in children in relation to prior BCG vaccination and infection with atypical mycobacteria. *Allergy* 1998; 53(3):249-54.
230. Dockery DW, Pope CA, 3rd. Acute respiratory effects of particulate air pollution. *Annu Rev Public Health* 1994; 15:107-32.
231. Schwartz J. Air pollution and daily mortality: a review and meta analysis. *Environ Res* 1994; 64(1):36-52.
232. von Mutius E, Fritzsch C, Weiland SK, Roll G, Magnussen H. Prevalence of asthma and allergic disorders among children in united Germany: a descriptive comparison. *BMJ* 1992; 305(6866):1395-9.
233. Nowak D, Heinrich J, Jorres R, Wassmer G, Berger J, *et al.* Prevalence of respiratory symptoms, bronchial hyperresponsiveness and atopy among adults: West and East Germany. *Eur Respir J* 1996; 9(12):2541-52.
234. Braback L, Breborowicz A, Julge K, Knutsson A, Riikjarv MA, *et al.* Risk factors for respiratory symptoms and atopic sensitisation in the Baltic area. *Arch Dis Child* 1995; 72(6):487-93.
235. Braback L, Breborowicz A, Dreborg S, Knutsson A, Pieklik H, Bjorksten B. Atopic sensitization and respiratory symptoms among Polish and Swedish school children. *Clin Exp Allergy* 1994; 24(9):826-35.
236. Becker S, Soukup J, Gilmour M, Devlin R. Stimulation of human and rat alveolar macrophages by urban air particulates: effects on oxidant radical generation and cytokine production. *Toxicol Appl Pharmacol* 1996; 141:637-648.
237. Kaan PM, Hegele RG. Effect of PM10 on cytokine production by guinea pig alveolar macrophages. *Am J Respir Crit Care Med* 2001; 163(5):A362.
238. Kaan PM, Hegele RG. Effect of PM10 on cell viability and cytokine production by subpopulations of guinea pig alveolar macrophages. *Am J Respir Crit Care Med* 2001; 163(6):A188.

239. Vincent R, Bjarnason SG, Adamson IY, Hedgecock C, Kumarathasan P, *et al.* Acute pulmonary toxicity of urban particulate matter and ozone. *Am J Pathol* 1997; 151(6):1563-70.
240. Goldsmith C-A, Imrich A, Danaee H, Kobzik L, Ning YY. Analysis of air pollution particulate-mediated oxidant stress in alveolar macrophages. *J Toxicol Environ Health* 1998; 54:529-545.
241. Ghio AJ, Carter JD, Richards JH, Brighton LE, Lay JC, Devlin RB. Disruption of normal iron homeostasis after bronchial instillation of an iron-containing particle. *Am J Physiol* 1998; 274:L396-L403.
242. Kennedy T, Ghio AJ, Reed W, Samet JM, Zagorski J, *et al.* Copper-dependent inflammation and nuclear factor-kappa B activation by particulate air pollution. *Am J Respir Cell Mol Biol* 1998; 19:366-378.
243. Carter JD, Ghio AJ, Reed W, Devlin RB. Cytokine production by human airway epithelial cells after exposure to an air pollution particle is metal-dependent. *Toxicol Appl Pharmacol* 1997; 146:180-188.
244. Hallden G, Skold CM, Eklund A, Forslid J, Hed J. Quenching of intracellular autofluorescence in alveolar macrophages permits analysis of fluorochrome labelled surface antigens by flow cytofluorometry. *J Immunol Methods* 1991; 142(2):207-14.
245. Lundborg M, Johard U, Lastbom L, Gerde P, Camner P. Human alveolar macrophage phagocytic function is impaired by aggregates of ultrafine carbon particles. *Environ Res* 2001; 86(3):244-53.
246. Lundborg M, Johansson A, Lastbom L, Camner P. Ingested aggregates of ultrafine carbon particles and interferon-gamma impair rat alveolar macrophage function. *Environ Res* 1999; 81(4):309-15.
247. Renwick LC, Donaldson K, Clouter A. Impairment of alveolar macrophage phagocytosis by ultrafine particles. *Toxicol Appl Pharmacol* 2001; 172(2):119-27.
248. Li XY, Gilmour PS, Donaldson K, MacNee W. *In vivo* and *in vitro* proinflammatory effects of particulate air pollution (PM10). *Environ Health Perspect* 1997; 105 Suppl 5:1279-83.
249. Tsutsumi H, Takeuchi R, Ohsaki M, Seki K, Chiba S. Respiratory syncytial virus infection of human respiratory epithelial cells enhances inducible nitric oxide synthase gene expression. *J Leukoc Biol* 1999; 66(1):99-104.
250. Asano K, Chee CB, Gaston B, Lilly CM, Gerard C, *et al.* Constitutive and inducible nitric oxide synthase gene expression, regulation, and activity in human lung epithelial cells. *PNAS* 1994; 91(21):10089-93.

251. Majano PL, Garcia-Monzon C, Lopez-Cabrera M, Lara-Pezzi E, Fernandez-Ruiz E, *et al.* Inducible nitric oxide synthase expression in chronic viral hepatitis. Evidence for a virus-induced gene upregulation. *J Clin Invest* 1998; 101(7):1343-52.
252. Reiss CS, Komatsu T. Does nitric oxide play a critical role in viral infections? *J Virol* 1998; 72(6):4547-51.
253. Lopez-Guerrero JA, Carrasco L. Effect of nitric oxide on poliovirus infection of two human cell lines. *J Virol* 1998; 72(3):2538-40.
254. Harris N, Buller RM, Karupiah G. Gamma interferon-induced, nitric oxide-mediated inhibition of vaccinia virus replication. *J Virol* 1995; 69(2):910-5.
255. Zaragoza C, Ocampo CJ, Saura M, McMillan A, Lowenstein CJ. Nitric oxide inhibition of coxsackievirus replication *in vitro*. *J Clin Invest* 1997; 100(7):1760-7.
256. Sanders SP, Siekierski ES, Porter JD, Richards SM, Proud D. Nitric oxide inhibits rhinovirus-induced cytokine production and viral replication in a human respiratory epithelial cell line. *J Virol* 1998; 72(2):934-42.
257. Geist LJ, Hunninghake GW. Role of viruses in cytokine induction from lung cells. In: Nelson S, Martin TR, editors. *Cytokines in pulmonary disease. Infection and inflammation*. New York: Marcel Dekker, Inc.; 2000. p. 293-305.
258. Hamilton TA, Ohmori Y, Tebo JM, Kishore R. Regulation of macrophage gene expression by pro- and anti-inflammatory cytokines. *Pathobiology* 1999; 67(5-6):241-4.
259. Mastronarde JG, He B, Monick MM, Mukaida N, Matsushima K, Hunninghake GW. Induction of interleukin (IL)-8 gene expression by respiratory syncytial virus involves activation of nuclear factor (NF)-kappa B and NF-IL-6. *J Infect Dis* 1996; 174(2):262-7.
260. Bitko V, Velazquez A, Yang L, Yang YC, Barik S. Transcriptional induction of multiple cytokines by human respiratory syncytial virus requires activation of NF-kappa B and is inhibited by sodium salicylate and aspirin. *Virology* 1997; 232(2):369-78.
261. Thomas LH, Friedland JS, Sharland M, Becker S. Respiratory syncytial virus-induced RANTES production from human bronchial epithelial cells is dependent on nuclear factor-kappa B nuclear binding and is inhibited by adenovirus-mediated expression of inhibitor of kappa B alpha. *J Immunol* 1998; 161(2):1007-16.
262. Fiedler MA, Wernke-Dollries K, Stark JM. Inhibition of viral replication reverses respiratory syncytial virus-induced NF-kappaB activation and interleukin-8 gene expression in A549 cells. *J Virol* 1996; 70(12):9079-82.
263. Sen R, Baltimore D. Inducibility of kappa immunoglobulin enhancer-binding protein Nf-kappa B by a posttranslational mechanism. *Cell* 1986; 47(6):921-8.
264. Ghosh S, Baltimore D. Activation *in vitro* of NF-kappa B by phosphorylation of its inhibitor I kappa B. *Nature* 1990; 344(6267):678-82.

265. Baeuerle PA, Henkel T. Function and activation of NF-kappa B in the immune system. *Annu Rev Immunol* 1994; 12:141-79.
266. Foo SY, Nolan GP. NF-kappaB to the rescue: RELs, apoptosis and cellular transformation. *Trends Genet* 1999; 15(6):229-35.
267. Baeuerle PA, Baltimore D. NF-kappa B: ten years after. *Cell* 1996; 87(1):13-20.
268. Kunsch C, Lang RK, Rosen CA, Shannon MF. Synergistic transcriptional activation of the IL-8 gene by NF-kappa B p65 (RelA) and NF-IL-6. *J Immunol* 1994; 153(1):153-64.
269. Collart MA, Baeuerle P, Vassalli P. Regulation of tumor necrosis factor alpha transcription in macrophages: involvement of four kappa B-like motifs and of constitutive and inducible forms of NF-kappa B. *Mol Cell Biol* 1990; 10(4):1498-506.
270. Drouet C, Shakhov AN, Jongeneel CV. Enhancers and transcription factors controlling the inducibility of the tumor necrosis factor-alpha promoter in primary macrophages. *J Immunol* 1991; 147(5):1694-700.
271. Libermann TA, Baltimore D. Activation of interleukin-6 gene expression through the NF-kappa B transcription factor. *Mol Cell Biol* 1990; 10(5):2327-34.
272. Matsusaka T, Fujikawa K, Nishio Y, Mukaida N, Matsushima K, *et al.* Transcription factors NF-IL6 and NF-kappa B synergistically activate transcription of the inflammatory cytokines, interleukin 6 and interleukin 8. *PNAS* 1993; 90(21):10193-7.
273. Baichwal VR, Baeuerle PA. Activate NF-kappa B or die? *Curr Biol* 1997; 7(2):R94-6.
274. Marianneau P, Cardona A, Edelman L, Deubel V, Despres P. Dengue virus replication in human hepatoma cells activates NF-kappaB which in turn induces apoptotic cell death. *J Virol* 1997; 71(4):3244-9.
275. Garofalo R, Sabry M, Jamaluddin M, Yu RK, Casola A, *et al.* Transcriptional activation of the interleukin-8 gene by respiratory syncytial virus infection in alveolar epithelial cells: nuclear translocation of the RelA transcription factor as a mechanism producing airway mucosal inflammation. *J Virol* 1996; 70(12):8773-81.
276. Mastronarde JG, Monick MM, Gross TJ, Hunninghake GW. Amiloride inhibits cytokine production in epithelium infected with respiratory syncytial virus. *Am J Physiol* 1996; 271(2 Pt 1):L201-7.
277. Jamaluddin M, Garofalo R, Ogra PL, Brasier AR. Inducible translational regulation of the NF-IL6 transcription factor by respiratory syncytial virus infection in pulmonary epithelial cells. *J Virol* 1996; 70(3):1554-63.
278. Mukaida N, Okamoto S, Ishikawa Y, Matsushima K. Molecular mechanism of interleukin-8 gene expression. *J Leukoc Biol* 1994; 56(5):554-8.

279. Casola A, Garofalo RP, Jamaluddin M, Vlahopoulos S, Brasier AR. Requirement of a novel upstream response element in respiratory syncytial virus-induced IL-8 gene expression. *J Immunol* 2000; 164(11):5944-51.
280. Bitko V, Barik S. Persistent activation of RelA by respiratory syncytial virus involves protein kinase C, underphosphorylated IkappaBbeta, and sequestration of protein phosphatase 2A by the viral phosphoprotein. *J Virol* 1998; 72(7):5610-8.
281. Baeuerle PA, Baichwal VR. NF-kappa B as a frequent target for immunosuppressive and anti-inflammatory molecules. *Adv Immunol* 1997; 65:111-37.
282. Kopp EB, Ghosh S. NF-kappa B and rel proteins in innate immunity. *Adv Immunol* 1995; 58:1-27.
283. Delhase M, Li N, Karin M. Kinase regulation in inflammatory response. *Nature* 2000; 406(6794):367-8.
284. Ozes ON, Akca H, Mayo LD, Gustin JA, Maehama T, *et al.* A phosphatidylinositol 3-kinase/Akt/mTOR pathway mediates and PTEN antagonizes tumor necrosis factor inhibition of insulin signaling through insulin receptor substrate-1. *PNAS* 2001; 98(8):4640-5.
285. Karin M, Delhase M. The I kappa B kinase (IKK) and NF-kappa B: key elements of proinflammatory signalling. *Semin Immunol* 2000; 12(1):85-98.
286. Muzio M, Natoli G, Saccani S, Levrero M, Mantovani A. The human toll signaling pathway: divergence of nuclear factor kappaB and JNK/SAPK activation upstream of tumor necrosis factor receptor-associated factor 6 (TRAF6). *J Exp Med* 1998; 187(12):2097-101.
287. Benn J, Schneider RJ. Hepatitis B virus HBx protein activates Ras-GTP complex formation and establishes a Ras, Raf, MAP kinase signaling cascade. *PNAS* 1994; 91(22):10350-4.
288. Doria M, Klein N, Lucito R, Schneider RJ. The hepatitis B virus HBx protein is a dual specificity cytoplasmic activator of Ras and nuclear activator of transcription factors. *EMBO J* 1995; 14(19):4747-57.
289. Bruder JT, Kovacs I. Adenovirus infection stimulates the Raf/MAPK signaling pathway and induces interleukin-8 expression. *J Virol* 1997; 71(1):398-404.
290. Chen W, Monick MM, Carter AB, Hunninghake GW. Activation of ERK2 by respiratory syncytial virus in A549 cells is linked to the production of interleukin 8. *Exp Lung Res* 2000; 26(1):13-26.
291. Lange-Carter CA, Pleiman CM, Gardner AM, Blumer KJ, Johnson GL. A divergence in the MAP kinase regulatory network defined by MEK kinase and Raf. *Science* 1993; 260(5106):315-9.

292. Moodie SA, Willumsen BM, Weber MJ, Wolfman A. Complexes of Ras.GTP with Raf-1 and mitogen-activated protein kinase kinase. *Science* 1993; 260(5114):1658-61.
293. Denhardt DT. Signal-transducing protein phosphorylation cascades mediated by Ras/Rho proteins in the mammalian cell: the potential for multiplex signaling. *Biochem J* 1996; 318(Pt 3):729-47.
294. Lewis TS, Shapiro PS, Ahn NG. Signal transduction through MAP kinase cascades. *Adv Cancer Res* 1998; 74:49-139.
295. Monick M, Staber J, Thomas K, Hunninghake G. Respiratory syncytial virus infection results in activation of multiple protein kinase C isoforms leading to activation of mitogen-activated protein kinase. *J Immunol* 2001; 166(4):2681-7.
296. Duke RC. Apoptosis in cell-mediated immunity. In: Tomei LD, Cope FO, editors. *Apoptosis: the molecular basis of cell death*. Cold Spring Harbor, NY: Cold Spring Harbor Laboratory; 1991. p. 209-226.
297. Gougeon ML, Montagnier L. Apoptosis in AIDS. *Science* 1993; 260(5112):1269-70.
298. Terai C, Kornbluth RS, Pauza CD, Richman DD, Carson DA. Apoptosis as a mechanism of cell death in cultured T lymphoblasts acutely infected with HIV-1. *J Clin Invest* 1991; 87(5):1710-5.
299. Hinshaw VS, Olsen CW, Dybdahl-Sissoko N, Evans D. Apoptosis: a mechanism of cell killing by influenza A and B viruses. *J Virol* 1994; 68(6):3667-73.
300. Takizawa T, Matsukawa S, Higuchi Y, Nakamura S, Nakanishi Y, Fukuda R. Induction of programmed cell death (apoptosis) by influenza virus infection in tissue culture cells. *J Gen Virol* 1993; 74(Pt 11):2347-55.
301. Teodoro JG, Branton PE. Regulation of apoptosis by viral gene products. *J Virol* 1997; 71(3):1739-46.
302. McFadden G. Even viruses can learn to cope with stress. *Science* 1998; 279(5347):40-1.
303. Henderson S, Huen D, Rowe M, Dawson C, Johnson G, Rickinson A. Epstein-Barr virus-coded BHRF1 protein, a viral homologue of Bcl-2, protects human B cells from programmed cell death. *PNAS* 1993; 90(18):8479-83.
304. Rao L, Debbas M, Sabbatini P, Hockenberry D, Korsmeyer S, White E. The adenovirus E1A proteins induce apoptosis, which is inhibited by the E1B 19-kDa and Bcl-2 proteins. *PNAS* 1992; 89(16):7742-6.
305. Schreiber M, Sedger L, McFadden G. Distinct domains of M-T2, the myxoma virus tumor necrosis factor (TNF) receptor homolog, mediate extracellular TNF binding and intracellular apoptosis inhibition. *J Virol* 1997; 71(3):2171-81.

306. O'Donnell D R, Milligan L, Stark JM. Induction of CD95 (Fas) and apoptosis in respiratory epithelial cell cultures following respiratory syncytial virus infection. *Virology* 1999; 257(1):198-207.
307. Bitko V, Barik S. An endoplasmic reticulum-specific stress-activated caspase (caspase-12) is implicated in the apoptosis of A549 epithelial cells by respiratory syncytial virus. *J Cell Biochem* 2001; 80(3):441-54.
308. Nakagawa T, Zhu H, Morishima N, Li E, Xu J, *et al*. Caspase-12 mediates endoplasmic-reticulum-specific apoptosis and cytotoxicity by amyloid-beta. *Nature* 2000; 403(6765):98-103.
309. Takeuchi R, Tsutsumi H, Osaki M, Haseyama K, Mizue N, Chiba S. Respiratory syncytial virus infection of human alveolar epithelial cells enhances interferon regulatory factor 1 and interleukin-1beta-converting enzyme gene expression but does not cause apoptosis. *J Virol* 1998; 72(5):4498-502.
310. Cohen GM. Caspases: the executioners of apoptosis. *Biochem J* 1997; 326(Pt 1):1-16.
311. Domachowske JB, Bonville CA, Mortelliti AJ, Colella CB, Kim U, Rosenberg HF. Respiratory syncytial virus infection induces expression of the anti-apoptosis gene IEX-1L in human respiratory epithelial cells. *J Infect Dis* 2000; 181(3):824-30.
312. Kondratyev AD, Chung KN, Jung MO. Identification and characterization of a radiation-inducible glycosylated human early-response gene. *Cancer Res* 1996; 56(7):1498-502.
313. Wu MX, Ao Z, Prasad KV, Wu R, Schlossman SF. IEX-1L, an apoptosis inhibitor involved in NF-kappaB-mediated cell survival. *Science* 1998; 281(5379):998-1001.
314. Krilov LR, McCloskey TW, Harkness SH, Pontrelli L, Pahwa S. Alterations in apoptosis of cord and adult peripheral blood mononuclear cells induced by *in vitro* infection with respiratory syncytial virus. *J Infect Dis* 2000; 181(1):349-53.
315. Laemmli UK. Cleavage of structural proteins during the assembly of the head of bacteriophage T4. *Nature* 1970; 227(259):680-5.
316. Lowry OH. Protein measurement with the Folin Phenol reagent. *J Biol Chem* 1951; 193:265-275.
317. Peterson GL. Review of the Folin phenol protein quantitation method of Lowry, Rosebrough, Farr and Randall. *Anal Biochem* 1979; 100(2):201-20.
318. Riches DW, Chan ED, Winston BW. TNF-alpha-induced regulation and signalling in macrophages. *Immunobiol* 1996; 195(4-5):477-90.
319. Frodin M, Gammeltoft S. Role and regulation of 90 kDa ribosomal S6 kinase (RSK) in signal transduction. *Mol Cell Endocrinol* 1999; 151(1-2):65-77.

320. Shimamura A, Ballif BA, Richards SA, Blenis J. Rsk1 mediates a MEK-MAP kinase cell survival signal. *Curr Biol* 2000; 10(3):127-35.
321. Schouten GJ, Vertegaal AC, Whiteside ST, Israel A, Toebe M, *et al.* IkappaB alpha is a target for the mitogen-activated 90 kDa ribosomal S6 kinase. *EMBO J* 1997; 16(11):3133-44.
322. Ghoda L, Lin X, Greene WC. The 90-kDa ribosomal S6 kinase (pp90rsk) phosphorylates the N-terminal regulatory domain of IkappaBalph α and stimulates its degradation *in vitro*. *J Biol Chem* 1997; 272(34):21281-8.
323. Luo H, Yanagawa B, Zhang J, Luo Z, Zhang M, *et al.* Coxsackievirus B3 replication is reduced by inhibition of the extracellular signal-regulated kinase (ERK) signaling pathway. *J Virol* 2002; [In Press].
324. Datta SR, Brunet A, Greenberg ME. Cellular survival: a play in three Akts. *Genes Dev* 1999; 13(22):2905-27.
325. Fruman DA, Meyers RE, Cantley LC. Phosphoinositide kinases. *Annu Rev Biochem* 1998; 67:481-507.
326. Cross DA, Alessi DR, Cohen P, Andjelkovich M, Hemmings BA. Inhibition of glycogen synthase kinase-3 by insulin mediated by protein kinase B. *Nature* 1995; 378(6559):785-9.
327. Kulik G, Klippe A, Weber MJ. Antiapoptotic signalling by the insulin-like growth factor I receptor, phosphatidylinositol 3-kinase, and Akt. *Mol Cell Biol* 1997; 17(3):1595-606.
328. Dudek H, Datta SR, Franke TF, Birnbaum MJ, Yao R, *et al.* Regulation of neuronal survival by the serine-threonine protein kinase Akt. *Science* 1997; 275(5300):661-5.
329. Kennedy SG, Wagner AJ, Conzen SD, Jordan J, Bellacosa A, *et al.* The PI 3-kinase/Akt signaling pathway delivers an anti-apoptotic signal. *Genes Dev* 1997; 11(6):701-13.
330. Staal SP. Molecular cloning of the akt oncogene and its human homologues AKT1 and AKT2: amplification of AKT1 in a primary human gastric adenocarcinoma. *PNAS* 1987; 84(14):5034-7.
331. Miwa W, Yasuda J, Murakami Y, Yashima K, Sugano K, *et al.* Isolation of DNA sequences amplified at chromosome 19q13.1-q13.2 including the AKT2 locus in human pancreatic cancer. *Biochem Biophys Res Commun* 1996; 225(3):968-74.
332. Cheng JQ, Ruggeri B, Klein WM, Sonoda G, Altomare DA, *et al.* Amplification of AKT2 in human pancreatic cells and inhibition of AKT2 expression and tumorigenicity by antisense RNA. *PNAS* 1996; 93(8):3636-41.
333. Bellacosa A, de Feo D, Godwin AK, Bell DW, Cheng JQ, *et al.* Molecular alterations of the AKT2 oncogene in ovarian and breast carcinomas. *Int J Cancer* 1995; 64(4):280-5.

334. Carson JP, Kulik G, Weber MJ. Antiapoptotic signaling in LNCaP prostate cancer cells: a survival signaling pathway independent of phosphatidylinositol 3'-kinase and Akt/protein kinase B. *Cancer Res* 1999; 59(7):1449-53.
335. Khwaja A, Rodriguez-Viciiana P, Wennstrom S, Warne PH, Downward J. Matrix adhesion and Ras transformation both activate a phosphoinositide 3-OH kinase and protein kinase B/Akt cellular survival pathway. *EMBO J* 1997; 16(10):2783-93.
336. Bellacosa A, Testa JR, Staal SP, Tsichlis PN. A retroviral oncogene, akt, encoding a serine-threonine kinase containing an SH2-like region. *Science* 1991; 254(5029):274-7.
337. Franke TF, Yang SI, Chan TO, Datta K, Kazlauskas A, *et al*. The protein kinase encoded by the Akt proto-oncogene is a target of the PDGF-activated phosphatidylinositol 3-kinase. *Cell* 1995; 81(5):727-36.
338. Burgering BM, Coffer PJ. Protein kinase B (c-Akt) in phosphatidylinositol-3-OH kinase signal transduction. *Nature* 1995; 376(6541):599-602.
339. Franke TF, Kaplan DR, Cantley LC, Toker A. Direct regulation of the Akt proto-oncogene product by phosphatidylinositol-3,4-bisphosphate. *Science* 1997; 275(5300):665-8.
340. Alessi DR, James SR, Downes CP, Holmes AB, Gaffney PR, *et al*. Characterization of a 3-phosphoinositide-dependent protein kinase which phosphorylates and activates protein kinase Balpha. *Curr Biol* 1997; 7(4):261-9.
341. Stokoe D, Stephens LR, Copeland T, Gaffney PR, Reese CB, *et al*. Dual role of phosphatidylinositol-3,4,5-trisphosphate in the activation of protein kinase B. *Science* 1997; 277(5325):567-70.
342. Toker A, Newton AC. Cellular signaling: pivoting around PDK-1. *Cell* 2000; 103(2):185-8.
343. Deprez J, Vertommen D, Alessi DR, Hue L, Rider MH. Phosphorylation and activation of heart 6-phosphofructo-2-kinase by protein kinase B and other protein kinases of the insulin signaling cascades. *J Biol Chem* 1997; 272(28):17269-75.
344. Datta SR, Dudek H, Tao X, Masters S, Fu H, *et al*. Akt phosphorylation of BAD couples survival signals to the cell-intrinsic death machinery. *Cell* 1997; 91(2):231-41.
345. del Peso L, Gonzalez-Garcia M, Page C, Herrera R, Nunez G. Interleukin-3-induced phosphorylation of BAD through the protein kinase Akt. *Science* 1997; 278(5338):687-9.
346. Alessi DR, Caudwell FB, Andjelkovic M, Hemmings BA, Cohen P. Molecular basis for the substrate specificity of protein kinase B; comparison with MAPKAP kinase-1 and p70 S6 kinase. *FEBS Lett* 1996; 399(3):333-8.
347. Kandel ES, Hay N. The regulation and activities of the multifunctional serine/threonine kinase Akt/PKB. *Exp Cell Res* 1999; 253(1):210-29.

348. Cardone MH, Roy N, Stennicke HR, Salvesen GS, Franke TF, *et al.* Regulation of cell death protease caspase-9 by phosphorylation. *Science* 1998; 282(5392):1318-21.
349. Du K, Montminy M. CREB is a regulatory target for the protein kinase Akt/PKB. *J Biol Chem* 1998; 273(49):32377-9.
350. Pap M, Cooper GM. Role of glycogen synthase kinase-3 in the phosphatidylinositol 3-Kinase/Akt cell survival pathway. *J Biol Chem* 1998; 273(32):19929-32.
351. Brunet A, Bonni A, Zigmond MJ, Lin MZ, Juo P, *et al.* Akt promotes cell survival by phosphorylating and inhibiting a Forkhead transcription factor. *Cell* 1999; 96(6):857-68.
352. Romashkova JA, Makarov SS. NF-kappaB is a target of AKT in anti-apoptotic PDGF signalling. *Nature* 1999; 401(6748):86-90.
353. Borgatti P, Zauli G, Colamussi ML, Gibellini D, Previati M, *et al.* Extracellular HIV-1 Tat protein activates phosphatidylinositol 3- and Akt/PKB kinases in CD4+ T lymphoblastoid Jurkat cells. *Eur J Immunol* 1997; 27(11):2805-11.
354. Meili R, Cron P, Hemmings BA, Ballmer-Hofer K. Protein kinase B/Akt is activated by polyomavirus middle-T antigen via a phosphatidylinositol 3-kinase-dependent mechanism. *Oncogene* 1998; 16(7):903-7.
355. Pullen N, Thomas G. The modular phosphorylation and activation of p70S6K. *FEBS Lett* 1997; 410(1):78-82.
356. Pullen N, Dennis PB, Andjelkovic M, Dufner A, Kozma SC, *et al.* Phosphorylation and activation of p70s6k by PDK1. *Science* 1998; 279(5351):707-10.
357. Westphal RS, Coffee RL, Jr., Marotta A, Pelech SL, Wadzinski BE. Identification of kinase-phosphatase signaling modules composed of p70 S6 kinase-protein phosphatase 2A (PP2A) and p21-activated kinase-PP2A. *J Biol Chem* 1999; 274(2):687-92.

APPENDIX

Raw data for Chapter 6 – Effect of age of host animal on *in vitro* RSV infection.

RSV immunostaining on cytopsin preparations.

Proportion of RSV-immunopositive AM from adult and juvenile guinea pigs.

| Adult | | | Juvenile | | |
|--------|--------------|----------|----------|--------------|----------|
| Mature | Intermediate | Immature | Mature | Intermediate | Immature |
| 1.3 | 1.7 | 1.3 | 13.0 | 21.0 | 20.0 |
| 2.6 | 4.0 | 1.0 | 11.0 | 13.0 | 17.0 |
| 0.7 | 0.3 | 1.3 | 10.0 | 20.0 | 24.0 |
| 0.7 | 1.3 | 0.3 | 9.0 | 17.0 | 23.0 |
| 1.7 | 2.0 | 2.0 | 10.0 | 16.0 | 19.0 |
| 0.7 | 1.7 | 1.0 | - | - | - |

Plaque Assay.

Number of syncytia per million AM from adult and juvenile guinea pigs.

| Adult | | | Juvenile | | |
|--------|--------------|----------|----------|--------------|----------|
| Mature | Intermediate | Immature | Mature | Intermediate | Immature |
| 80 | 88 | 80 | 220 | 1710 | 2500 |
| 6 | 71 | 68 | 300 | 930 | 5330 |
| 20 | 112 | 32 | 160 | 950 | 5330 |
| 35 | 0 | 27 | 290 | 110 | 3110 |
| 67 | 71 | 17 | 290 | 1170 | 6500 |
| 42 | 67 | 67 | - | - | - |

Raw data for Chapter 7 – Effect of sex of host animal on *in vitro* RSV infection.

RSV immunostaining on cytopsin preparations.

Proportion of RSV-immunopositive AM from male and female guinea pigs.

| Male | | Female | |
|--------|----------|--------|----------|
| Mature | Immature | Mature | Immature |
| 10.0 | 23.3 | 12.0 | 25.0 |
| 9.7 | 23.0 | 13.7 | 25.3 |
| 9.0 | 21.0 | 13.0 | 23.0 |
| 11.0 | 19.7 | 15.0 | 27.0 |

Plaque Assay.

Number of syncytia per million AM from male and female guinea pigs.

| Male | | Female | |
|--------|----------|--------|----------|
| Mature | Immature | Mature | Immature |
| 330 | 6500 | 420 | 7100 |
| 400 | 5700 | 350 | 6700 |
| 410 | 8300 | 380 | 7000 |
| 500 | 6500 | 330 | 8600 |

IL-6 production by RSV-infected AM subpopulations from male and female guinea pigs.

| Male | | Female | |
|--------|----------|--------|----------|
| Mature | Immature | Mature | Immature |
| 158.5 | 124.6 | 179.0 | 155.9 |
| 395.9 | 349.0 | 318.0 | 300.3 |
| 458.9 | 508.1 | 407.4 | 395.3 |
| 500.3 | 416.7 | 491.0 | 473.1 |

IL-8 production by RSV-infected AM subpopulations from male and female guinea pigs.

| Male | | Female | |
|--------|----------|--------|----------|
| Mature | Immature | Mature | Immature |
| 682 | 952 | 207 | 507 |
| 617 | 737 | 582 | 767 |
| 892 | 1137 | 957 | 1457 |
| 727 | 657 | 762 | 722 |

TNF α production by RSV-infected AM subpopulations from male and female guinea pigs.

| Male | | Female | |
|--------|----------|--------|----------|
| Mature | Immature | Mature | Immature |
| 3.2 | 23.1 | 3.8 | 2.2 |
| 5.9 | 4.3 | 6.6 | 6.3 |
| 40.7 | 6.5 | 11.8 | 18.6 |
| 14.2 | 18.7 | 12.6 | 14.3 |

Raw data for Chapter 8 – PM10-RSV interaction in guinea pig alveolar macrophages.

Side scatter measurements by flow cytometry.

| PM10+RSV | RSV+PM10 | PM10 | RSV | NEG |
|----------|----------|------|------|------|
| 88.0 | 88.8 | 88.4 | 76.7 | 70.2 |
| 88.8 | 94.9 | 91.9 | 86.7 | 86.8 |
| 86.0 | 87.8 | 86.9 | 61.9 | 64.4 |
| 83.0 | 90.5 | 84.2 | 73.4 | 82.6 |

RSV immunopositivity as measured by flow cytometry.

Proportion of RSV-immunopositive AM.

| PM10+RSV | RSV+PM10 | PM10 | RSV | NEG |
|----------|----------|------|-------|------|
| 3.9 | 12.02 | 1.89 | 5.08 | 0.18 |
| 4.95 | 11.6 | 1.59 | 16.41 | 0.0 |
| 3.69 | 13.7 | 1.97 | 7.6 | 0.15 |
| 5.45 | 12.9 | 2.48 | 12.9 | 0.0 |

Plaque Assay.

Number of syncytia per million AM from male and female guinea pigs.

| PM10+RSV | RSV+PM10 | PM10 | RSV | NEG |
|----------|----------|------|------|-----|
| 363 | 575 | 0 | 4375 | 0 |
| 150 | 725 | 0 | 1488 | 0 |
| 400 | 1038 | 0 | 4750 | 0 |
| 650 | 1700 | 0 | 3525 | 0 |

IL-6 production by guinea pig AM subjected to different treatments.

| PM10+RSV | RSV+PM10 | PM10 | RSV | NEG |
|----------|----------|------|-------|-----|
| 67.0 | 10.5 | 9.1 | 335.9 | 3.0 |
| 78.0 | 10.5 | 0.5 | 337.7 | 5.2 |
| 62.8 | 9.8 | 0.3 | 355.9 | 9.9 |
| 69.5 | 14.5 | 0.7 | 282.3 | 7.0 |

IL-8 production by guinea pig AM subjected to different treatments.

| PM10+RSV | RSV+PM10 | PM10 | RSV | NEG |
|----------|----------|------|-------|-------|
| 214.2 | 187.9 | 32.8 | 534.6 | 288.6 |
| 185.4 | 209.2 | 66.2 | 344.6 | 199.8 |
| 217.3 | 187.3 | 41.2 | 470.9 | 334.6 |
| 282.3 | 292.3 | 41.2 | 530.9 | 201.7 |

TNF production by guinea pig AM subjected to different treatments.

| PM10+RSV | RSV+PM10 | PM10 | RSV | NEG |
|----------|----------|-------|-------|-------|
| 232.0 | 264.0 | 249.0 | 317.8 | 119.3 |
| 308.9 | 351.3 | 333.1 | 247.9 | 235.4 |
| 282.2 | 372.9 | 251.7 | 422.6 | 150.0 |
| 346.3 | 197.2 | 281.0 | 298.4 | 105.8 |

Raw data for Chapter 9 – Summary of AM data from KPKS-1.0

| Species | GuineaPig | GuineaPig | GuineaPig | Species | GuineaPig | GuineaPig | GuineaPig |
|-------------|-----------|-----------|-----------|-------------|-----------|-----------|-----------|
| Tissue | Lung | Lung | Lung | Tissue | Lung | Lung | Lung |
| Cell line | AM | AM | AM | Cell line | AM | AM | AM |
| KPKS1 gels | 368,369 | 372,373 | 376,377 | KPKS1 gels | 368,369 | 372,373 | 376,377 |
| Kinexus ID | 330 | 332 | 332 | Kinexus ID | 330 | 332 | 332 |
| | Untreated | RSV | RSV | | Untreated | RSV | RSV |
| Exposure | 160 sec | 160 sec | 300 sec | Exposure | 160 sec | 160 sec | 300 sec |
| | | | | | | | |
| RafB | 0 | 0 | 0 | p52 S6K | 7029 | 500 | 500 |
| Erk3 | 0 | 0 | 0 | Rsk1 | 5365 | 0 | 0 |
| p45 | 0 | 0 | 0 | Rsk2 | 0 | 3780 | 5918 |
| p43 | 1559 | 500 | 6170 | Cot | 7192 | 4941 | 7203 |
| PKB-alpha | 0 | 1007 | 1646 | Pim 1 | 0 | 0 | 0 |
| Erk1-A2 | 2180 | 2513 | 4278 | CK2-alpha | 5344 | 11603 | 19759 |
| Erk2-A2 | 2515 | 7704 | 12950 | CK2-alpha' | 6140 | 0 | 0 |
| Erk2-A3 | 3357 | 4422 | 7750 | CK2-alpha'' | 0 | 0 | 0 |
| PDK1 | 0 | 0 | 0 | Erk1-B1 | 3279 | 1702 | 2856 |
| Cdk1 | 0 | 0 | 0 | Erk2-B1 | 3284 | 4987 | 8766 |
| Cdk2 | 6244 | 0 | 0 | Yes | 0 | 0 | 0 |
| Cdk4 | 0 | 3988 | 4191 | IKK-alpha | 0 | 0 | 0 |
| Cdk5 | 4042 | 0 | 3580 | DAPK | 0 | 0 | 0 |
| Cdk6 | 1263 | 1467 | 2181 | Lck | 0 | 0 | 0 |
| Cdk7 | 6082 | 2874 | 4822 | BMX | 1495 | 2157 | 3743 |
| Cdk9 | 0 | 0 | 0 | Ksr1 | 0 | 0 | 0 |
| p38-alpha | 15004 | 11289 | 18506 | Csk | 0 | 0 | 0 |
| PKC-mu | 0 | 0 | 0 | Lyn | 6815 | 6831 | 11611 |
| PKC-alpha | 3779 | 2808 | 4558 | Fyn-L | 5431 | 500 | 500 |
| PKC-beta | 11726 | 4041 | 6285 | Fyn-U | 6610 | 8608 | 15820 |
| PKC-gamma | 0 | 0 | 0 | Syk | 3894 | 500 | 6026 |
| PKC-epsilon | 0 | 0 | 0 | Pyk2 | 0 | 0 | 0 |
| PKC-delta | 0 | 0 | 0 | Btk | 0 | 0 | 0 |
| PKC-lambda | 0 | 0 | 0 | CK1-delta | 0 | 0 | 0 |
| PKC-theta | 0 | 0 | 0 | CK1-epsilon | 0 | 0 | 0 |
| PKC-zeta | 3096 | 2736 | 3947 | ZAP70 | 0 | 0 | 0 |
| Erk6 | 0 | 0 | 0 | GCK | 0 | 0 | 0 |
| SAPK p46 | 0 | 1344 | 0 | CaMK4 | 0 | 0 | 0 |
| SAPK p54 | 0 | 0 | 0 | CaMKK | 0 | 0 | 0 |
| Mos | 0 | 0 | 0 | CaMK1 | 0 | 0 | 0 |
| Mek1 | 1264 | 4473 | 7037 | Mnk2 | 0 | 0 | 0 |
| Mek2 | 0 | 0 | 0 | Nek2 | 0 | 0 | 0 |
| Mek4 | 0 | 0 | 0 | Raf1 | 16108 | 7197 | 11971 |
| Mek6 | 5922 | 0 | 0 | PKG | 0 | 0 | 0 |
| Mek7 | 6 | 0 | 0 | PKA | 1044 | 1831 | 2902 |
| PAK-alpha | 7599 | 3781 | 5698 | FAK | 500 | 4567 | 500 |
| ROK-alpha | 0 | 0 | 0 | GRK2 | 6219 | 2998 | 4833 |

| | | | | | | | |
|------------|------|------|------|------|-------|-------|-------|
| RKR | 0 | 0 | 0 | Hpk | 5181 | 0 | 0 |
| GSK3-alpha | 4662 | 4212 | 6135 | ZIPK | 37748 | 11193 | 21213 |
| GSK3-beta | 0 | 0 | 0 | JAK1 | 17068 | 500 | 500 |
| p90 S6K | 9428 | 5614 | 8468 | JAK2 | 0 | 0 | 0 |
| p70 S6K U | 0 | 0 | 0 | Src | 0 | 1210 | 0 |
| p70 S6K L | 0 | 3686 | 5427 | Mst1 | 0 | 0 | 0 |